

M.Sc. (Ocean Science & Technology)

(Integrated Five Years Programme)

IOST 62 AIR :: SEA INTERACTION

VI – SEMESTER

Objective:

The student's undergoing this course will get a sufficient knowledge about the various meteorological events in the atmosphere and its impact on sea surface. Significant attention is also focused on weather forecasting technique and satellite in forecasting technique.

Unit – I : Introduction to Atmosphere

Meteorology-weather and climate-composition, extent, thermal and vertical structure of the atmosphere-heat and temperature, mechanism of heat transfer-incoming solar radiation-heat budget-latitudinal heat balance.

Unit – II : Moisture, Atmospheric stability and Precipitation

Hydrological cycle-changes of state-humidity and its measurement-condensation-adiabatic process-atmospheric stability-lapse rate-lifting process-convection lifting-orographic lifting condensation and cloud formation-cloud-fog-formation of precipitation and its types measurement.

Unit – III : Air pressure, Wind and circulation of Atmosphere

Factors affecting air pressure-measurement-wind pressure-coriolis effect-friction-surface wind-vertical air motion-wind measurement-scale of atmospheric motion-local winds-land and sea breezes-distribution of surface pressure and winds-monsoon circulation-global wind and ocean currents.

Unit – IV : Upper ocean dynamics

Oceanic heat budget, factors influencing heat budget terms, radiative and turbulent fluxes, bulk method for computation of fluxes, dominant forces for ocean dynamics, and equation of motion.

Unit – V : Cyclone and thunderstorms, weather forecasting

Inter Tropical Convergence Zone (ITCZ), Tropical cyclones- formation, classification and structure, Storm surges, EL-Nino Southern Oscillation (ENSO), cyclone tracking thunderstorms-forecasting technique-standard tool in weather forecasting-satellite in weather forecasting.

PRACTICAL XV : IOSP 65 : AIR – SEA INTERACTION

1. Illustrating the concept of atmospheric pressure-construction of graph to measure how Pressure changes with height above earth surface.
2. Illustrating the temperature profile for various class of stability
 - i. Stable
 - ii. Unstable
 - iii. Inversion
3. Determination of Relative Humidity and Dew point temperature at a place.
4. Illustrating the effect of terrain roughness on the wind velocity profile for various Surface conditions.
5. Construction of wind rose diagram at a given location over a period
6. Rainfall measurement.
7. Analysis of rainfall (i.e.) determination of mean, monthly and annual rainfall etc.

REFERENCE BOOKS

1. Csanady, G. T., 2001. Air-Sea Interaction (Laws and Mechanisms) Cambridge University Press.
2. Geernaert, G.L., 1999. Air-Sea Exchange: Physics, Chemistry and Dynamics, Springer.
3. Gill A.E., 1982. Atmosphere- Ocean Dynamics, Academic Press.
4. Menon P.A., 1989. Our Weather, National Book Trust, India.
5. Patrick Santurette, Christo G. Georgiev, 2005. Weather analysis and forecasting, Academic Press.
6. Pickard G.L. and W.J.Emery, 1990. Descriptive Physical Oceanography, Pergamon Press, Newyork.
7. Roll H.U., 1965. Physics of the Marine Atmosphere, Academic Press, Newyork.

UNIT - 1

INTRODUCTION

Meteorology

Meteorology is a branch of the atmospheric sciences which includes atmospheric chemistry and atmospheric physics, with a major focus on weather forecasting. The study of meteorology dates back millennia, though significant progress in meteorology did not occur until the 18th century.

Weather and climate

Weather is the day-to-day state of the atmosphere, and its short-term variation in minutes to weeks. People generally think of **weather** as the combination of temperature, humidity, precipitation, cloudiness, visibility, and wind. **Climate** is the **weather** of a place averaged over a period of time, often 30 years.

Composition of atmosphere

The atmosphere is made up of different types of gases, water vapor and dust particles. The composition of the atmosphere is not static. It changes according to the time and place.

(A) Gases of the atmosphere:

<i>Serial No.</i>	<i>Gas</i>	<i>Amount (in percentage)</i>
A.	Main	
1.	Nitrogen	78.1
2.	Oxygen	20.9
		} 99%
B.	Secondary	
1.	Organ	0.9
2.	Carbon Dioxide	0.03
3.	Hydrogen	0.01
4.	Nion	0.0018
5.	Helium	0.0005
6.	Ozone	0.00006
7.	Others	
		} 0.99%

(B) Water vapour

Gaseous form of water present in the atmosphere is called water vapour. Water vapour present in the atmosphere has made life possible on the earth. Water vapour is the source of all kinds of precipitation. Its maximum amount in the atmosphere could be up to 4 percent. Maximum amount of water vapour is found in hot-wet regions and its least amount is found in the dry regions. Generally, the amount of water vapour goes on decreasing from low latitudes to high latitudes.

(C) Dust Particles

Dust particles are generally found in the lower layers of the atmosphere. These particles are found in the form of sand, smoke and oceanic salt. Sand particles have an important place in the atmosphere. These dust particles help in the condensation of water vapour. During condensation, water vapour gets condensed in the form of droplets around these dust particles. Due to this process, the clouds are formed and precipitation is made possible.

Structure of the atmosphere

The atmosphere is an integral part of the earth. It surrounds the earth from all sides. Generally it extends upto about 1600 kilometres from the earth's surface. 97 percent of the total amount of weight of the atmosphere is limited upto the height of about 30 kilometres. The atmosphere can be divided into five layers according to the diversity of temperature and density.

- (a) Troposphere
- (b) Stratosphere
- (c) Mesosphere
- (d) Ionosphere
- (e) Exosphere

(a) TROPOSPHERE :-

- (i) This is the lowest layer of the atmosphere.
- (ii) The height of this layer is about 18 kms on the equator and 8 kms on the poles. The main reason of higher height at the equator is due to presence of hot convection currents that push the gases upward.
- (iii) This is the most important layer of the atmosphere because all kinds of weather changes take place only in this layer. Due to these changes development of living world take place on the earth. The air never remains static in this layer. Therefore this layer is called changing sphere or troposphere.
- (iv) The environmental temperature decreases with increasing height of atmosphere. It decreases at the rate of 10C at the height of 165 metre. This is called Normal lapse rate.
- (v) The upper limit of the troposphere is called tropopause. This is a transitional zone. In this zone characteristics of both the troposphere and ionosphere are found

(b) STRATOSPHERE

- (i) This layer is above the troposphere.
- (ii) This layer is spread upto the height of 50 kms from the Earth's surface. Its average extent 40 kms

- (iii) The temperature remains almost the same in the lower part of this layer upto the height of 20 kms. After this the temperature increases slowly with the increase in the height. The temperature increases due to the presence of ozone gas in the upper part of this layer.
- (iv) Weather related incidents do not take place in this layer. The air blows horizontally here. Therefore this layer is considered ideal for flying of aircrafts

(c) MESOSPHERE

- (i) It is the third layer of the atmosphere spreading over stratosphere
- (ii) It spreads upto the height of 80 kms. from the surface of the earth. It's extent is 30 kms.
- (iii) Temperature goes on decreasing and drops upto – 1000C.
- (iv) 'Meteors' or falling stars occur in this layer.

(d) IONOSPHERE

- (i) This is the fourth layer of the atmosphere. It is located above the mesosphere.
- (ii) This layer spreads upto the height of 400 kms. from the surface of the earth. The width of this layer is about 300 kms.
- (iii) The temperature starts increasing again with increasing height in this layer.
- (iv) Electrically charged currents flows in the air in this sphere. Radio waves are reflected back on the earth from this sphere and due to this radio broadcasting has become possible.

(e) EXOSPHERE

- (i) This is the last layer of the atmosphere located above ionosphere and extends to beyond 400 km above the earth.
- (ii) Gases are very sparse in this sphere due to the lack of gravitational force. Therefore, the density of air is very less here.

Heat and temperature

Heat and temperature are related to each other, but are different concepts. **Heat** is the total energy of molecular motion in a substance while **temperature** is a measure of the average energy of molecular motion in a substance.

Heat transfer mechanism

Heat transfer mechanisms are simply ways, by which thermal energy can be transferred between objects, and they all rely on the basic principle that kinetic energy or heat wants to be at equilibrium or at *equal energy states*. There are three different ways for heat transfer to occur: conduction, convection, and radiant heat (often referred to as radiation, but that's a more general term that includes many other phenomena). There is a related phenomenon that transfers latent heat called evapotranspiration.

Conduction

Conduction is the simplest heat transfer model in terms of being able to create a mathematical explanation for what's happening. It is the movement of kinetic energy in materials from higher temperature areas to lower temperature areas through a substance. The molecules will simply give their energy to adjacent molecules until equilibrium is reached. Conduction models do not deal with the movement of particles within the material.

Convection

Convection is heat transfer through fluid (like air or water) motion. The difference between conduction and convection is the motion of a material carrier; convection is the movement of the thermal energy by moving hot fluid (as opposed to making other material hot by wiggling atoms). Usually this motion occurs as a result of differences in density. Warmer particles are less dense, so particles with higher temperature will move to regions where the temperature is cooler and the particles with lower temperature will move to areas of higher temperature. The fluid will remain in motion until equilibrium is reached.

Radiation

Heat transferred by radiation is called radiant heat. Like light, radiant heat is radiant energy, and does not necessarily require a medium to carry it. This form of energy transfer is facilitated through a type of electromagnetic radiation.^[6] All moving charged particles emit electromagnetic radiation. This emitted wave will travel until it hits another particle. The particle that receives this radiation will receive it as kinetic energy. Particles will receive and emit radiation even after

everything is at the same temperature, but it's not noticed due to the fact that the material is at equilibrium at this point.

This type of heat transfer is particularly important in the setting the temperature of Earth. Radiation, as heat transfer, is how the Earth gets energy from the sun. Radiation is also important for the greenhouse effect.

Incoming solar radiation

Effect of Earth's atmosphere on incoming solar radiation.

A. Reflectivity: 35% of incoming solar radiation is reflected back to space

Clouds; Twenty-four percent of incoming solar radiation is reflected by clouds, 4% by the Earth's surface.

Scattering; Seven percent of incoming solar radiation is scattered back to space. Particles in the atmosphere can scatter incoming solar radiation. This process works as follows: a particle momentarily traps some part of the solar spectrum that strikes it and then releases that same energy in all directions. Consequently one half of the radiation scattered is returned to space and the other half is sent down to the Earth's surface.

The wavelengths scattered depends on the size of the scattering particle. Haze and smog particles are relatively large and they scatter all wavelengths. The presence of particles of smog and haze (small water droplets) gives the sky a milky appearance. Contrast the color of the sky on a hot humid summer day with its appearance on a cold clear winter day.

Small particles, such as air molecules (molecules of nitrogen or oxygen), scatter a larger proportion of short wavelength light (blue and violet) rather than longer wavelengths (red). This preferential scattering of blue light is what gives the sky its blue color. This effect is also responsible for red Sunsets. At Sunset, if you look directly at the Sun, the Sun rays have traveled through a much greater thickness of the Earth's atmosphere than they do when the Sun is directly overhead at noon. Consequently, because of the preferential scattering of blue light by the atmosphere, only red and yellow light reach your eyes, hence red Sunsets.

B. Absorption: about 17% of incoming solar radiation is absorbed at various levels in the atmosphere

Absorption is the process by which radiant energy is transferred to matter. If the matter is a gas, radiation can affect it in a number of ways. The ways it can absorb energy depends on the size and complexity of the gas molecule. The gas molecule can be rotated and a variety of vibratory modes can be excited depending on the nature of the molecule. If the energy is strong enough the molecule can be broken apart. Each mode of energy absorption occurs at a specific narrow band of the solar spectrum. Gases, therefore, are not like black bodies that absorb equally and completely at all wavelengths. Rather, they absorb only at specific, often narrow ranges of wavelengths. Diatomic molecules such as nitrogen and oxygen (most of our atmosphere) can absorb energy by increasing the vibration of the bond between the two atoms. If the energy absorbed is great enough it may break the bond resulting in two freewheeling oxygen or nitrogen atoms traveling at high speeds.



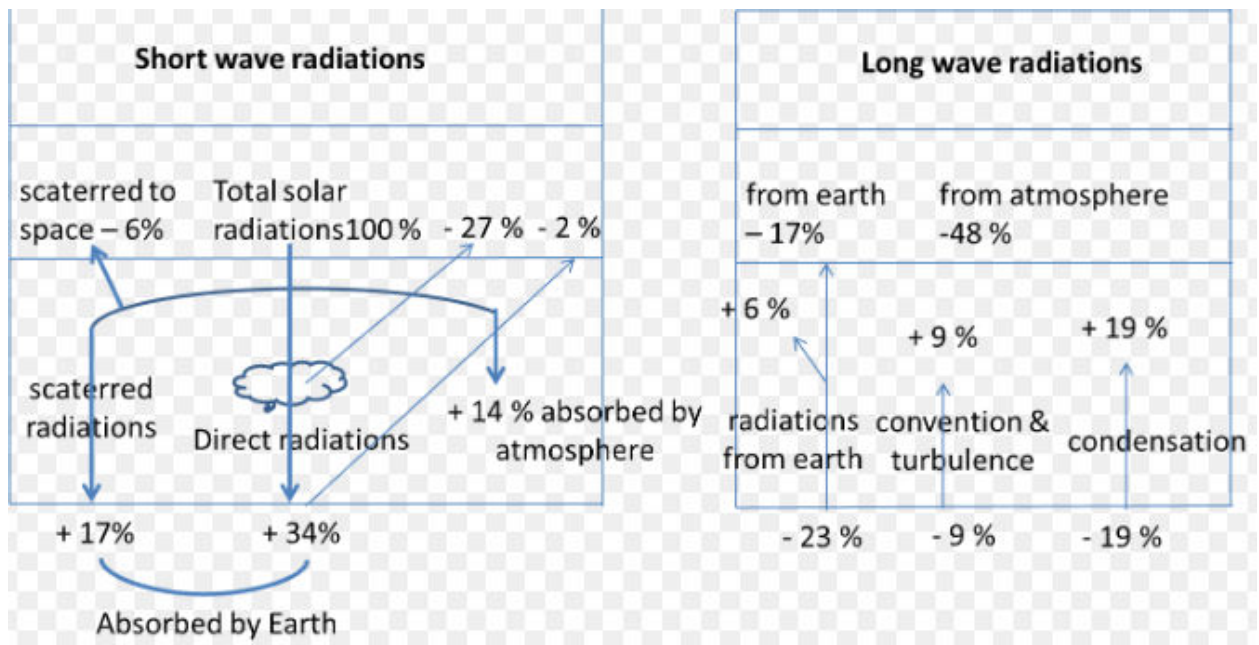
Heat budget

There is a state of balance between the incoming solar radiation and the outgoing terrestrial radiation. This equilibrium, in which the temperature of the earth as a whole remains constant, is known as the heat budget or heat balance.

The budget of solar radiation is as follows:

	percent
Reflected	35
Absorbed by atmosphere	17.5
Scattered to the Earth from blue sky	10.5
Scattered to the Earth from clouds	14.5
Radiation going directly to Earth's surface	22.5

	100



Latitudinal heat balance

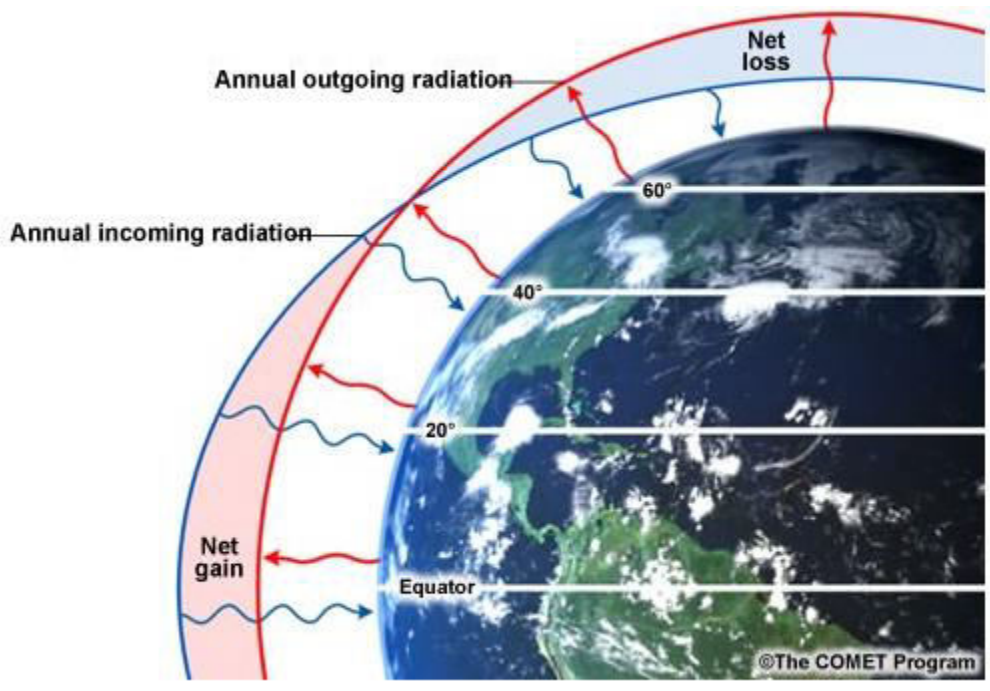
Latitudinal heat balance means the state of balance which exists between the latitudinal belts.

The insulation on the surface of the earth varies because of its tilted axis.

- (i) Insulation decreases pole wards from the equator.
- (ii) Between 37° N and 37° S, maximum insulation is received. It is a zone surplus heat.
- (iii) Beyond 37° N and 37° S to the poles, insulation decreases. It is a zone of deficit heat.

If the heat is not transferred from one latitudinal belt to the other, the surplus heat belt will become too hot to live in and the deficit heat belt will become too cold. Hence, transfer of heat takes from surplus heat zone to the deficit heat zone by ocean currents and winds.

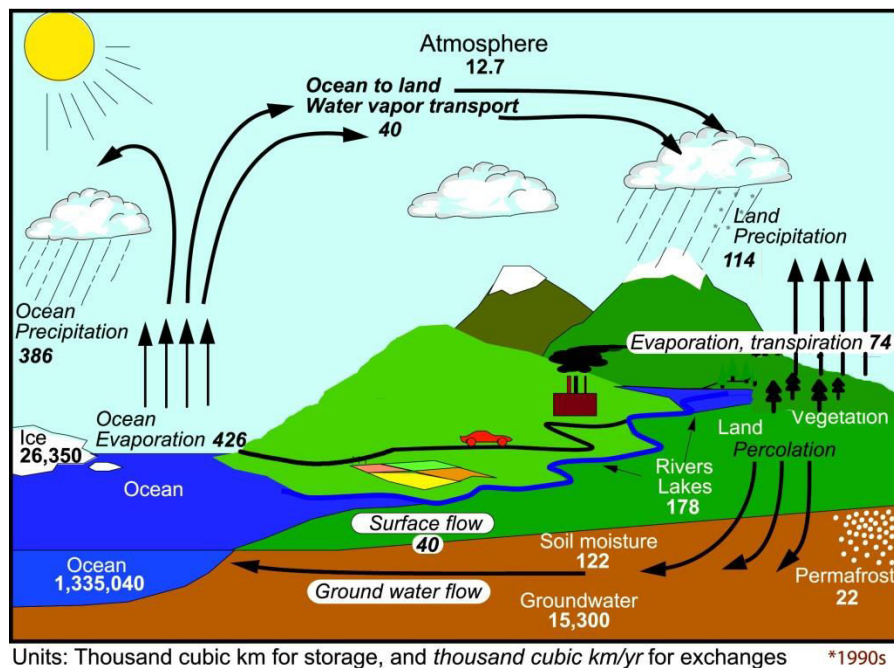
- The amount of insolation received varies from latitude to latitude.
- Regions within the equator and 40° N and S latitudes receive abundant sunlight and hence more heat will be gained than lost. Hence they are **energy surplus regions**.
- Regions beyond 40° N and S latitudes lose more heat than that gained from sunlight. Hence they are **energy deficit regions** (This is because of **slant sunlight and high albedo of Polar Regions**).
- Going by this logic, the tropics should have been getting progressively hotter and the poles getting progressively cooler. And the planet would have been inhospitable except for few regions near mid-latitudes. But, in reality, this does not happen.
- The atmosphere (**planetary winds**) and the oceans (**ocean currents**) transfer excess heat from the tropics (energy surplus region) towards the poles (energy deficit regions) making up for heat loss at higher latitudes.
- And most of the heat transfer takes place across the mid-latitudes (30° to 50°)[more while studding jet streams and cyclones], and hence much of the stormy weather is associated with this region.



UNIT - 2

Hydrological cycle

The hydrologic cycle begins with the evaporation of water from the surface of the ocean. As moist air is lifted, it cools and water vapor condenses to form clouds. Moisture is transported around the globe until it returns to the surface as precipitation. Once the water reaches the ground, one of two processes may occur; 1) some of the water may evaporate back into the atmosphere or 2) the water may penetrate the surface and become groundwater. Groundwater either seeps its way to into the oceans, rivers, and streams, or is released back into the atmosphere through transpiration. The balance of water that remains on the earth's surface is runoff, which empties into lakes, rivers and streams and is carried back to the oceans, where the cycle begins again.



Humidity and its measurement

Humidity is the amount of water vapour present in air. Water vapour, the gaseous state of water, is generally invisible to the human eye. Humidity indicates the likelihood for precipitation, dew,

or fog to be present. The amount of water vapour needed to achieve saturation increases as the temperature increases.

Hygrometer

A **hygrometer** is a weather instrument used to measure the amount of humidity in the atmosphere. There are two main types of **hygrometers** -- a dry and wet bulb psychrometer and a mechanical **hygrometer**.

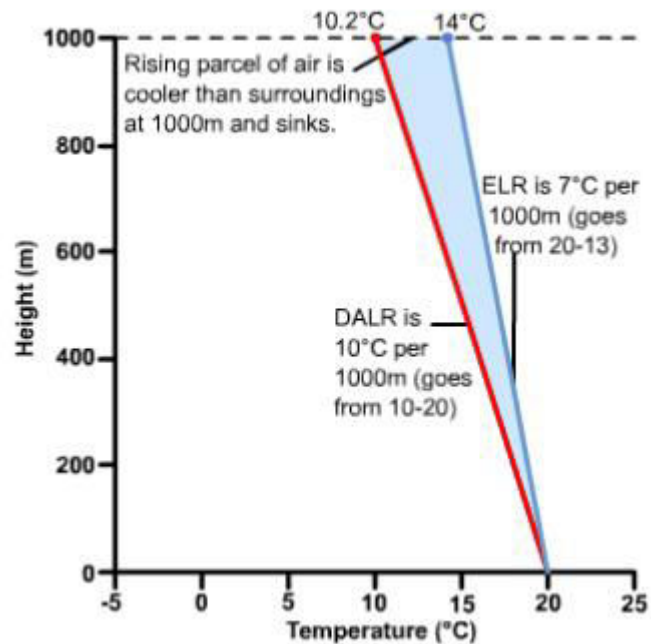
A common way these devices work is by using a material that attracts moisture, and that changes depending on how moist it is. The probably simplest method of these is to use a human hair. The hair will change length, depending on the moisture. Hence, it calculates the relative humidity of a particular place. A hygrometer has two bulbs: one wet and one dry. Both bulbs are thermometers, though one is covered with a wet towel. After a period of time, the water on the wet bulb evaporates and at that time, the temperature is measured on each bulb. The difference between the temperatures is noted. Then each is used on a chart to find the relative humidity of that temperature and area. A small difference between the temperature of the bulbs shows a high relative humidity coming from a low evaporation rate. In dry air, evaporation happens faster showing a large difference in temperature thus giving you a low relative humidity

Example: 30°C Dry Bulb + 20°C Wet Bulb = ~40% relative humidity

Condensation

Condensation is the change of the physical state of matter from gas phase into liquid phase, and is the reverse of vapourisation. The word most often refers to the water cycle. It can also be defined as the change in the state of water vapour to liquid water when in contact with a liquid or solid surface or cloud condensation nuclei within the atmosphere. When the transition happens from the gaseous phase into the solid phase directly, the change is called deposition.

Lapse rate



Lapse Rate is a term that refers to the rate at which temperature varies in the vertical. There are various types of Lapse Rates.

Environmental lapse rate

The environmental lapse rate is the rate at which temperature changes in the vertical in the troposphere, as observed by an upwards moving radiosonde. This varies greatly from day to day. When this lapse rate is averaged out for all places and times, it is called the Standard (or Average) Lapse Rate, which is around 3.0F/1000 ft. It's important to keep in mind that this lapse rate is determined by a vertically moving radiosonde. The air itself is not moving up or down.

Dry adiabatic lapse rate

The lapse rate that occurs in a vertically moving air parcel in which no condensation is occurring. The temperature change is related to the expansional cooling (compressional

warming) that occurs when the air moves upward (downward). It is entirely determined by the pressure distribution in the atmosphere in question. For earth's atmosphere, in the troposphere, for example, the pressure is 200 mb at the top and 1000 mb at the bottom. Thus, the dry adiabatic lapse rate is constant, 5.5F/1000 ft (1C/100m). This is known as the dry adiabatic lapse rate because no heat is added or subtracted from the moving air parcel (adiabatic) and no moisture is condensing (dry).

Wet adiabatic lapse rate

The lapse rate that occurs in a vertically moving air parcel in which condensation is occurring. For example, although an upwards moving air parcel will always experience expansional cooling as a dominant effect, a certain amount of heating offsets that cooling due to latent heat release associated with condensation. This latent heat release is dependent upon temperature and pressure, so the wet adiabatic rate is not a constant. It averages around 3.5F/1000 ft in the lower troposphere.

Adiabatic lapse rate

The atmosphere is restless, always in motion either horizontally or vertically, or both. As air rises, pressure on it decreases and in response it expands. The act of expansion to encompass its new and larger dimensions requires an expenditure of energy; since temperature is a measure of internal energy, this use of energy makes its temperature drop—this is an important point—an important process in physics (especially in air physics). This phenomenon is known as the *adiabatic lapse rate*. Simply, *adiabatic* refers to a process that occurs with or without loss of heat, especially the expansion or contraction of a gas in which a change takes place in the pressure or volume, although no heat is allowed to enter or leave. *Lapse rate* refers to the rate at which air temperature decreases with height. The normal lapse rate in stationary air is on the order of 3.5°F/1,000 ft (6.5°C/km). This value may vary with latitude and changing atmospheric conditions (e.g., seasonal changes). A parcel of air that is not immediately next to the earth's surface is sufficiently well insulated by its surroundings that either expansion or compression of the parcel may be assumed to be adiabatic.

Atmospheric stability

Stability is divided into three classes: stable, unstable, and neutral. A *stable atmosphere* is marked by air cooler at the ground than aloft, low wind speeds, and consequently, a low degree of turbulence. A plume of pollutants released into a stable lower layer of the atmosphere can remain relatively intact for long distances. Thus, we can say that stable air discourages the dispersion and dilution of pollutants. An *unstable atmosphere* is marked by a high degree of turbulence. A plume of pollutants released into an unstable atmosphere may exhibit a characteristic looping appearance produced by turbulent eddies. A *neutrally stable atmosphere* is an intermediate class between stable and unstable conditions. A plume of pollutants released into a neutral stability condition is often characterized by a coning appearance as the edges of the plume spread out in a V shape.

The importance of the state of the atmosphere and stability's effects cannot be overstated. The ease with which pollutants can disperse vertically into the atmosphere is mainly determined by the rate of change of air temperature with height (altitude). Therefore, air stability is a primary factor in determining where pollutants will travel, and how long they will remain aloft. Stable air discourages the dispersion and dilution of pollutants. Conversely, in unstable air conditions, rapid vertical mixing takes place, encouraging pollutant dispersal, which increases air quality.

Lifting process

Convection lift

In meteorology, **convection** refers primarily to atmospheric motions in the vertical direction. As the earth is heated by the sun, bubbles of hot air (called thermals) rise upward from the warm surface. An air parcel will rise naturally if the air within the parcel is warmer than the surrounding air (like a hot air balloon). Therefore, if cool air is present aloft with warm air at lower levels, thermals can rise to great heights before losing their buoyancy.

Orographic lifting

Orographic lift occurs when an air mass is forced from a low elevation to a higher elevation as it moves over rising terrain. As the air mass gains altitude it quickly cools down adiabatically,

which can raise the relative humidity to 100% and create clouds and, under the right conditions, precipitation.

Condensation

Condensation is the change of the physical state of matter from gas phase into liquid phase, and is the reverse of vapourisation. The word most often refers to the water cycle. It can also be defined as the change in the state of water vapour to liquid water when in contact with a liquid or solid surface or cloud condensation nuclei within the atmosphere. When the transition happens from the gaseous phase into the solid phase directly, the change is called deposition.

Condensation is initiated by the formation of atomic/molecular clusters of that species within its gaseous volume—like rain drop or snow flake formation within clouds—or at the contact between such gaseous phase and a liquid or solid surface. In clouds, this can be catalyzed by water-nucleating proteins, produced by atmospheric microbes, which are capable of binding gaseous or liquid water molecules.

Cloud Formation

The atmosphere is a highly complex system, and the effects of the changes in any single property tend to be transmitted to many other properties. The most profound effect on the atmosphere is the result of alternate heating and cooling of the air, which causes adjustments in relative humidity and buoyancy; they cause condensation, evaporation, and cloud formation.

The temperature structure of the atmosphere (along with other forces that propel the moist air upward) is the main force behind the form and size of clouds. Temperature (that is, heating and cooling of the surface atmosphere) causes vertical air movements. Let us take a look at what happens when air is heated. As the ground is heated, the air in contact with it will warm also. This warm air increases in temperature and expands. Remember, gases expand on heating much more than liquids or solids, so this expansion is quite marked. In addition, as the air expands, its density falls (meaning that the same mass of air now occupies a larger volume). Because of its lessened density, this parcel of air is now lighter than the surrounding air and tends to rise. Conversely, if the air cools, the opposite occurs—it contracts, its density increases, and it sinks. Actually, alternate heating and cooling are intimately linked with the process of evaporation,

condensation, and precipitation. As the surface temperature increases, heat passes to the overlying air. Later, by mid-morning, a bulbous mass of warm, moisture-laden air rises from the ground. This mass of air cools as it meets lower atmospheric pressure at higher altitudes. If cooled to its dew point temperature, condensation follows and a small cloud forms. This cloud breaks free from the heated patch of ground and drifts with the wind. If it passes over other rising air masses, it may grow in height. The cloud may encounter a mountain and be forced higher still into the air. Condensation continues as the cloud cools, and if the droplets it holds become too heavy, they fall as rain.

Fog formation

Fog is a visible aerosol consisting of tiny water droplets or ice crystals suspended in the air at or near the Earth's surface. Fog can be considered a type of low-lying cloud, usually resembling stratus, and is heavily influenced by nearby bodies of water, topography, and wind conditions. In turn, fog has affected many human activities, such as shipping, travel, and warfare. Fog forms when the difference between air temperature and dew point is less than 2.5 °C (4.5 °F) Fog begins to form when water vapor condenses into tiny liquid water droplets that are suspended in the air. Six examples of ways that water vapor is added to the air are by wind convergence into areas of upward motion; precipitation or virga falling from above; daytime heating evaporating water from the surface of oceans, water bodies, or wet land; transpiration from plants; cool or dry air moving over warmer water; and lifting air over mountains. Water vapor normally begins to condense on condensation nuclei such as dust, ice, and salt in order to form clouds. Fog, like its elevated cousin stratus, is a stable cloud deck which tends to form when a cool, stable air mass is trapped underneath a warm air mass. Fog normally occurs at a relative humidity near 100%. This occurs from either added moisture in the air, or falling ambient air temperature. However, fog can form at lower humidities, and can sometimes fail to form with relative humidity at 100%. At 100% relative humidity, the air cannot hold additional moisture, thus, the air will become supersaturated if additional moisture is added.

Formation of precipitation and its types

Formation of precipitation; thermodynamic consideration

A necessary condition to the formation of precipitation is that the air becomes saturated with water vapor. Saturation is the first step in the formation of precipitation (i.e. it is necessary but not sufficient).

Saturation is typically quantified by relative humidity. The relative humidity (RH) is defined as:

$$RH = \frac{e_a}{e_s},$$

where $a e$ is the actual water vapor pressure (say in kPa or mbars) and $s e$ is the saturation vapor pressure. Air becomes saturated if RH is 100%.

The actual vapor pressure is dependent on the water vapor concentration (or density ρ_v) of the parcel of air. These variables are related through the ideal gas law, given by

$$\rho_v = \frac{0.622 e_a}{R_d T}$$

where:

ρ_v is the water vapor density

R_d is the gas constant of dry air (=287.04 Joules kg⁻¹ K⁻¹)

T is the absolute temperature (K)

NOTE: the 0.622 = 18/29 which is the ratio of the molecular weights of water and air.

The saturation vapor pressure is defined as the pressure at which the parcel of air is saturated with water vapor. That is - you cannot add more water vapor to this parcel of air without changing its temperature.

The saturation vapor pressure varies only with temperature. The relationship is known as the Clausius-Clapeyron equation. It can be approximated by

$$e_s(kPa) = 0.611 \text{Exp} \left[\frac{17.502 T_c}{T_c + 240.91} \right]$$

where T_c is the air temperature (degrees C). The relationship between e_s and T_c is shown in Figure 1. Hence, $RH \rightarrow 100\%$ if

- 1) ρ_v increases (for a fixed temperature) or
- 2) if temperature decreases.

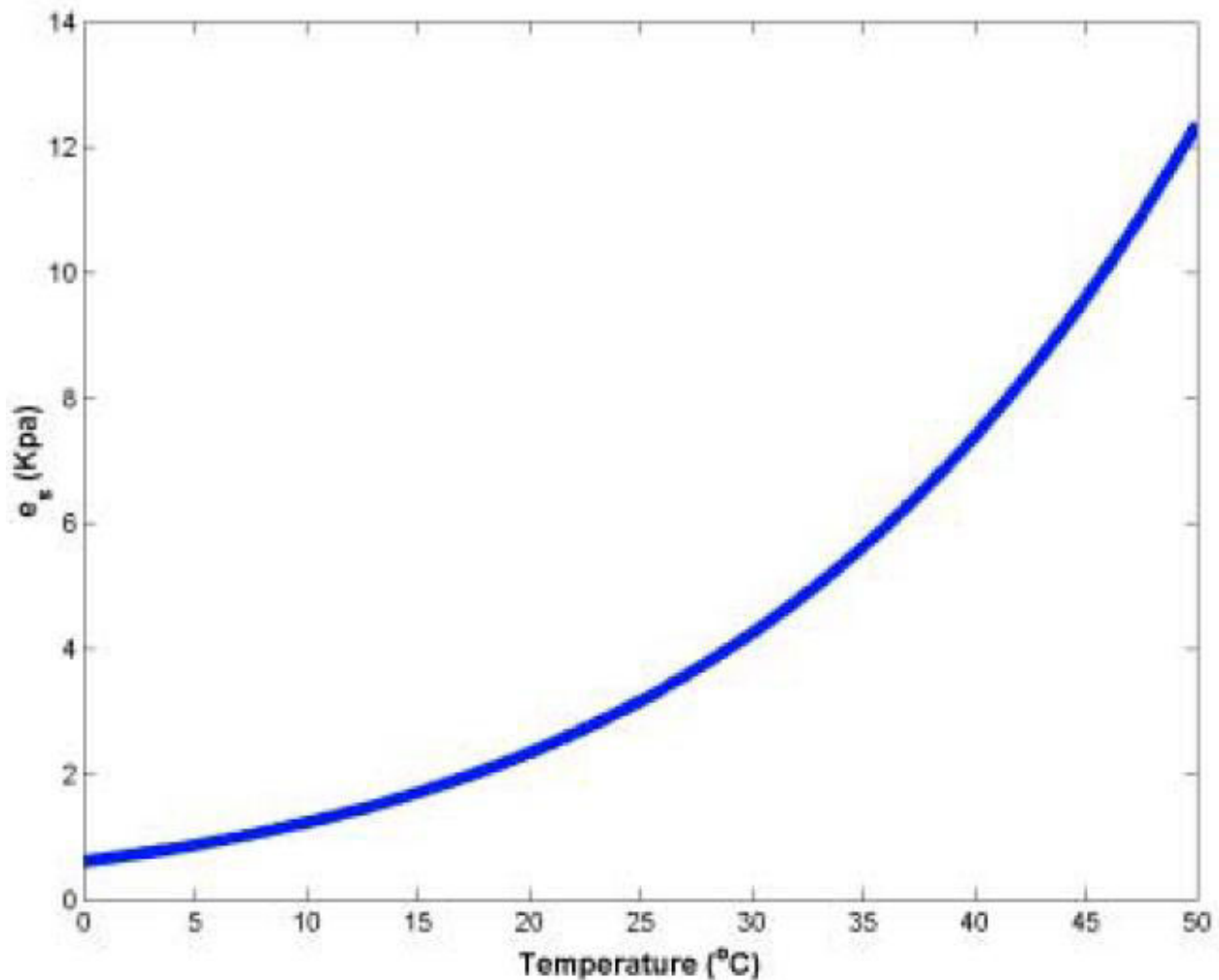


Figure 1: Exponential variation of saturation vapor pressure with air temperature.

Decreasing temperature decreases exponentially e_s (see Figure 1) thereby forcing $e_s = ea$

One key mechanism for decreasing temperature is LIFTING the parcel of air to higher elevation. As a parcel of air is lifted to higher elevations – it becomes cooler, and its e_s drops. The height or elevation at which $e_s = e_a$, clouds will form. The term LIFTING CONDENSATION LEVEL (LCL) is often used to describe this elevation or state. .

Roughly speaking, the air cools by about 10K per 1000 m (or 1 Km). This quantity is known as

the DRY ADIABATIC LAPSE RATE (Γ_d) By definition $\Gamma_d = \frac{g}{C_p}$, where g is the gravitational acceleration (=9.8 m s⁻²) and C_p is the specific heat capacity of dry air at constant pressure (=1005 Joules Kg⁻¹ K⁻¹).

As earlier stated, condensation is a NECESSARY but NOT SUFFICIENT condition to the formation of precipitation. Next, we briefly describe the remaining conditions necessary to the formation of precipitation

Condensation Nuclei: These are particles in the atmosphere of the order of 0.1 to 10 μ m. These particles originate from products of combustion, oxides of nitrogen, aerosols, salt particles, etc...

Growth of the water droplet: The saturated air tends to condense on these particles – and then water droplet grow in size, become heavier, and fall to the ground as precipitation.

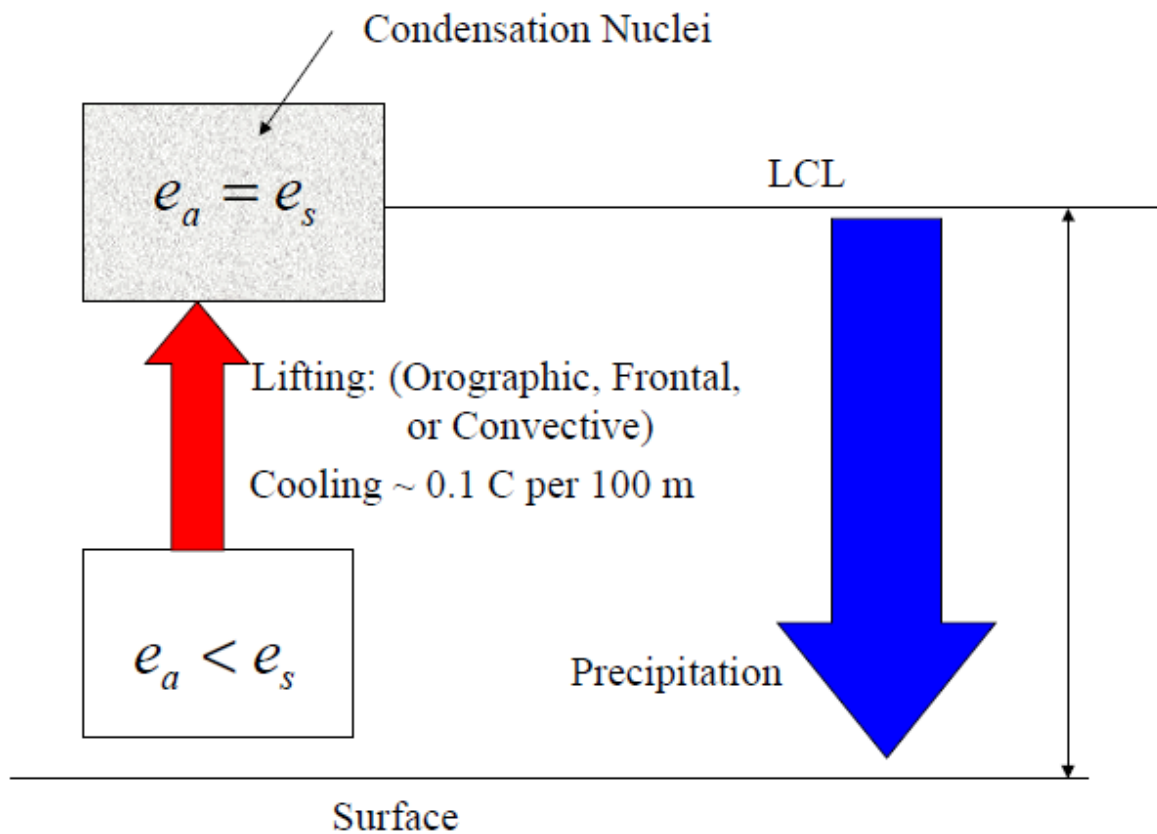


Figure 2: Summary of the key (idealized) processes leading to precipitation.

Measurement of precipitation

Instruments for measuring precipitation include rain gauges and snow gauges, and various types are manufactured according to the purpose at hand. Rain gauges are discussed below

Rain gauges are classified into recording and non-recording types. The latter include cylindrical and ordinary rain gauges, and measurement of precipitation with these types is performed manually by the observer. Some recording types such as siphon rain gauges have a built-in recorder, and the observer must physically visit the observation site to obtain data. Other types such as tipping bucket rain gauges have a recorder attached to them, and remote readings can be taken by setting a recorder at a site distant from the gauge itself to enable automatic observation.

As rain gauges measure the volume or weight of precipitation collected in a vessel with a fixed orifice diameter, the size of the orifice needs to be standardized. CIMO provides that its area

should be 200 cm² or more, and types with an orifice area of 200 to 500 cm² are widely used. In Japan, the rain gauge orifice diameter is set as 20 cm (314 cm²).

Cylindrical Rain Gauges

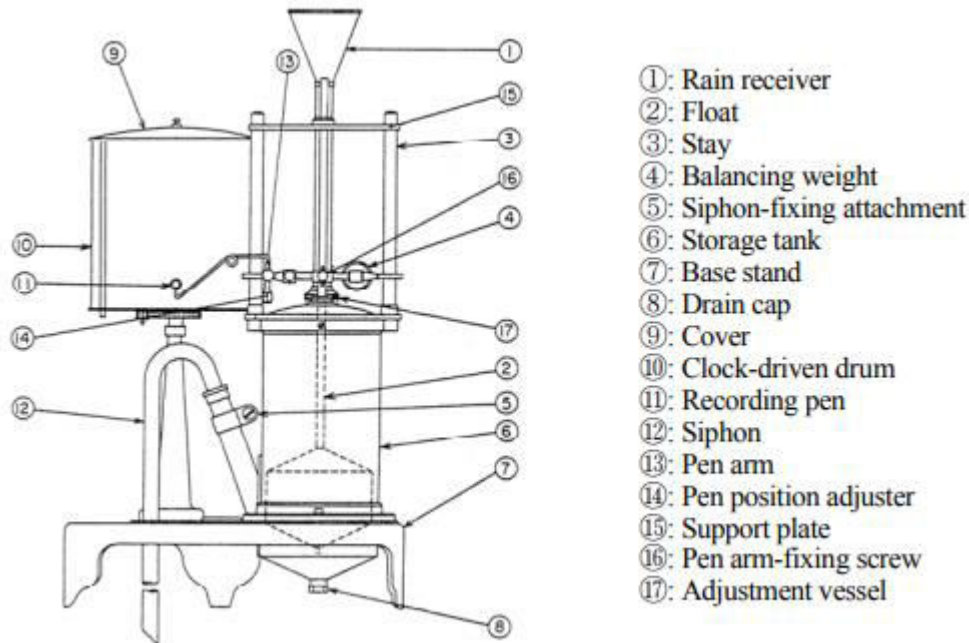
As this type of rain gauge can also be used to measure snow, it is alternatively known as a cylindrical rain/snow gauge. It consists of a cylindrical vessel with a uniform diameter from top to bottom and an orifice at the top. It does not have a funnel. Rainwater enters through the orifice and accumulates in the cylindrical vessel, which is weighed at regular intervals with a precipitation scale. As the amount of precipitation is determined by subtracting the vessel weight from the total weight, the dry vessel is weighed before observation. A rain-measuring glass may be used instead of a precipitation scale. To measure solid precipitation such as snow and hail with such a device, a known amount of warm water is added to melt the precipitation; the total amount is then measured with the measuring glass, and the amount of warm water added is subtracted from the total to obtain the precipitation amount. The precipitation scale is graduated in millimeters based on the size of the rain gauge orifice.

Ordinary Rain Gauges

Ordinary rain gauges are the type used at non-automated observatories. With such devices, the observer takes measurements using a rain-measuring glass at regular intervals. This type of rain gauge consists of a receptacle, a shell, a storage bottle, a storage vessel and a rain-measuring glass, which is a measuring cylinder graduated in precipitation amounts based on the diameter of the receptacle's orifice. The shell acts as a container for the storage bottle and the storage vessel. The storage vessel is a cylindrical metallic container that houses the storage bottle. The measuring cylinder is transparent, and is graduated in units of precipitation. Rainwater entering through the receptacle accumulates in the storage bottle, and the precipitation amount is measured with the measuring glass. Rainwater that overflows from the storage bottle enters the storage vessel. The amount of overflow is also measured with the measuring glass, and is added to the amount of precipitation in the storage bottle.

Siphon Rain Gauges

A siphon rain gauge enables automatic, continuous measurement and recording of precipitation.



Tipping Bucket Rain Gauges

This type of rain gauge generates an electric signal (i.e., a pulse) for each unit of precipitation collected, and allows automatic or remote observation with a recorder or a counter. The only requirement for the instrument connected to the rain gauge is that it must be able to count pulses. Thus, a wide selection of configurations and applications is possible for this measuring system. Solid precipitation can also be measured if a heater is set at the receptacle.

Classification of Precipitation Events:

Hence, the “mechanism” by which air is lifted is nominally used to classify the type of precipitation. Broadly speaking, there are 3 types of lifting mechanisms:

Orographic lifting: In which air is forced to go over mountains (and it’s the reason why windward slopes receive more precipitation).

Frontal surface lifting: In which warmer air is forced to go above cooler air in equilibrium with a cooler surface.

Convective Lifting: Warm air rises from a warm surface and progressively cools down.

All three mechanisms can lift air and hence result in the cooling process necessary to reduce s_e and attain $RH=100\%$.

Types of precipitation

Liquid precipitation

Drizzle

is a light liquid precipitation consisting of liquid water drops smaller than those of rain – generally smaller than 0.5 mm (0.02 in) in diameter.^[1] Drizzle is normally produced by low stratiform clouds and stratocumulus clouds. Precipitation rates from drizzle are on the order of a millimetre per day or less at the ground.

Rain

Rain is liquid water in the form of droplets that have condensed from atmospheric water vapor and then become heavy enough to fall under gravity. Rain is a major component of the water cycle and is responsible for depositing most of the fresh water on the Earth. It provides suitable conditions for many types of ecosystems, as well as water for hydroelectric power plants and crop irrigation.

Cloudburst

A **cloudburst** is an extreme amount of precipitation in a short period of time,^[1] sometimes accompanied by hail and thunder, which is capable of creating flood conditions. A cloudburst can suddenly dump large amounts of water e.g. 25 mm of precipitation corresponds to 25,000 metric tons/km² (1 inch corresponds to 72,300 short tons over one square mile).

Sunshower

A **sunshower** or **sun shower** is a meteorological phenomenon in which rain falls while the sun is shining.^[1] A sunshower is usually the result of accompanying winds associated with a rain storm sometimes miles away, blowing the airborne raindrops into an area where there are no clouds, therefore causing a sunshower. Sometimes a sunshower is created when a single rain cloud

passes overhead, and the Sun's angle keeps the sunlight from being obstructed by overhead clouds.

Freezing precipitation:

Freezing drizzle

Freezing drizzle is drizzle that freezes on contact with the ground or an object at or near the surface

Freezing rain

Freezing rain is the name given to rain maintained at temperatures below freezing by the ambient air mass that causes freezing on contact with surfaces. Unlike a mixture of rain and snow, ice pellets, or hail, freezing rain is made entirely of liquid droplets. The raindrops become supercooled while passing through a sub-freezing layer of air hundreds of meters above the ground, and then freeze upon impact with any surface they encounter, including the ground, trees, electrical wires, aircraft, and automobiles.^[1] The resulting ice, called glaze ice, can accumulate to a thickness of several centimeters and cover all exposed surfaces

Frozen precipitation:

Snow

refers to forms of ice crystals that precipitate from the atmosphere (usually from clouds) and undergo changes on the Earth's surface.^[2] It pertains to frozen crystalline water throughout its life cycle, starting when, under suitable conditions, the ice crystals form in the atmosphere, increase to millimeter size, precipitate and accumulate on surfaces, then metamorphose in place, and ultimately melt, slide or sublimate away. Snowstorms organize and develop by feeding on sources of atmospheric moisture and cold air.

Hail

Hail is a form of solid precipitation. It is distinct from ice pellets (American English "sleet"), though the two are often confused.^[1] It consists of balls or irregular lumps of ice, each of which

is called a **hailstone**. Ice pellets fall generally in cold weather while hail growth is greatly inhibited during cold surface temperatures.^[2]

Graupel

also called **soft hail** or **snow pellets**,^[1] is precipitation that forms when supercooled water droplets are collected and freeze on falling snowflakes, forming 2–5 mm (0.08–0.20 in) balls of rime. The term *graupel* comes from the German language.

UNIT - 3

Weight of air is known as air pressure. Air is a composition of various gases therefore it has specific weight. Weight of air on any unit of area on Earth is known as air pressure while it is represented in Millibar unit. Air expands in summer due to high temperature and in winter it shrinks due to low temperature.

High temperature causes scanty air and less air pressure while low temperature brings thick air and higher air pressure. Thus difference between air pressures creates air movement from high pressure areas to low pressure areas which is known as wind. Temperature and Air pressure cause expansion and shrinking of air which further results into distribution of heat and moisture in the atmosphere. In normal circumstance average air pressure at sea level is 1013.2 milibar. Instrument used to measure air pressure is known as Barometer.

Factors Affecting Air Pressure:

1. Temperature:

As the temperature increases, air expands because of which its density decreases which results in low pressure. On the other hand air shrinks due to low temperature because of which its density increases which creates high pressure. The relation between air pressure and temperature is defined with following quote- **“When the mercury of thermometer rises, mercury of barometer falls”**. Equatorial regions have low pressure because of high temperatures. On the other hand Polar regions have high pressure due to low temperature.

2. Height from Sea Level:

Air pressure is created due to weight of air therefore sea level has highest air pressure. As we move upward from sea level leaving behind the heavy gases at lower layers of atmosphere, air pressure decreases because the upper air is light and its density is low. There is no fixed rate of fall in air pressure with increase in height but it decreases with increase in height. Air pressure is reduced to half at the height of 5 Kms from seal level and at the height of 11 kms it is reduces to one fourth. It is because of low pressure in mountainous regions that breathing gets hard.

3. - Moisture in Air (Humidity):

Conversion of water from liquid state to gaseous state because of evaporation is known as atmospheric humidity. Water vapours are light in weight therefore they rise up and pressure of humid air decreases as compared to dry air. Amount of water vapours changes with time and place and because of this the pressure of air also varies.

4. Gravitation of Earth:

Atmosphere glues around the Earth due to its gravitation. The intensity of gravitational pull decreases as we get away from core of Earth. Another fact is that as Earth rotates round its axis, average distance of Polar Regions and equatorial regions varies from the core of Earth. For example Polar Regions are nearer to core of the Earth as compared to Equatorial regions and hence have higher air pressure.

5. Rotation of Earth:

Rotation of Earth produces centrifugal force which has more effect in Equatorial region while lesser effect on Polar regions. Centrifugal force Pushes things away from its core. Same is the effect on air pressure which results into lesser pressure in Equatorial regions as compared to that in polar regions.

Measurement of air pressure

For a long time, atmospheric pressure has been measured by a mercury barometer. The first was invented in 1643 by one of [Galileo's](#) assistants. A mercurial barometer has a section of mercury exposed to the atmosphere. The atmosphere pushes downward on the mercury (see image). If there is an increase in pressure, it forces the mercury to rise inside the glass tube and a higher measurement is shown. If atmospheric [pressure](#) lessens, downward force on the mercury lessens and the height of the mercury inside the tube lowers. A lower measurement would be shown. This type of instrument can be used in a lab or a weather station, but is not easy to move! Measurements from a mercury barometer are usually made in inches of Mercury (in Hg).

An aneroid barometer can be used in place of a mercury barometer. It is easier to move and is often easier to read. This instrument contains sealed wafers that shrink or spread out depending

on changes of atmospheric pressure. If atmospheric pressure is higher, the wafers will be squished together. If atmospheric pressure lessens, it allows the wafers to grow bigger. The changes in the wafers move a mechanical arm that shows higher or lower air pressure

Either a mercury barometer or an aneroid barometer can be set up to make constant measurements of atmospheric pressure. Then it is called a barograph. The barograph may constantly record pressure on paper or foil wrapped around a drum that makes one turn per day, per week, or per month. Nowadays, many mechanical weather instruments have been replaced by electronic instruments that record atmospheric pressure onto a computer.

Atmospheric pressure can be recorded and reported in *many* different units. This can get a little confusing! As mentioned, a mercury barometer makes measurements in inches of Mercury (in Hg). Pounds per square inch (abbreviated as p.s.i.) is common in the English system of units, and the pascal (abbreviated Pa) is the standard in the Metric (SI) system. Since the pressure exerted by [Earth's atmosphere](#) is of great importance, pressure is sometimes expressed in terms of "atmospheres" (abbreviated atm). In weather, the bar and millibar (mb) describe pressure. You'll often hear millibar used by meteorologists when describing low or high pressure [weather](#) systems.

n summary, at sea level when it is 0°C,

atmosphere = 29.92 in Hg = 14.7 psi = 101,325 Pa = 1,013.25 mb = 1.013 bar

Coriolis effect

The **Coriolis effect** is most apparent in the path of an object moving longitudinally. On the Earth an object that moves along a north-south path, or longitudinal line, will undergo apparent deflection to the right in the Northern Hemisphere and to the left in the Southern Hemisphere.

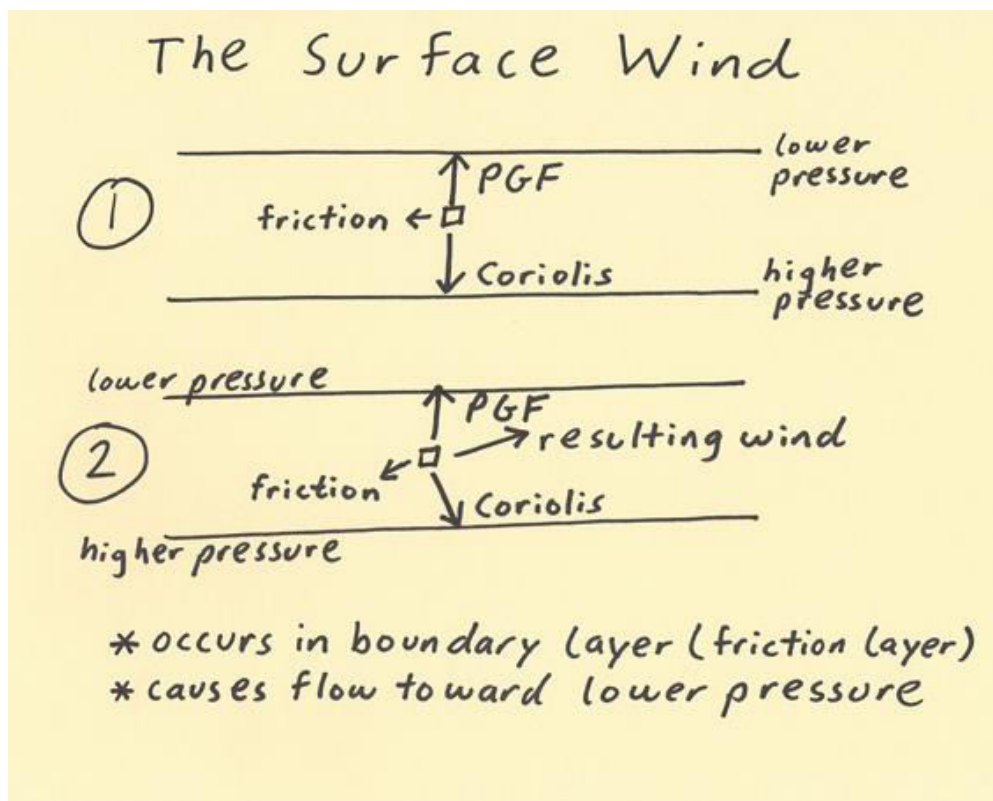
Surface wind

Surface wind is the wind blowing near the Earth's surface. It is measured by an anemometer (speed) or wind vane (wind direction) at a standard height of 10 m above ground in an area

where the distance between the instrument and any obstruction is at least 10 times the height of the obstruction. This distance is known as **fetch** and is kept in order to avoid the influence of eddies.

The surface wind is the balance of forces on the wind that occurs at and near the Earth's surface. The contrast to the geostrophic wind is that the surface wind introduces the force of friction. In the diagram below labeled (1) we start with geostrophic balance and introduce friction. Friction is a force that slows the wind and this is why the friction vector is in the opposite direction to the resulting wind labeled on (2).

Hence friction slows the wind it causes a reduction in the Coriolis force since the magnitude of the Coriolis force is directly related to the wind speed. Although the Coriolis force decreases, the Pressure Gradient Force (PGF) stays the same. This results in an imbalance between the Coriolis and Pressure Gradient Force. The PGF has a greater magnitude as compared to Coriolis. This results in the wind crossing the isobars at an angle from higher pressure toward lower pressure. In the diagram (2), it shows the balance of the forces between Coriolis, friction and PGF along with the resulting wind.



Vertical air movement

The density of air is the main factor that determines whether air rises or sinks. Warm air is less dense than cooler air because the air molecules are spread out more. Think of a hot air balloon. They can rise because air is heated inside the balloon. A **parcel of air** is a significant amount of air, but not so large that the properties of the air are inconsistent within it. When a warm air parcel rises, it cools in the upper part of the troposphere, which is the layer of the atmosphere where weather occurs. When the air cools, the water vapor in it condenses into water droplets that form clouds. Enough cloud formation can lead to precipitation and even to stormy weather. This is the typical pattern for a **low pressure cell**.

Scale of motion

Weather phenomena are analyzed at a variety of scales of motion. Four scales of motion that will be focused on in this writing from largest to smallest land area are the global scale, synoptic scale, mesoscale and microscale.

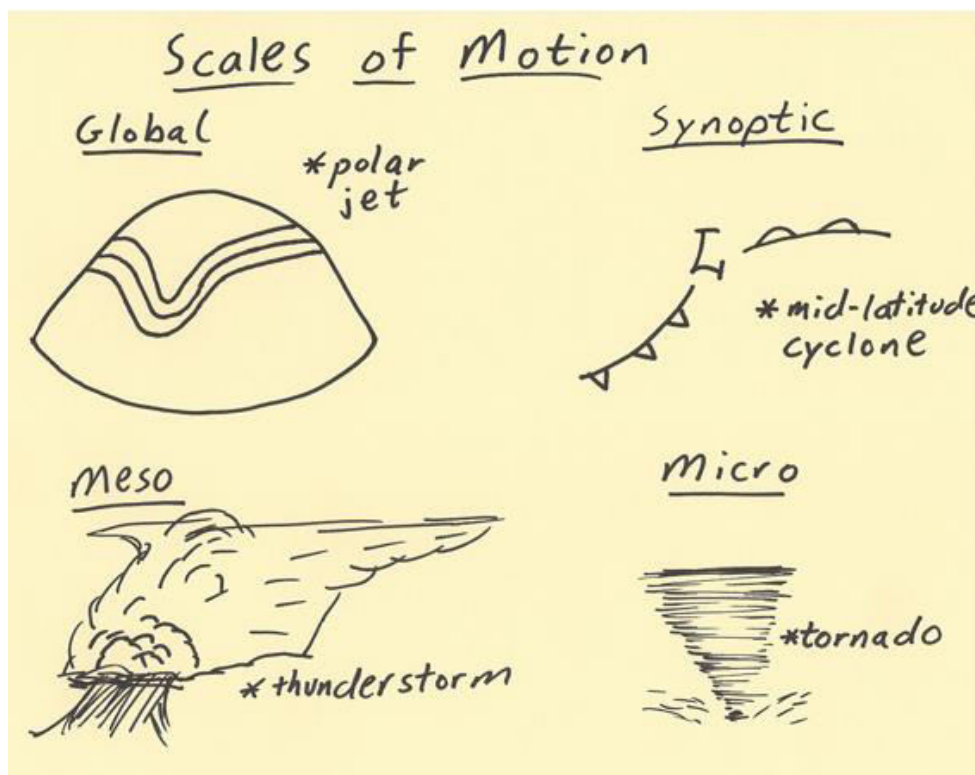
The global scale includes events that impact large areas of the globe and last for weeks and even months at a time. Features such as the polar jet stream can be found just about any time somewhere. The polar jet stream is an example of a global scale phenomenon. Its influence circles the globe and influences the polar and middle latitudes with varying extent throughout the year. Another example of a global scale phenomenon is the position of subtropical highs. The position and strength of subtropical highs can influence weather across the globe.

The next scale is the synoptic scale. Phenomena on the synoptic scale can span over 1000s of kilometers and last for many days. Mid-latitude cyclones, hurricanes, and fronts are examples of synoptic weather events. A weather forecaster looks closely at the global scale and synoptic scale when making weather forecasts beyond 1 day out.

The mesoscale is the next scale that will be discussed. These weather phenomena typically last from an hour to a day and influence 10s to 100s of kilometers of distance. Examples of mesoscale weather events include thunderstorms (especially complexes of thunderstorms such as MCCs and squall lines), differential heating boundaries (i.e. sea breeze), and mesolows. A weather forecaster will integrate an increasing amount of mesoscale analyses into their

forecasting technique when making short term forecasts such as over the next several hours to 1 day.

The last scale of motion that will be mentioned is the microscale. These events occur typically from minutes up to an hour and cover small distances such as less than 10 kilometers. Examples of microscale phenomena include tornadoes, rainbows, convective updrafts, and downdrafts. This scale is important since it is the scale most experienced with the eyes in-person. These are the weather events that are witnessed when going outside.



Local winds

Local winds occur on a small spatial scale, their horizontal dimensions typically several tens to a few hundreds of kilometres. They also tend to be short-lived lasting typically several hours to a day. There are many such winds around the world, some of them cold, some warm, some wet, some dry. There are many hazards associated with the winds.

The main types of local winds are: Sea breezes and land breezes, Anabatic and katabatic winds, and Foehn winds.

Sea and land breezes

Sea breezes and land breezes are two familiar categories of local winds that are driven by differences in temperature and in air pressure, which is the pressure exerted by air on a given area. A sea breeze blows from the water to the shore. It comes as a welcome relief to coastal inhabitants on a hot day. A land breeze, in contrast, blows from the shore toward the water. Land breezes occur in the evening.

Sea breezes form on hot days because the land warms more rapidly than does the water. As a result, a low-pressure area develops over warm ground and a high-pressure area over the cooler water. A mild wind blows across the pressure gradient, from the high-pressure area (over the water) to the low-pressure area (over the land). At night, the process is reversed as the land loses heat more quickly than does the water. The resultant land breeze flows from the high-pressure area, over the shore, out to the low-pressure area, over the water.

Sea breezes and land breezes are strongest at the shoreline, where temperature and pressure differences are most pronounced. They lose intensity as they travel inland or out to sea. The time of day when temperature and pressure differences are greatest, and therefore the breezes are strongest, is midafternoon, when land reaches its maximum.

Monsoon circulation

Monsoons are caused by differences in solar heating between the oceans and continents, and they are most likely to form where a large continental land mass meets a major [ocean basin](#). During the early summer, the increasing solar [energy](#) heats up the land surfaces fairly quickly. [Water](#), on the other hand, heats much more slowly in response to the sun. This is one reason why we cool off by swimming in lakes during the summer—the water is still chilled from the recent winter and takes much of the summer to warm up. The enormous quantity of water in the oceans guarantees they will remain cooler than the nearby continents during the early summer. The relatively warm land surface will [heat](#) the air over it, causing it to rise, or convect. The [convection](#) of warm air produces an area of low [pressure](#) near the land surface. Meanwhile,

the air over the cooler [ocean](#) will be more dense and tend to stay at the surface or sink downwards from aloft. Thus during the summer, oceanic air flows onshore toward the low pressure over land. This onshore flow is continually supplied by cooler oceanic air sinking from higher levels in the atmosphere. In the upper atmosphere, the rising continental air is drawn outward over the oceans to replace the sinking oceanic air, thus completing the cycle. In this way a large vertical circulation cell is set up, driven by solar heating. At the surface, the result is a constant wind flowing from sea to land.

The oceanic air moving onto the land is usually quite humid, due to its prolonged contact with the sea surface. As it flows on shore the moist marine air is pulled upward as part of the convecting half of the circulation cell. The rising air cools and eventually forms rain [clouds](#). Rain clouds are especially likely when the continental areas have higher elevations ([mountains](#), plateaus, etc.), because the humid sea air is forced upward over these barriers, causing widespread cloud formation and heavy rains. This is the reason why the summer monsoon forms the rainy season in many tropical areas.

In the late fall and early winter, the situation is reversed. Land surfaces cool off quickly in response to cooler weather, but the same property of water that makes it slow to absorb heat, called [heat capacity](#), also causes it to cool slowly. As a result, continents are usually cooler than the oceans surrounding them during the winter. This sets up a new circulation in the reverse direction: air over the sea, now warmer than that over the land, rises and is replaced by winds flowing off the [continent](#). The continental winds are supplied by cooler air sinking from aloft. At upper atmospheric levels the rising oceanic air moves over the land to replace the sinking continental air. Sinking air prevents the development of clouds and rain, so during the winter monsoon continental areas are typically very dry. This winter circulation causes a prevailing land to sea wind until it collapses with the coming of spring.

Wind and Ocean Currents

Global winds and ocean currents are responsible for distributing global heat, which directly affects continental climates. To understand how these currents form, a knowledge of the impacts of Earth's motion is necessary.

- The earth rotates on an axis at 23.5 degrees. The axis slowly wobbles and may tilt anywhere from 22.1° to 24.5° throughout a cycle of 40,000 years.
- Due to the tilt and position when the earth revolves around the sun, solar radiation strikes the earth at varying intensities, creating differences in temperature. These different temperatures form a pattern for climates and air/water circulation according to latitude (the degree distance north and south from the equator to poles, not east to west).
- The atmosphere has mass. Depending on different air densities that are influenced by hot and cold temperatures, the atmosphere will either sink to Earth's surface or rise further into the atmosphere. The hot and cold temperatures at specific latitudes are due to uneven solar radiation.
- Friction between the atmosphere and Earth's surface causes the air to be dragged as the earth rotates. The colder air is denser and sinks to Earth's surface, causing it to drag faster than aloft warm air in the atmosphere.
- The resulting rotations in the atmosphere, known as the Coriolis effect, create wind currents. Like the atmosphere, ocean water is also dragged counterclockwise while Earth rotates. Earth's rotation and wind currents influence oceans, forming ocean currents.

Global Winds

Global winds are strong winds that always flow in the depicted pattern because of the earth's rotation. Within the region from the equator (0° latitudes) to 30° N and 30° S, these strong global wind currents are called the Westerlies. Wind direction is always named according to the direction from which it comes. Therefore, wind flowing from the west is a westerly wind. The Trade Winds, named for supplying trade ships with a fast and steady wind to sail around the globe, flow from the east between latitudes 30° and 60° N and 30° and 60° S. Lastly, the Polar Easterlies flow from the east at each pole. Notice that the airflow rotates circularly where opposing wind directions converge. In the Northern Hemisphere the circulation is clockwise, and the Southern Hemisphere is counterclockwise. The same pattern of circulation exists in oceans.

Ocean Currents

Like air currents in the Northern Hemisphere, the ocean currents of the Northern Hemisphere are also clockwise. The opposite is true for the Southern Hemisphere in which ocean currents circulate counterclockwise. The warm water that builds along the equator is distributed through

these ocean circulations to latitudes further north or south, warming the climates of adjacent continents.

Global Ocean Conveyor Belt

Ocean currents circulate the same way that the atmosphere circulates, horizontally around the globe, and vertically from ocean depths to the surface. Water moves up and down in the ocean due to temperature differences, just as it does in the air. Warm water will rise towards the surface and colder; denser water will sink to lower ocean depths. In addition to temperature, salinity (how much salt is in the water) will add to the density differences. Salt increases the mass per unit of water; therefore, the saltier the water is, the denser it becomes. These enormous movements of ocean water, vertically and horizontally, forms a giant water circulation system that distributes cold and warm water across the globe. This deep-ocean circulation, driven by salinity and temperature, is known as the "global ocean conveyor belt."

UNIT - 4

OCEAN HEAT BUDGET

Ocean temperature varies from place to place and time to time.

- Increase in ocean temperature should be due to an advection of warm water, or an increase in heat input.
- Decrease in temperature should be due to the advection of cooler water or an increase in heat loss.
- Hence the change in temperature is due to either advection or net heat input.
- The amount of heat into or out through the ocean surface per unit area per unit time is called as heat flux.
- Unit of heat flux is Wm^{-2} .

Heat budget

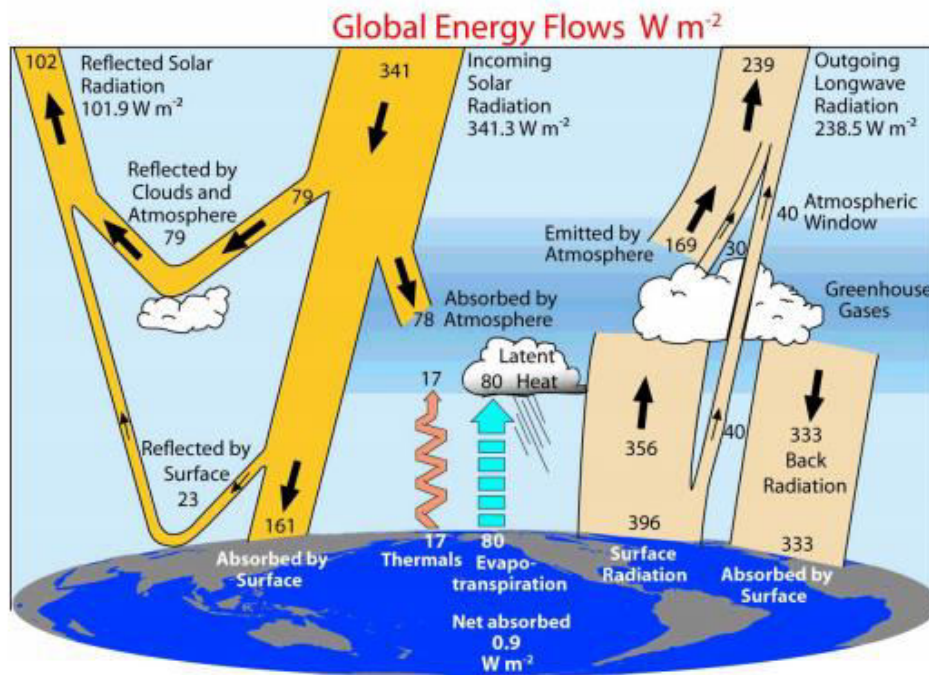
- Heat flux occurs due to
 1. Input of solar energy to ocean (shortwave radiation) (Q_s)
 2. Net heat loss by ocean as longwave radiation to atmosphere or space (back radiation) (Q_b)
 3. Heat loss/gain by evaporation/condensation (latent heat flux) (Q_e)
 4. Heat loss/gain due to conduction with atmosphere (Q_h)
 5. Heat gain/loss due to currents (Q_v)
- Calculations of heat fluxes are referred to as 'heat budget' studies
- Heat fluxes are computed as daily, monthly or yearly averages
- Other source of heat such as heat from earth's interior, change in kinetic energy to heat, heat from chemical reactions etc are very small and neglected.
- Heat gain terms are positive and heat loss terms are negative. Heat budget is computed as the sum of heat gain and heat loss terms.

$$Q_T = Q_s + Q_b + Q_e + Q_h + Q_v$$

where Q_T is the net heat gain or loss of the water.

- If the temperature of the water is not changing then QT is constant. The individual fluxes may vary.
- If the heat budget for the global ocean is done, then QT = 0.

Annual Global mean Heat balance



Heat Budget Terms

(1) Short-wave Radiation (Qs)

Radiation laws

- According to Stefan's law, all body radiate energy at a rate proportional to the fourth power of their absolute temperature.
- The energy is in the form of electromagnetic radiation with a range of wavelengths.
- But the concentration of energy is not the same at all wavelengths but has a peak at a particular wavelength given by Wien's law

$$\lambda_{max} = \frac{2897}{T}$$

- Sun has a surface temperature of about 6000K and radiate energy proportional to the fourth power of its temperature.

- According to Wien's law,

$$\lambda_{\max} = 0.5\mu\text{m}$$

- 90% of energy is contained in wavelengths shorter than 4 μm and 50% of energy is in the visible part (0.3 to 0.7 μm) which is less than that for earth's radiation. Hence solar radiation is called short wave radiation.

Computation of Shortwave radiation

- Length of the day (varies with season and latitude)
- Absorption in the atmosphere due to gases, dust, water vapour etc.
- Daily mean shortwave radiation assuming average atmospheric absorption and no clouds.
- Highest values occur at about 30 degree latitude during summer.
- No radiation at higher latitudes during polar winter.
- Southern hemisphere receive more radiation than northern hemisphere.
- Clouds reduce the amount of radiation by reflection, absorption and scattering. Hence multiply the cloud-free radiation with a value called as cloud factor.

$$Q_s = Q_{s0}(1 - 0.0012C^3)$$

(2) Long-wave Back Radiation (Qb)

Computation of Longwave Radiation

- Earth (land and ocean) emit radiation proportional to its temperature.
- Emission occurs from the top few millimeters of sea. • The λ_{\max} for earth is 10 μm which is in the infra-red band of the spectrum.
- 90% of earth's radiation is in the region 3 to 80 μm and is hence called as long-wave radiation as compared to that of sun.
- Qb represent the net longwave radiation (energy lost by sea as longwave (negative) minus energy received by sea from atmosphere (positive)). Since sea emission is always greater than that of the atmosphere, this term is always negative.

- Q_b depends on sea temperature (sea surface long-wave radiation) and the water vapour content (humidity) above the sea (atmospheric longwave radiation).

(3) Latent Heat flux

Computation of Latent Heat flux

Heat loss due to evaporation.

Evaporation requires energy that is taken from the ocean itself and hence ocean loses heat.

Latent heat is estimated using Bulk formula as

$$Q_e = -\rho_e C_e U (q_s - q_a)$$

(4) Sensible Heat (Heat conduction) (Q_h)

- Heat conducted between ocean and atmosphere due to conduction.
- If sea is warmer, then heat is transferred from ocean to atmosphere and vice versa.
- Bulk formula

$$Q_h = -\rho C_p C_h U (T_s - T_a)$$

Bulk Method for Computation of Fluxes (Refer the following):

JOURNAL OF GEOPHYSICAL RESEARCH, VOL. 101, NO. C2, PAGES 3747-3764, FEBRUARY 15, 1996 Bulk parameterization of air-sea fluxes for Tropical Ocean Global Atmosphere Coupled-Ocean Atmosphere Response Experiment C. W. Fairall, • E. F. Bradley, • D. P. Rogers, 3 J. B. Edson, 4 and G. S. Young.

Dominant Forces for Ocean Dynamics

Gravity

Pressure

- ◇ Buoyancy Friction
- ◇ Wind, bottom, shear currents inertial forces
- ◇ Coriolis, centrifugal force

Terminology for describing the flow in the ocean

- General Circulation.
- Abyssal Deep (thermohaline circulation)
- Wind-Driven Circulation
- Gyres (mainly clockwise/anticlockwise in the North/south hemisphere)
- Boundary Currents : western and eastern currents flowing parallel to coasts
- Squirts or Jets are long narrow currents
- Mesoscale Eddies (current instability, topographically trapped)

Waves in the ocean

- Planetary Waves depend on the rotation of the earth for a restoring force
- Surface Waves sometimes called gravity waves and wind waves. The restoring force is due to the large density contrast between air and water at the sea surface.
- Internal Waves are subsea wave similar in some respects to surface waves. The restoring force is due to change in density with depth.
- Tsunamis are surface waves with periods near 15 minutes generated by earthquakes.
- Tidal Currents (waves) are horizontal currents and currents associated with internal waves driven by the tidal potential.
- Edge Waves are surface waves with periods of a few minutes confined to shallow regions near shore. The amplitude of the waves drops off exponentially with distance from shore.

EQUATION OF MOTION (Refer the following)



Air-Sea Interaction and Surface Waves

Peter A.E.M. Janssen, Øyvind Breivik,
Kristian Mogensen, Frédéric Vitart,
Magdalena Balmaseda, Jean-Raymond
Bidlot, Sarah Keeley, Martin Leutbecher,
Linus Magnusson, and Franco Molteni.

Research Department

November 2013

This paper has not been published and should be regarded as an Internal Report from ECMWF.

Permission to quote from it should be obtained from the ECMWF.



European Centre for Medium-Range Weather Forecasts
Europäisches Zentrum für mittelfristige Wettervorhersage
Centre européen pour les prévisions météorologiques à moyen terme

Series: ECMWF Technical Memoranda

A full list of ECMWF Publications can be found on our web site under:

<http://www.ecmwf.int/publications/>

Contact: library@ecmwf.int

©Copyright 2013

European Centre for Medium-Range Weather Forecasts
Shinfield Park, Reading, RG2 9AX, England

Literary and scientific copyrights belong to ECMWF and are reserved in all countries. This publication is not to be reprinted or translated in whole or in part without the written permission of the Director-General. Appropriate non-commercial use will normally be granted under the condition that reference is made to ECMWF.

The information within this publication is given in good faith and considered to be true, but ECMWF accepts no liability for error, omission and for loss or damage arising from its use.

1 Introduction

Presently we are developing a coupled earth system model that allows for efficient, sequential interaction of the ocean/sea-ice, atmosphere and ocean waves components, and, therefore it becomes feasible to introduce sea state effects on the upper ocean mixing and dynamics (Mogensen *et al.*, 2012). By the end of 2013, a first version of this system will be introduced in operations in the medium-range/monthly ensemble forecasting system. The main purpose of this operational change is that coupling between atmosphere and ocean is switched on from initial time, rather than from day 9-10 in the forecast. This version will also include a number of changes to the air-sea interaction that explicitly use information on the sea state from the wave model. These changes will be described in this report. In the mean time, work is in progress to introduce the sea-ice component in the forecasting and assimilation system while also a considerable amount of effort is devoted to the development of a weakly coupled data assimilation system. A first prototype of such a weakly coupled system is near completion and will be thoroughly tested in the context of the reanalysis effort.

Ocean waves represent the interface between the ocean and the atmosphere, the two most important systems governing the dynamics of weather, climate and global change. A realistic description of the physical processes occurring at the ocean-atmosphere interface is essential for a reliable determination of the air-sea fluxes of momentum, sensible and latent heat, CO_2 and other trace gases, and aerosols. It is known that the wave field is intimately involved in these exchange processes, and, therefore, wave models are needed to compute not only the wave spectrum, but also the processes at the air-sea interface that govern the fluxes across the interface.

In the context of these ideas, a wave prediction system, called the WAM model, was developed that determines the sea state dependence of the air-sea fluxes (Komen *et al.*, 1994). As a first step, the study of the two-way interaction between ocean waves and atmospheric circulation was undertaken. This interaction takes place on a relatively short time scale of a few days. Modest improvements in medium-range forecasting of waves and winds were obtained (Janssen *et al.*, 2002; Janssen, 2004) and, as a consequence, since the 29th of June 1998 ECMWF has been producing weather and ocean wave analyses and forecasts, using a coupled atmosphere, ocean-wave forecasting system. On a seasonal time scale, depending on spatial resolution, however, a more substantial impact of ocean waves on the atmospheric climate was found (Janssen and Viterbo, 1996). The next step in the development of one model for ocean and atmosphere is to study the impact of the sea state on the ocean circulation. These studies are only beginning and therefore we are, in this respect, still in an exploration phase. Nevertheless, already some promising developments may be reported.

In this paper we start with a discussion of the details of air-sea interaction, assuming that ocean waves play an important role in this interaction. Growing ocean waves play a role in the air-sea momentum and heat transfer while breaking ocean waves affect the upper ocean mixing. If the ocean model is regarded as a system that describes the evolution of the ocean circulation velocity then it will be found that there is, because of the presence of ocean waves, an additional force on the mean circulation, which is called the Stokes-Coriolis force. Furthermore, the surface stress felt by the mean circulation is the total surface stress applied by the atmosphere minus the net stress going into the waves. Finally, momentum transfer and the sea state are affected by surface currents, hence it makes sense to introduce a three-way coupling between atmosphere, ocean circulation/sea-ice and surface waves.

The programme of this paper is as follows. In §2 we briefly describe the most salient features of the role of ocean waves in air-sea interaction. Next, we indicate how sea state effects may be incorporated into large scale ocean circulation system. For reasons of economy compromises have to be made in the representation of processes such as wave-induced upper ocean mixing and the Stokes-Coriolis force. In

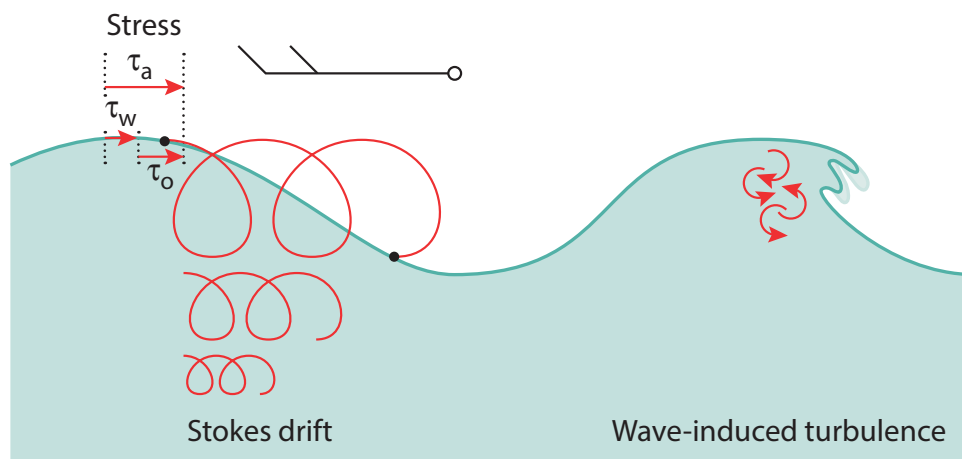


Figure 1: Wave-ocean interaction. As waves grow under the influence of the wind (left), the waves will absorb momentum which otherwise would have gone into the ocean directly. As waves break, turbulent kinetic energy is injected into the ocean mixed layer, significantly enhancing the mixing. The Stokes drift, caused by finite amplitude waves, sets up a current in the along-wave direction which decays rapidly with depth. Near the surface it may become substantial (≈ 1 m/s). The Coriolis effect works on the Stokes drift and adds a new term to the momentum equations known as the Stokes-Coriolis force.

§3 we present results of simulations with the NEMO model, which has been modified to include sea state effects on surface forcing, upper ocean mixing and including the additional Stokes-Coriolis force. Using in-situ observations we study the quality of the resulting SST fields by inspecting maps of systematic error and the standard deviation of error. The default of version 3.4 of NEMO includes sea state effects, but as there is no knowledge on the actual sea state it is assumed that the sea state is in equilibrium with the wind (in the field of ocean waves this is called 'old' windsea) and the energy flux due to breaking waves is a simple function of the friction velocity. Results with this version of NEMO are referred to as the control (CTRL). We assess the impact of sea state effects on the twenty year climate of the ocean circulation by comparing with CTRL, and typically differences of ± 1.5 -2 °K in SST have been found, which are fairly substantial. We also try to assess whether these differences at the surface result in changes to the deep circulation. After studying results with NEMO in forced mode, we continue in §4 with presenting results from fully coupled integrations on the seasonal timescale, where we concentrate on aspects of model drift and possible impact on predictability.

In the present operational medium-range/monthly ensemble forecasting system (ENS) the ocean becomes dynamically active from day 10 and onwards. First results using the new version of NEMO from day 0 in the ensemble prediction system and in the monthly system are presented in §5. Coupling from day 0 results in substantial improvements in probabilistic skill of ENS and in predicting the MJO. Finally, it is well-known that during the generation of hurricanes there is a strong interaction between ocean and atmosphere. ENS was run for a number of special cases, and, in particular for slowly moving hurricanes a beneficial impact on the deepening of a low is found.

A summary of conclusions will be presented in §6.

2 Sea state effects

Over the past 40 years a considerable amount of research has been devoted to investigate the role of ocean waves in air-sea interaction. Important contributions to be mentioned are the pioneering work of Hasselmann (1971) on what is nowadays called the Stokes-Coriolis force, the thought-provoking work of McWilliams and Restrepo (1999) on the wave-driven ocean circulation and the courageous efforts by Craig and Banner (1994) on upper ocean mixing by wave breaking. In this Section we briefly discuss a number of sea state related processes that are thought to be important in the interaction between ocean and atmosphere. A pictorial view of the relevant processes is shown in Fig. 1.

Before we discuss some of the mathematical details of the processes involved it is important to realize that ocean waves give rise to transport of momentum. Therefore one needs to separate the contribution of the ocean waves from the total transport as an ocean model gives the evolution of the ocean circulation only. As a consequence, in a rotating ocean the ocean waves exert a wave-induced stress on the mean ocean circulation which results in a force equal to $\mathbf{u}_s \times \mathbf{f}$, where \mathbf{f} is the Coriolis parameter, and \mathbf{u}_s equals the Stokes drift. This additional force may have impact on the Ekman turning of the surface current. Secondly, the surface stress felt by the ocean circulation is the atmospheric stress minus the net stress going into the waves. Therefore, when waves are growing, momentum and energy is spent in growth which is not available for forcing the mean circulation while in the opposite case of a decaying sea state more momentum is available for forcing the ocean. Only when the sea state is in equilibrium the ocean is forced by the atmospheric stress, but in practice an equilibrium sea state is a fairly rare event. We will refer to this as sea-state dependent forcing.

Thirdly, starting with the work of Craig and Banner (1994) it is well-known that breaking ocean waves affect mixing of ocean current and temperature by enhancing turbulence in the upper ocean. The energy flux by surface wave breaking affects the upper-ocean mixing up to a depth of the order of the wave height. Transport to the deeper layers of the ocean is possible because work against the shear in the Stokes drift generates Langmuir cells and wave-induced turbulence which have a penetration depth of the order of the typical wavelength of the wave field (see e.g. Grant and Belcher, 2009).

In the following §'s some of the mathematical details of the sea state dependent processes will be given. For example, we have to give a clear distinction between wave momentum and momentum for the ocean circulation and we have to work out the consequences of this separation for the momentum budget of the ocean. This separation has consequences for how the ocean is being forced and it introduces the Stokes-Coriolis force. We also have to explain how effects of breaking ocean waves are introduced in upper-ocean mixing. A brief summary of this development is offered in §2.3.

2.1 Conservation of total mass and momentum

In order to understand better why one needs to include the Stokes-Coriolis forcing and why the mean ocean circulation is forced by the sea-state dependent stress, we need to study the conservation laws for total column mass and momentum in the presence of ocean waves. For a similar discussion see Janssen (2004).

Consider an incompressible fluid (water) in a constant gravitational field on a rotating earth. Let the body of water with air above it be of infinite extent in the horizontal while in the vertical it extends from $z = -D$ (with D the water depth) to $z = \eta$, with $\eta(x, y, t)$ the unknown surface elevation. Let us assume

that the water motion is governed by the continuity equation

$$\frac{\partial}{\partial t} \rho + \nabla \cdot (\rho \mathbf{u}) = 0. \quad (1)$$

and the momentum equation

$$\frac{\partial}{\partial t} \rho \mathbf{u} + \nabla \cdot \rho \mathbf{u} \mathbf{u} = -\nabla p + \rho \mathbf{g} + \rho \mathbf{u} \times \mathbf{f}. \quad (2)$$

These equations apply to the domain $-D < z < \eta$ and the boundary conditions are

$$z = \eta(x, y, t) : \frac{\partial}{\partial t} \eta + \mathbf{u} \cdot \nabla_h \eta = w, \quad p = p_a, \quad (3)$$

where p_a is the given air pressure at the sea surface and $\nabla_h = (\partial/\partial x, \partial/\partial y)$ is the horizontal gradient operator. At the flat bottom $D = D_0$ we impose the condition that no fluid penetrates the bottom

$$z = -D : w = 0. \quad (4)$$

Following Longuet-Higgins and Stewart (1961), Whitham (1962), and Phillips (1977) conservation laws for the mean surface elevation ζ and the mean horizontal velocity \mathbf{U} may now be obtained by integration of the continuity equation and the momentum equation over the depth of the water, followed by a suitable ensemble averaging. The ensemble average $\langle \cdot \rangle$ is supposed to filter the linear gravity wave motion. Here, the mean surface elevation ζ is defined as

$$\zeta = \langle \eta \rangle, \quad (5)$$

while the mean horizontal velocity \mathbf{U} follows from

$$\mathbf{U} = \frac{\mathbf{P}}{\rho h}, \quad (6)$$

with $h = D + \zeta$ the slowly varying water depth. Note that \mathbf{P} is the *total* mass flux

$$\mathbf{P} = \left\langle \int_{-D}^{\eta} dz \rho \mathbf{u} \right\rangle, \quad (7)$$

i.e., it consists of the sum of the water column mean \mathbf{P}^m and the surface layer mean \mathbf{P}^w , defined as (Hasselmann, 1971)

$$\mathbf{P}^m = \left\langle \int_{-D}^{\zeta} dz \rho \mathbf{u} \right\rangle, \quad \mathbf{P}^w = \left\langle \int_{\zeta}^{\eta} dz \rho \mathbf{u} \right\rangle. \quad (8)$$

In the linear approximation the surface layer mean mass flux may be expressed in terms of the wave momentum

$$\mathbf{P}^w = \rho g \int d\mathbf{k} \mathbf{l} F / c, \quad (9)$$

where c is the phase speed of the gravity waves and $\mathbf{l} = \mathbf{k}/k$ is a unit vector pointing in the direction of the wave propagation. As a consequence, the mean horizontal velocity \mathbf{U} is the sum of the ocean circulation velocity \mathbf{U}_c and the wave-induced drift \mathbf{U}_{surf} ,

$$\mathbf{U} = \mathbf{U}_c + \mathbf{U}_{surf}. \quad (10)$$

Note that the total momentum in the mean surface drift equals the total momentum in the Stokes drift.

The conservation laws become (Mastenbroek et al, 1993)

$$\frac{\partial}{\partial t} \zeta + \nabla_h \cdot (h\mathbf{U}) = 0, \quad (11)$$

and

$$\left(\frac{\partial}{\partial t} + \mathbf{U} \cdot \nabla_h \right) \mathbf{U} + g \nabla_h \zeta + \frac{1}{\rho} \nabla_h p_a = \mathbf{U} \times \mathbf{f} + \frac{\tau_a - \tau_b}{\rho h} - \frac{1}{\rho h} \nabla_h \cdot \mathbf{S}, \quad (12)$$

where τ_a and τ_b represent the atmospheric surface stress and the bottom stress. The radiation stress tensor \mathbf{S} represents the contribution of the wave motions to the mean horizontal flux of horizontal momentum. In terms of the wave spectrum $F(\mathbf{k})$, which gives the energy distribution of the ocean waves over wavenumber \mathbf{k} , the stress tensor is given by

$$S_{ij} = \rho g \int d\mathbf{k} \left\{ \frac{v_g}{c} l_i l_j + \left(\frac{v_g}{c} - \frac{1}{2} \right) \delta_{ij} \right\} F(\mathbf{k}). \quad (13)$$

Note that the first term corresponds to advection of wave momentum, while the second term consists of a combination of contributions from the wave-induced pressure and the wave-induced stress (Phillips, 1977).

As pointed out by Whitham (1974) the momentum conservation law (12) assumes its most simple form when the mass transport velocity including the wave momentum is used. In this formulation of the conservation laws, ocean waves only appear explicitly through the radiation stress tensor \mathbf{S} . Implicitly wave effects also appear through parametrizations of the stress. For example, in case the bottom stress τ_b is modelled in terms of the current velocity \mathbf{U}_c rather than the total velocity \mathbf{U} .

Although the depth-averaged continuity and momentum equations show their simplest form in terms of the total velocity, there is a definite need to know the ocean circulation velocity \mathbf{U}_c . Following Hasselmann (1971) one obtains the corresponding evolution equations for the current velocity \mathbf{U}_c by eliminating from (12) the rate of change in time of the wave momentum by means of the energy balance equation for surface gravity waves.

The energy balance equation reads (Komen *et al.*, 1996)

$$\frac{\partial}{\partial t} F + \frac{\partial}{\partial \mathbf{x}} \cdot (\mathbf{v}_g F) = S_{in} + S_{nl} + S_{diss} + S_{bot},$$

where $\mathbf{v}_g = \partial \omega / \partial \mathbf{k}$ is the group velocity and ω is the angular frequency. Our discussion will concentrate on the deep water case. Then, the angular frequency obeys the dispersion relation $\omega^2 = gk$, where k is the magnitude of the wavenumber vector. While the left-hand side of the energy balance equation describes advection of wave energy, on the right-hand side there are four source terms that represent the physics of ocean waves. The first one, S_{in} describes the generation of ocean waves by wind and therefore represents the momentum and energy transfer from air to ocean waves. The third and fourth term describe the dissipation of waves by processes such as white-capping, large scale breaking eddy-induced damping and bottom friction, while the second terms denotes nonlinear transfer by resonant four-wave interactions. The nonlinear transfer conserves total energy and momentum and is important in shaping the wave spectrum and in the down-shift towards lower frequencies.

Noting that wave momentum is wave energy divided by the phase speed of the waves, one obtains the rate of change of total wave momentum by dividing the energy balance equation by the phase speed and

by integration over wavenumber \mathbf{k} . The result is

$$\frac{\partial}{\partial t} \mathbf{P}^w = -\rho g \nabla \cdot \int d\mathbf{k} \frac{\mathbf{v}_g}{c} F + \rho g \int \frac{d\mathbf{k}}{c} (S_{in} + S_{nl} + S_{diss} + S_{bot}). \quad (14)$$

Substitution of (14) into (12) gives the following evolution equation for the ocean circulation velocity \mathbf{U}_c

$$\left(\frac{\partial}{\partial t} + \mathbf{U}_c \cdot \nabla_h \right) \mathbf{U}_c + g \nabla_h \zeta + \frac{1}{\rho} \nabla_h p_a = (\mathbf{U}_c + \mathbf{U}_{surf}) \times \mathbf{f} + \frac{\tau_{oc,a} - \tau_{oc,b}}{\rho h} - \frac{1}{\rho h} \nabla_h \cdot \mathbb{T}, \quad (15)$$

and it is straightforward to rewrite the continuity equation:

$$\frac{\partial}{\partial t} \zeta + \nabla_h \cdot (h \mathbf{U}_c) = -\nabla_h \cdot (h \mathbf{U}_{surf}). \quad (16)$$

The conservation laws for the mean ocean circulation differ in a number of respects from the laws for the total current. First, the continuity equation now shows an explicit dependence on the mass flux related to the ocean waves. Second, in the momentum equation effects of the advection of wave momentum have been eliminated, therefore, S is replaced by T with

$$\mathbb{T}_{ij} = \rho g \int d\mathbf{k} \left(\frac{v_g}{c} - \frac{1}{2} \right) \delta_{ij} F(\mathbf{k}). \quad (17)$$

The stress \mathbb{T} vanishes in deep water because according to the dispersion relation for surface gravity waves the group speed v_g equals one-half the phase speed c . Thus, only in shallow water there will be a finite contribution, which will be ignored for the moment. Third, the surface stress and the bottom stress are modified accordingly. For example, the surface stress felt by the mean circulation is the total stress minus the net stress going into the waves, or,

$$\tau_{oc,a} = \tau_a - \rho g \int \frac{d\mathbf{k}}{c} (S_{in} + S_{nl} + S_{diss}), \quad (18)$$

and the bottom stress becomes

$$\tau_{oc,b} = \tau_b + \rho g \int \frac{d\mathbf{k}}{c} S_{bot}, \quad (19)$$

Fourth, the wave momentum equation (14) does not involve an explicit Coriolis term, and therefore the mean circulation experiences an additional force given by $\rho \mathbf{U}_{surf} \times \mathbf{f}$. It is this additional force, which recently has been given considerable attention.

Since ocean modelling is about evolution of the mean ocean circulation we need to follow the approach suggested by Eq. (15). This means that in the ocean model one needs to introduce the Stokes-Coriolis force while the ocean is driven by the difference between atmospheric stress and the net stress going into the waves.

2.2 Wave breaking and upper ocean mixing

In the past 20 years evidence has been presented on the role of wave breaking and Langmuir turbulence in the upper ocean mixing. Because wave breaking generates turbulence near the surface, in a layer of the order of the wave height H_S , the turbulent velocity is enhanced by a factor of 2-3, while, in agreement with observations there is an enhanced turbulent dissipation. This gives deviations from Monin-Obukhov similarity and the dissipation profile deviates from the usual 'law-of-the-wall'. In addition, an enhanced

transport to the deeper layers of the ocean is possible because work against the shear in the Stokes drift generates Langmuir cells and wave-induced turbulence which has a penetration depth of the order of the inverse of a characteristic wavenumber of the wavefield.

Before sea state effects on the upper ocean mixing are discussed, we briefly describe the 'standard' turbulence model which is based on Monin-Obukhov similarity. Effects of turbulence are modelled by means of a version of the Mellor-Yamada scheme. Here, effects of turbulence on momentum, heat and turbulent kinetic energy are modelled by means of an eddy-viscosity model, where the eddy viscosity ν is proportional to the product of a mixing length $l(z)$, a turbulent velocity $q(z)$ and a factor ST which depends on stratification (as measured by a Richardson number Ri), or,

$$\nu = l(z)q(z)ST(Ri), \quad (20)$$

while the turbulent velocity is obtained from solving the turbulent kinetic energy (TKE) equation. If effects of advection are ignored, the TKE equation describes the rate of change of turbulent kinetic energy e due to processes such as shear production, damping by buoyancy, vertical transport of pressure and TKE, and turbulent dissipation ε . It reads

$$\frac{\partial e}{\partial t} = \nu_m S^2 - \nu_h N^2 - \frac{1}{\rho_w} \frac{\partial}{\partial z} (\overline{\delta p \delta w}) - \frac{\partial}{\partial z} (e \overline{\delta w}) - \varepsilon, \quad (21)$$

where $e = q^2/2$, with q the turbulent velocity, $\mathbf{S} = \partial \mathbf{U} / \partial z$ and $N^2 = g \rho_0^{-1} \partial \rho / \partial z$, with N the Brunt-Väisälä frequency, ρ_w is the water density, δp and δw are the pressure and vertical velocity fluctuations and the over-bar denotes an average taken over a time scale that removes linear turbulent fluctuations. Normally, pressure and TKE vertical transport is ignored, while the dissipation term is taken to be proportional to the cube of the turbulent velocity divided by the mixing length,

$$\varepsilon = \frac{q^3}{Bl}, \quad (22)$$

where, B is a dimensionless constant. Assuming steady state one then obtains the turbulent velocity from the balance between shear production, buoyancy and turbulent dissipation, i.e.

$$\nu_m S^2 - \nu_h N^2 - \varepsilon = 0. \quad (23)$$

The 'law-of-the wall' is now obtained from the reasonable assumption that close to the surface effects of stratification may be ignored while the stress, and hence, the turbulent velocity q is a constant. For a mixing length given by $l(z) = \kappa z$ it then follows immediately from Eq. (22) that close to the surface dissipation increases with the inverse of the distance to the surface.

Sea state effects such as wave breaking and Langmuir turbulence will give rise to considerable deviations from the 'law-of-the-wall'. In order to introduce these sea state effects the TKE equation is extended in the following manner. As suggested by Grant and Belcher (2009) the turbulent production by Langmuir circulation is represented by introducing an additional term that is related to work against the shear in the Stokes drift \mathbf{u}_S , i.e. $\nu_m \mathbf{S} \cdot \partial \mathbf{u}_S / \partial z$. Although in principle the depth dependence of the Stokes drift is known theoretically it is computationally very expensive to use the exact expression so we will use the approximate expression

$$\mathbf{u}_S = \mathbf{u}_S(0) e^{-2k_e |z|} / (1 + 8k_e |z|), \quad (24)$$

where $\mathbf{u}_S(0)$ is the value of the Stokes drift at the surface and k_e is an appropriately chosen wave number scale that both follow from the wave model. For a more detailed discussion see §3.

Furthermore, following Craig and Banner (1994), effects by breaking waves on upper ocean mixing are explicitly taken into account by the introduction of the energy flux from waves to the ocean column. As a consequence, transport of turbulent kinetic energy needs to be introduced as well. It is parametrized by means of a turbulent diffusion model, i.e. $\overline{e\delta w} = v_q \partial e / \partial z$. Hence, ignoring the pressure transport, the TKE equation becomes

$$\frac{\partial e}{\partial t} = \frac{\partial}{\partial z} \left(v_q \frac{\partial e}{\partial z} \right) + v_m S^2 + v_m \mathbf{S} \cdot \frac{\partial \mathbf{u}_S}{\partial z} - v_h N^2 - \frac{q^3}{Bl(z)}. \quad (25)$$

Craig and Banner now assumed that at the surface there is a direct conversion of mechanical energy to turbulent energy and therefore the turbulent energy flux is assumed to be given by the energy flux from waves to ocean column Φ_{oc} which follows from the dissipation term in the energy balance equation:

$$\Phi_{oc} = -\rho_w g \int d\mathbf{k} S_{diss}. \quad (26)$$

Remark that in the absence of relevant information on the sea state the energy flux is often parametrized as $\Phi_{oc} = m \rho_a u_*^3$, where u_* is the air friction velocity while m is in the range of 1-10. The energy flux may also be expressed in terms of the water friction velocity w_* which gives $\Phi_{oc} = \alpha \rho_w w_*^3$ with $\alpha = m(\rho_w/\rho_a)^{1/2}$ having values of the order 30-300.

Hence the boundary conditions become

$$lqS_q \frac{\partial e}{\partial z} = \Phi_{oc}/\rho_w \text{ for } z = 0, \quad \frac{\partial e}{\partial z} = 0 \text{ for } z \rightarrow \infty. \quad (27)$$

In the Craig and Banner model turbulent transport of TKE plays an essential role. This follows from an analysis of the TKE equation which reveals that very close to the surface there is a balance between turbulent transport of TKE and dissipation. In fact, from this balance one may obtain the value of TKE at the surface (cf. Mellor and Blumberg, 2004),

$$e(z=0) = \left(\frac{3B}{8S_q} \right)^{1/3} (\Phi_{oc}/\rho_w)^{2/3}, \quad (28)$$

and this is the boundary condition that is usually applied in ocean circulation models, e.g. in the NEMO model. In terms of the water friction velocity the boundary condition for TKE may be written as

$$e(z=0) = e_{bb} w_*^2, \quad e_{bb} = \left(\frac{3B\alpha^2}{8S_q} \right)^{1/3}.$$

For old windsea, a typical value for the dimensionless energy flux (in terms of w_*) is $\alpha = 100$ and using from the Mellor-Yamada scheme the standard values $B = 16.6$ and $S_q = 0.2$ one finds that $e_{bb} \approx 68$. This is the default value used in the present NEMO model.

However, the assumption that at the surface there is a direct conversion of mechanical energy into turbulence may be questioned. For example, observations of TKE dissipation in the wave crest region (Gemrich, 2010) suggest that TKE vanishes at the surface. An alternative approach, which avoids the assumption of direct energy conversion, was suggested by Saetra and Janssen some time ago (Janssen *et al.*, 2004) and this approach was extensively validated (Janssen, 2012) by comparing simulated sea surface temperature with in-situ observations. Thus far, the pressure transport has been ignored but it should be realized that this term may be related to the work done by white capping/wave breaking on the ocean surface. Denoting the negative of the correlation between pressure and velocity fluctuations by

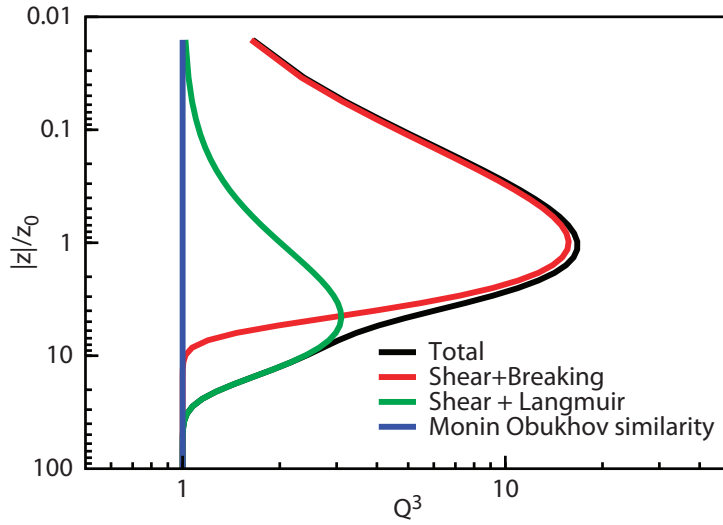


Figure 2: Profile of Q^3 according to the local approximation in the ocean column near the surface. The contributions by wave dissipation (red line) and Langmuir turbulence (green line) are shown as well. Finally, the Q^3 -profile according to Monin-Obukhov similarity, which is basically the balance between shear production and dissipation, is shown as the blue line.

$I_w(z)$ it turns out that at the surface the correlation can be written in terms of an integral of the dissipation term in the energy balance equation, e.g.,

$$I_w(0) = -\frac{1}{\rho_w} \overline{\delta p \delta w}(z=0) = \frac{\Phi_{oc}}{\rho_w} = -g \int_0^\infty S_{diss}(\mathbf{k}) d\mathbf{k} = m \frac{\rho_a}{\rho_w} u_*^3. \quad (29)$$

The main problem is now how to model the depth dependence of $I_w(z)$, in particular how deep the breaking-induced turbulence will penetrate in the upper ocean. Because breaking is a nonlinear process it is assumed that the depth scale is controlled by the significant wave height H_S (rather than a depth dependence that follows from potential flow). Therefore, the following depth dependence for $I_w(z)$ is suggested:

$$I_w(z) = I_w(0) \times \hat{I}(z), \quad \hat{I}(z) = e^{-|z|/z_0}, \quad (30)$$

where the depth scale $z_0 \sim H_S$ will basically play the role of a roughness length. Based on a comparison between modelled and observed turbulent dissipation, which will be discussed later, we choose

$$z_0 = 0.5H_S. \quad (31)$$

In contrast to the Craig and Banner model one now obtains the following TKE equation

$$\frac{\partial e}{\partial t} = \frac{\partial}{\partial z} \left(lqS_q \frac{\partial e}{\partial z} \right) + \frac{\partial I_w(z)}{\partial z} + v_m S^2 + v_m \mathbf{S} \cdot \frac{\partial \mathbf{u}_S}{\partial z} - v_h N^2 - \frac{q^3}{Bl(z)}. \quad (32)$$

At the surface there is no direct conversion of mechanical energy to turbulent energy and therefore the turbulent energy flux is assumed to vanish. Hence the boundary conditions become

$$lqS_q \frac{\partial e}{\partial z} = 0 \text{ for } z = 0, \quad \frac{\partial e}{\partial z} = 0 \text{ for } z \rightarrow \infty. \quad (33)$$

In this alternative approach some analysis (Janssen, 2012) shows that in the upper part of the ocean the main players are the pressure transport term and the dissipation, while turbulent transport of TKE can

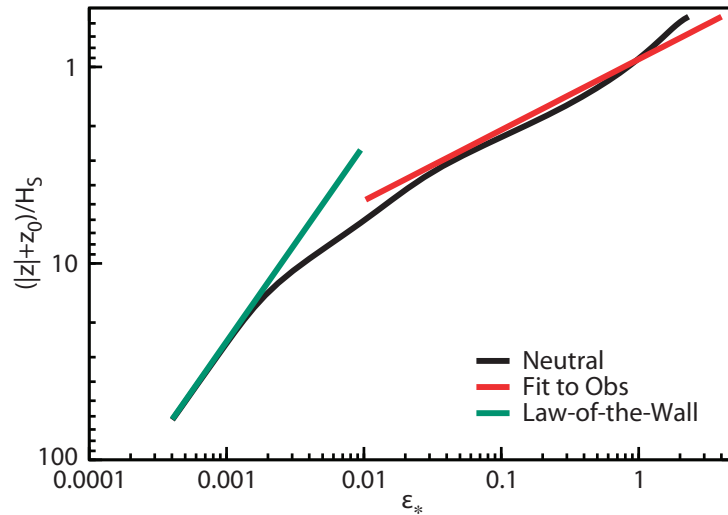


Figure 3: Dimensionless dissipation ϵ_* versus $(|z| + z_0)/H_S$.

be safely ignored. Without presenting any of the details, for neutral stratification in the steady state, the following '1/3'-rule for the turbulent velocity is then found. Introducing the dimensionless turbulent velocity $Q = (S_M/B)^{1/4} \times q/w_*$ the approximate solution of the TKE equation (32) becomes

$$Q^3 \approx 1 + \alpha \kappa |z| \frac{d\hat{I}_w}{dz} + La^{-2} \kappa |z| \frac{d\hat{U}_S}{dz}, \quad (34)$$

where $La = (w_*/u_S(0))^{1/2}$ is the turbulent Langmuir number which measures the importance of Langmuir turbulence. Therefore, in terms of Q^3 there is a *superposition principle*, so that contributions due to wave dissipation and Langmuir turbulence may be added to the shear production term.

Let us now discuss a 'typical' solution in more detail, namely the one for 'old' windsea. This is a pure windsea state (hence swell is absent) that occurs when a steady wind has been blowing for sufficiently long time so that a steady state has been achieved. A dimensional analysis suggests that the profiles depend on four parameters, namely $\alpha, La, z_0/H_S$, and the integral steepness parameter $s = k_s H_S/2$. We have chosen the typical values $\alpha = 100, La = 1/4, z_0/H_S = 1/2$ and $s = 0.11$. The approximate solution (34) has been plotted in Fig. 2, while in addition the solution without Langmuir turbulence (in red), without wave breaking (in green) and without breaking and Langmuir (Monin-Obukhov similarity, in blue) have been plotted as well. From Fig. 2 we immediately infer that the maximum in Q^3 by wave breaking is close to the sea surface at a depth z_0 while the maximum by Langmuir turbulence is at the larger depth of $1/2k_s$. These scales are widely different because ocean waves are weakly nonlinear which means that their 'typical' steepness $s = k_s H_S \ll 1$.

The enhanced turbulence in the surface layer is accompanied by deviations from the law-of-the wall, as illustrated in Fig. 3. In this figure we have plotted the dimensionless dissipation $\epsilon_* = \rho_w \epsilon H_S / \Phi_{oc}$ as function of the dimensionless depth $Z = (|z| + z_0)/H_S$. For comparison, we have also shown the law-of-the wall which holds for the deeper parts of the ocean. Finally, also shown is a fit that summarizes the observational evidence of dissipation near the surface. The empirical fit is given by (see e.g. Burchard, 2001)

$$\epsilon_* = 0.78 Z^{-2.78}.$$

We used the fit to the observational data to determine the ratio of the roughness length and the significant wave height, resulting in the choice given in Eq. (31)

2.3 Summary

To summarize, a brief overview has been given of possible sea state effects that may be relevant in a more accurate description of the mixed layer of the upper ocean. Possible candidates are the Stokes-Coriolis force, sea-state dependent forcing and two versions of upper ocean mixing induced by wave breaking. The Stokes-Coriolis force, given by $\rho_w \mathbf{u}_{st} \times \mathbf{f}$, will be added to the ocean momentum equations. Here, the Stokes drift profile \mathbf{u}_{st} is given in Eq. (35). In the case where sea-state dependent forcing of the momentum equation is used the air-side stress τ_a is replaced by the ocean stress τ_{oc} shown in Eq. (18). If sea-state dependent upper ocean mixing is switched on then for option 1 the TKE equation is run using the boundary condition for the energy flux in Eq. 28 while for option 2 the modelled pressure vertical velocity correlation due to wave breaking (see Eq. (29-30)) is introduced in the TKE equation, while the energy flux vanishes at the surface.

In the next §'s we will test these candidates by doing standalone runs over a 20 year period using forcing from ERA-interim. Noting that ERA-interim has been produced with a coupled ocean-wave, atmosphere system, the sea state parameters such as Stokes drift, sea-state dependent stress and energy flux from the breaking waves have been explicitly calculated from the archived wave spectra from ERA-interim. As control we use the default version of the NEMO model which uses sea-state parameters valid for 'old' windsea.

As a final remark it is pointed out that there is a nontrivial dependence of parameters such as the momentum flux τ_{oc} and the energy flux Φ_{oc} on the sea state. In order to measure this we remark that in the absence of sea state information one often parametrizes the energy flux as $\Phi_{oc} = m \rho_a u_*^3$ with m having a typical value of 5. Using the wave model, the energy flux can be explicitly evaluated, and it turns out that there is a considerable daily variability in the value of m . In the bottom half of Fig. 4 a map of the dimensionless energy flux m is shown for a two-year period, illustrating that there is a considerable spatial dependence of the dimensionless energy flux as on average in the extra-tropics mixing of the upper ocean is more intense than in the tropics. The reason for this spatial dependence is related to the fact that the age of the sea state (usually measured in terms of the wave age c_p/u_* , with c_p the phase speed of the peak of the spectrum) is younger in the extra-tropics than in the tropics. Younger waves have higher steepness and since wave breaking is nonlinear in the wave steepness there is higher dissipation for young waves than for old waves. This is in agreement with observations from Terray *et al* (1996) and is also found in the ECMWF wave model when the sea state is dominated by windsea.

In the same Figure we also show a map of the monthly mean momentum flux going into the ocean normalized with the air-side stress. Also here some interesting spatial patterns are to be noted, but, to be definite, the variability of the pattern is considerably smaller when compared to the one for the dimensionless energy flux.

The key question to ask now is whether a time and spatially dependent dimensionless normalized momentum and energy flux will result in realistic upper ocean dynamics and mixing. We will try to answer this question in §3 by doing simulations with the NEMO model in which time-varying sea state effects, as obtained from the wave model, have been introduced.

3 Forcing NEMO with wave model fields

Wave model forcing has been implemented in the ECMWF version of NEMO v3.4.1. Here we describe how fields are ingested in *forced mode*, i.e., when NEMO is run in stand-alone mode. Using NEMO in

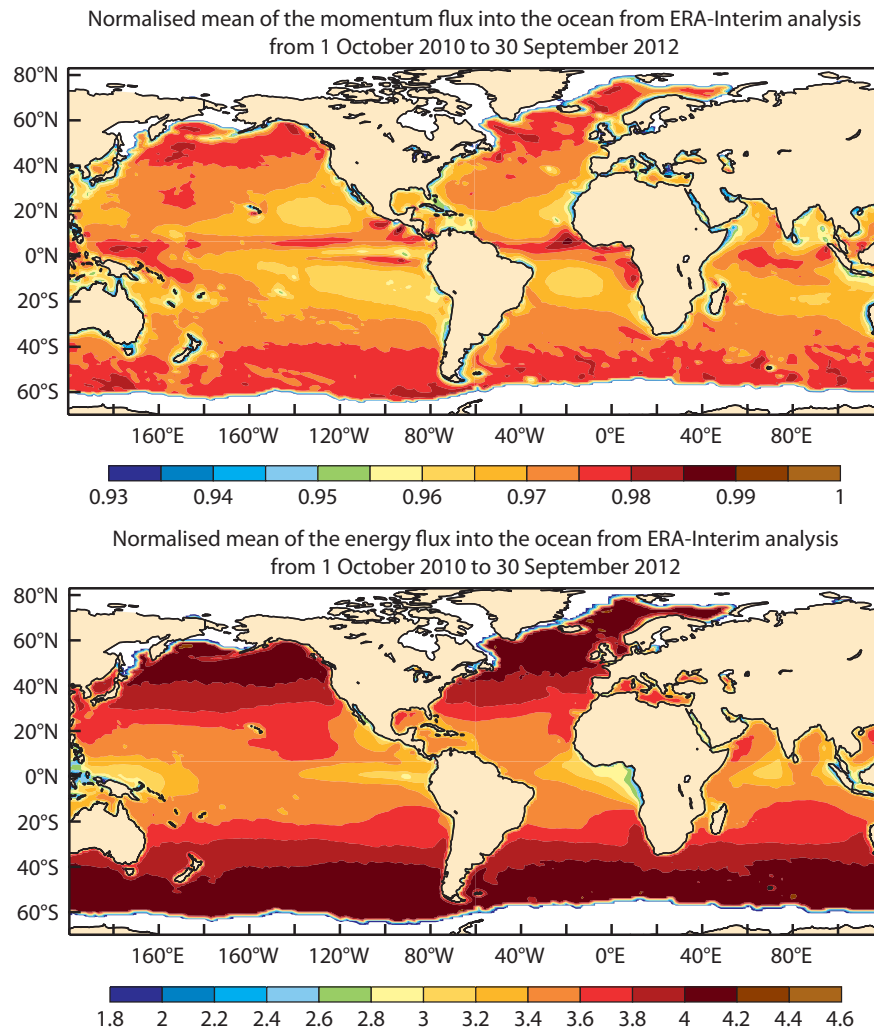


Figure 4: Top: Average of τ_{oc} normalized with the average of the surface stress. Bottom: Average of energy flux into the ocean, normalized with the average of $\rho_a u_*^3$. Averaging period is two years.

forced mode we study the impact of sea state effects in surface stress and upper ocean mixing and we study the impact of the Stokes-Coriolis force on the resulting SST fields. The control run also includes sea state effects, but normally there is no knowledge on the sea state and therefore it is assumed that the sea state is in equilibrium with the wind. This sea state is called 'old' windsea and the energy flux due to breaking waves becomes a simple function of the friction velocity while the ocean surface stress equals the air-side stress.

3.1 Forced mode experiments

A standard experiment setup is adhered to where the model is run for the period 1979-2009 inclusive. All atmospheric forcing fields in the control run (CTRL hereafter) are taken from ERA-Interim (Dee *et al.*, 2011) and are daily averages, while sea state information is provided at six-hourly intervals.

In order to test sea state effects, the 31-yr integrations on 1° resolution (1979-2009) have been conducted using wave parameters from ERA-Interim and have been compared against the control run (CTRL). Two

different vertical resolutions have been tested, ORCA1Z42 with 42 vertical levels and a 10-m thick top level, and ORCA1Z75 with 75 vertical levels and a 1-m thick top level. In addition, all experiments are set up in such a way that there is no data assimilation, SST damping is off, there is a weak 3D damping towards climatology and the LIM2 ice model is switched on.

NEMO forced runs normally require computation of the stress using a bulk formula. In CTRL the surface stress is computed using the ECMWF bulk formula (Edson *et al.*, 2013)

$$C_{D10} = (a + b\Delta U_{10}^{p_1})/\Delta U_{10}^{p_2},$$

where $a = 1.03 \times 10^{-3}$, $b = 0.04 \times 10^{-3}$, $p_1 = 1.48$ and $p_2 = 0.21$, and the relative wind speed $\Delta U_{10} = |\mathbf{U}_{10} - \mathbf{u}_0|$ is found from the difference between the 10-m wind vector and the surface current vector from NEMO. For a discussion of the coefficients that are used in the drag law see Janssen (2008).

WAM computes the air-side stress from the atmosphere into the wave field based on the 10-m neutral wind,

$$\tau_a = \rho_a C_{dw} U_{10N}^2,$$

where C_{dw} is the sea-state dependent drag computed by the WAM model. Hence, this gives the option to compute the air-side stress in NEMO based on the wave-dependent drag coefficient and the 10-m neutral wind. The wind *direction* must still be taken from the atmospheric model, which may lead to minor inconsistencies. We also note here that subtracting the surface current before computing the stress will lead to further inconsistencies. It is however important to remember that these inconsistencies are unique to the forced runs since the coupled runs (to be discussed later) exchange vectorial stresses from WAM.

3.2 The momentum flux from waves into the ocean

As discussed in §2, the ocean feels the water-side stress τ_{oc} . This differs from the air-side stress τ_a by the amount of momentum absorbed (τ_{in}) by the wave field and the amount released from breaking waves (τ_{ds}), or, $\tau_{oc} = \tau_a - (\tau_{in} + \tau_{ds})$.

The absorption in the wave field and the subsequent release to the ocean through dissipation can be related to integrals over the source terms of the wave energy balance equation as shown in Eq. (18), and therefore τ_{oc} can be evaluated, when required.

The water-side stress normalized by the magnitude of the air-side stress, τ_a , is archived in ERA-Interim. Using the water-side stress gives differences in SST compared with CTRL, which are shown in Fig. A1 of Appendix A. The most persistent differences are found along the eastern edge of the Pacific where the modifications to the wind stress appear to lead to reduced upwelling. A cooling of up to 0.5 K is found in the Gulf Stream and Kuro-Shio regions. The eastern tropical Pacific experiences a slight warming. A comparison against all available SST observations (OIv2, Reynolds *et al.*, 2002), as shown in Fig. A2, gives a slight reduction in the SST bias when compared with the bias in the CTRL.

3.3 Impact of Stokes-Coriolis force

The Stokes-Coriolis force has been implemented as a tendency to the momentum equations in NEMO. The surface Stokes drift is taken from the ERA-Interim archive and an approximate Stokes-drift profile is used to estimate the transport caused by the Stokes-Coriolis force.

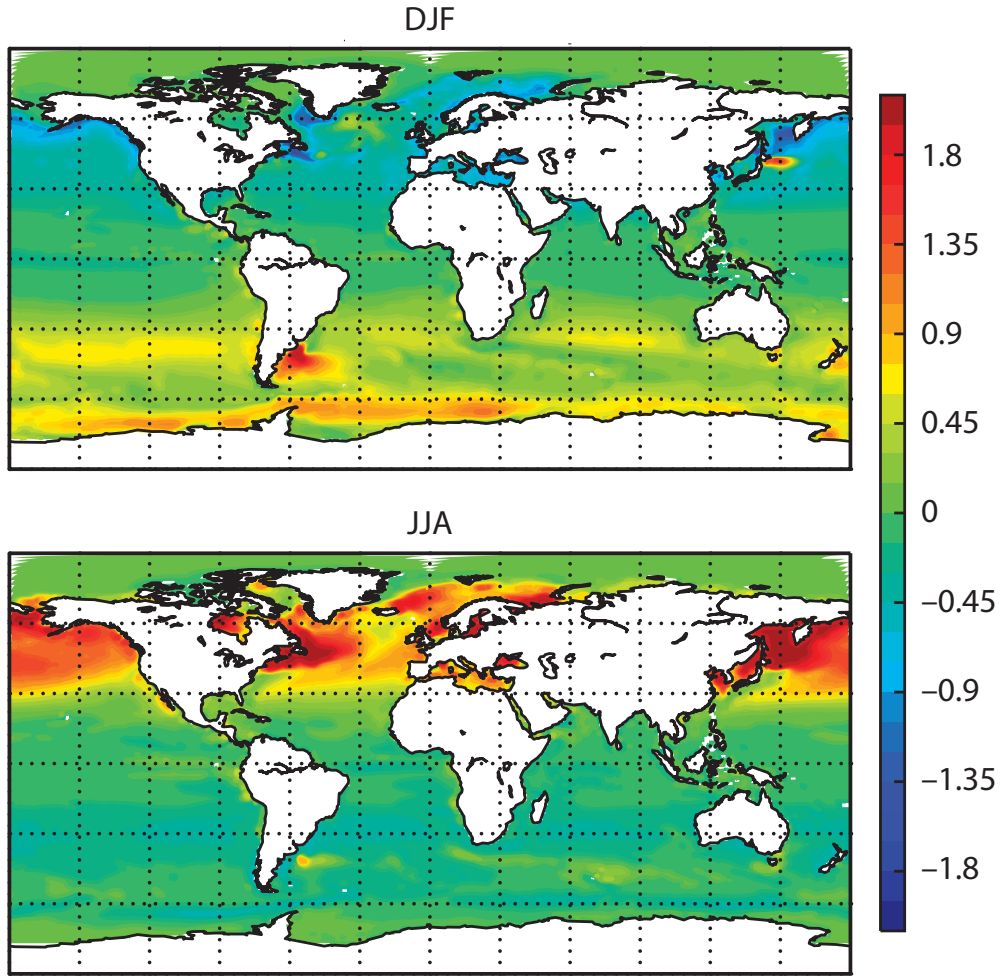


Figure 5: 20-yr average SST difference between CTRL and a run with TKE mixing dictated by the energy flux from the ERA-Interim WAM model plus the other wave effects. The differences are most pronounced in the summer hemisphere, where the mixing is reduced, leading to higher SST. The colour scale is ± 2 K.

In the deep-water limit, where the dispersion relation for water waves is given by $\omega^2 = gk$, the Stokes profile can be written as

$$\mathbf{u}_{st}(z) = 2 \int d\mathbf{k} \omega \mathbf{k} e^{2kz} F(\mathbf{k}). \quad (35)$$

Determining the full Stokes profile from Eq. (35) is expensive, and when the wave spectrum is not available the profile must be approximated in such a way that the surface Stokes drift vector \mathbf{u}_0 and the Stokes transport $\mathbf{T}_{st} = \int_{-\infty}^0 \mathbf{u}_{st}(z) dz$ are given correctly. In the deep-water limit the Stokes transport becomes

$$\mathbf{T}_{st} = \int d\mathbf{k} \omega \hat{\mathbf{k}} F(\mathbf{k}). \quad (36)$$

The integrand here is the first moment of the variance spectrum, m_1 , weighted by the unit vector $\hat{\mathbf{k}}$ of the wave component.

Because of the computational cost and often also due to lack of access to the full two-dimensional wave spectra it is customary (see e.g. Rascle *et al.*, 2006, Saetra *et al.*, 2007) to approximate Eq. (35) by the

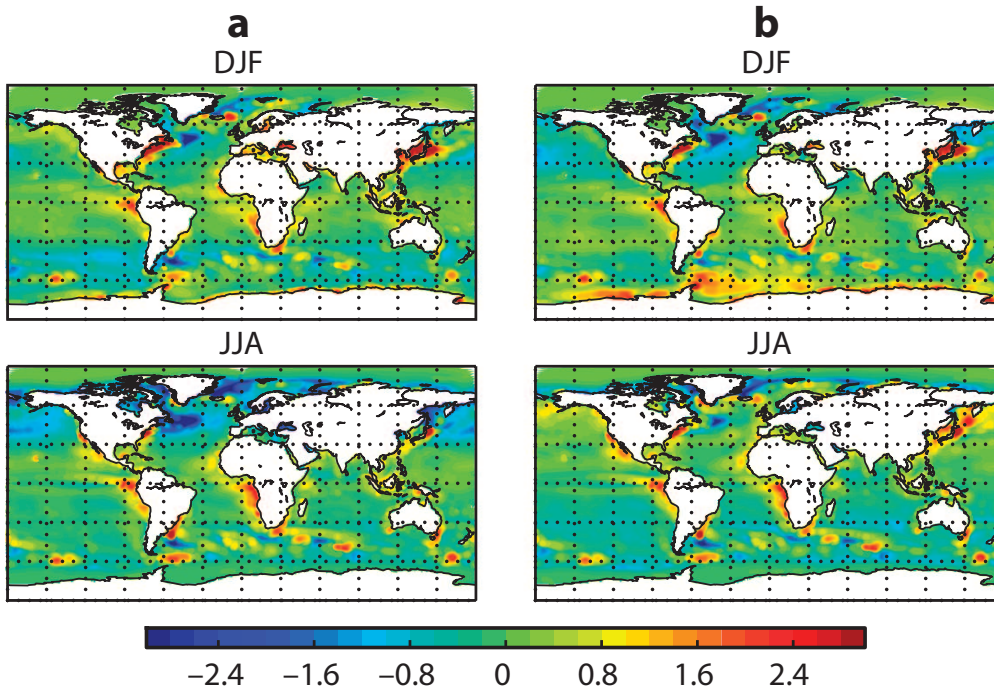


Figure 6: Panel a: 20-yr average SST difference between CTRL and OIv2. Panel b: difference between a run with TKE mixing dictated by the energy flux from the ERA-Interim WAM model and OIv2, giving smaller biases in the summer hemisphere.

exponential profile of a monochromatic wave,

$$\mathbf{u}_m = \mathbf{u}_0 e^{2k_m z}.$$

We have found that an alternative to the exponential profile of the form

$$\mathbf{u}_e = \mathbf{u}_0 \frac{e^{2k_e z}}{1 - 8k_e z}. \quad (37)$$

yields a closer agreement with the full profile than the monochromatic approximation. The transport under such a profile can be obtained analytically and involves the exponential integral E_1 (Abramowitz and Stegun, 1972, 5.1.28). It becomes

$$|\mathbf{T}_{st}| = \frac{|\mathbf{u}_0| e^{1/4} E_1(1/4)}{8k_e}$$

and by inverting this equation one obtains the effective wavenumber k_e as function of the Stokes drift at the surface and the Stokes transport, or,

$$k_e = \frac{|\mathbf{u}_0| e^{1/4} E_1(1/4)}{8|\mathbf{T}_{st}|} \approx \frac{|\mathbf{u}_0|}{5.97|\mathbf{T}_{st}|} \quad (38)$$

In a similar manner an expression for the typical wavenumber k_m of the monochromatic case can be obtained with the result that $k_m = |\mathbf{u}_0|/2|\mathbf{T}_{st}|$, implying that with the new, more accurate approximation (37) an increase in penetration depth by about a factor of 3 is found. Therefore, with the profile (37) Stokes-Coriolis effects are felt to much greater depth.

Finally, the Stokes transport is estimated from spectral information in the following manner. Introduce the mean angular frequency $\bar{\omega} = m_1/m_0$ and the significant wave height $H_S = 4\sqrt{m_0}$, then the following estimate of the Stokes transport may be found:

$$\mathbf{T}_{st} = \frac{1}{16} \bar{\omega} H_S^2 \hat{\mathbf{k}}_s. \quad (39)$$

Here $\hat{\mathbf{k}}_s = (\sin \theta_s, \cos \theta_s)$ is the unit vector in the direction θ_s of the Stokes transport.

The NEMO implementation computes the Stokes-Coriolis force and adds it to the momentum equation at the appropriate U and V points as a tendency. Contributions below 150 m are ignored because at those depths the Stokes drift is vanishingly small, even for strong wind speeds (for old windsea the Stokes profile has an e -folding depth of $(2k_e)^{-1} \approx 0.03U_{10}^2$, which for a 20 m/s wind equals 10 m). For real profiles the presence of swell may substantially increase the penetration depth, but even accounting for long swell a cutoff at 150 m depth is sufficient.

The effect of the Stokes-Coriolis forcing on SST is mainly seen in the extratropics, which is natural since it scales with the Coriolis frequency. The differences are on the order of 0.5 K compared with CTRL as can be seen in Fig. A3.

3.4 Impact of energy flux from waves on SST

The energy flux from breaking waves to the ocean is described in Sec 2.2. The implementation in NEMO also takes into account the thickness Δz of the uppermost model level.

If we assume, as do Craig and Banner (1994) and Mellor and Blumberg (2004), that in the uppermost, wave-affected layer, the roughness length can be set to a constant which we choose to be $z_w = 0.5H_S$ and that in this near-surface region diffusion balances dissipation, then Eq. (25) has the simple solution

$$e(z) = e_0 e^{z/z_{cb}},$$

where the decay length scale for TKE is given by

$$z_{cb} = \frac{1}{2} S_q B \kappa^2 z_w.$$

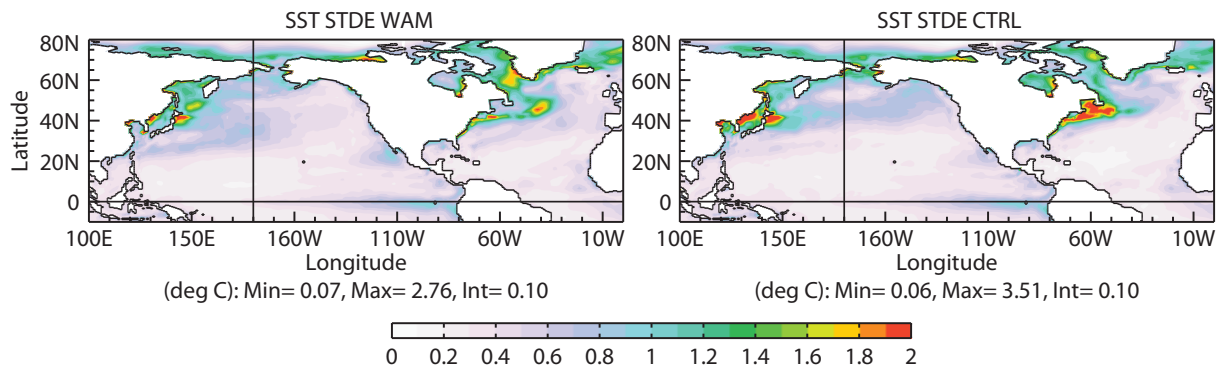


Figure 7: Standard deviation of errors in modelled SST, obtained from a comparison with OIv2 SST analyses. The left panel, labeled WAM, shows the STD errors when all sea state effects are switched on, while the right panel shows the STD errors obtained from CTRL.

It turns out that this decay length scale is quite small. For the parameters $S_q = 0.2$ and $B = 16.6$, as used in NEMO, one finds $z_{cb} \sim z_w/4$. For a wave height of 2.5 m, which is close to the global mean, the typical value of z_{cb} becomes of the order of 0.5 m.

In the present versions of NEMO the boundary condition (28) is applied, i.e. the value of TKE at the surface is specified. However, when TKE is varying rapidly in comparison to the coarse resolution in the vertical a too large mixing of the upper layer will result. It was therefore decided to use the average TKE as boundary condition at the surface. The average TKE for the uppermost level with thickness Δz is given by,

$$e_1 = e_0 \frac{z_{cb}}{\Delta z} \left(1 - e^{-\Delta z/z_{cb}} \right)$$

which will differ substantially from the surface value for a thick uppermost level, such as ORCA1Z42 has.

Fig. 5 compares a run with all wave effects included (TKE from breaking waves, modified stress and Stokes-Coriolis forcing) to the CTRL run. We see a substantial increase in the SST in the summer hemisphere due to reduced mixing when comparing with the CTRL run.

The changes to SST when comparing with OIv2 SST analyses are generally in the right direction, although there are notable regions where CTRL is closer to the observations (Fig. 6). In addition, as shown in Fig. 7, there are marked reductions in the standard deviation of error of SST when the above sea state effects are switched on, in particular in the Gulfstream area and near the Kuro-Shio current. A comparison with *in situ* observations has been done, and globally temperature biases in the mixed layer are reduced somewhat (Fig. A4), although much more at 25-50 m depth than at the surface. Finally, impact of sea-state dependent mixing is found down to 400 m depth as illustrated by a cross section at 170 E of the temperature difference between experiment and CTRL shown in Fig. A5.

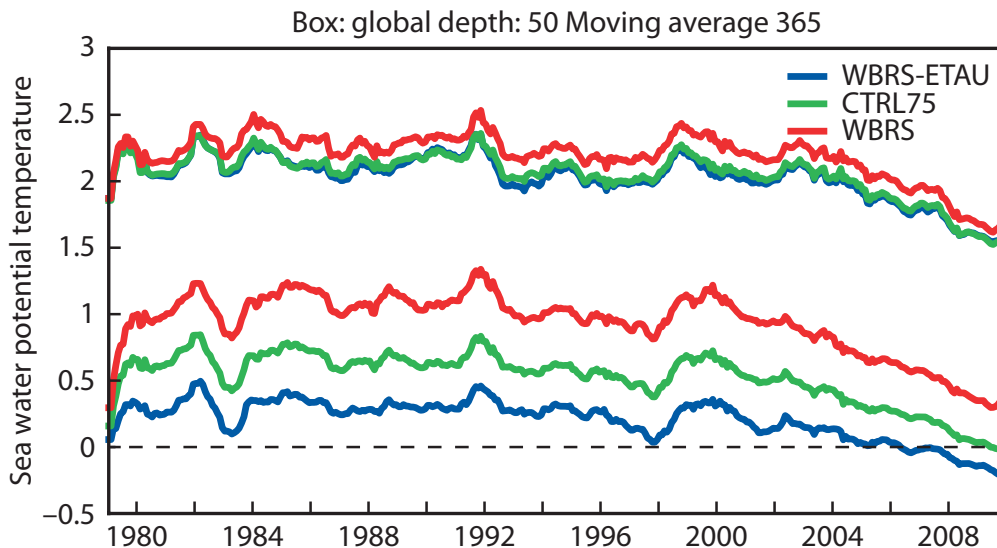


Figure 8: Time series of global model bias (lower curves) and standard deviation (upper curves) for observed temperature at 50 m depth globally (CTRL=green, WBRs-ETAU=blue, WBRs=red). Here WBRs includes mixing by wave breaking and unresolved surface wind variability while in WBRs-ETAU effects of unresolved surface wind variability are switched off. The range in biases gives an indication of the sensitivity to the additional mixing by the unresolved variability.

3.5 Wave breaking as a source term to the TKE equation

As outlined in Section 2.2, the injection of TKE from breaking waves can also be formulated as a source term to the TKE equation. In this case we must change the upper boundary condition accordingly. We have implemented this as an option in NEMO where the TKE from breaking waves is added as a tendency to the TKE equation. The e -folding depth is $z_0 = 0.5H_s$ and we can therefore safely confine the computation to the model levels in the upper 50 m of the ocean.

A number of experimental runs have been carried out with the source term formulation, and the preliminary conclusion is that it may prove a useful alternative for a 75-level model with a 1-metre thick uppermost level, but for a 42-level model we expect the flux boundary condition of Craig and Banner (1994), modified by using the average TKE at the surface, to work better.

However, for a 75-level model adding the source term may allow us to remove the additional mixing induced by unresolved surface wind variability (controlled by the `nn_etau` namelist variable). This has garnered some interest in the NEMO community recently as it adds in an *ad hoc* manner TKE to the lower levels based on the surface value to boost the mixing. Fig. 8 shows the sensitivity range to the additional mixing induced by `nn_etau` at 50 m depth. It is also interesting to note that the bias at this level is significantly reduced with a combination of a wave breaking source term and no additional mixing (blue curve). At the moment, it is too early to decide which of the two ways of injecting TKE will prove more beneficial in a future 75-level model setup.

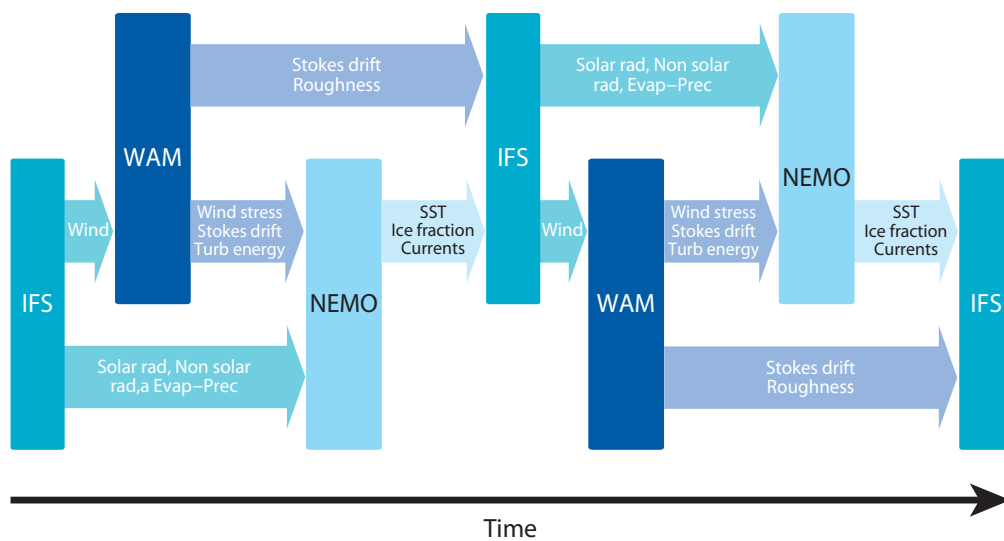


Figure 9: Flow chart of the coupled model, here two time steps are shown.

4 Coupled Simulations

After studying results with the standalone version of NEMO in forced mode we will now discuss results obtained with a coupled IFS-WAM-NEMO system on a seasonal timescale. First, some details of the coupled system are described, followed by a presentation of results obtained from the coupled simulations. In particular, impact of sea state information on the mean state and on the skill of seasonal forecasts is studied.

4.1 Description of the single executable coupled system

In the newly developed coupled atmosphere-wave-ocean system all components are integrated into the same executable with a sequential calling of each components. In the simplest configuration, without an active sea ice model in ocean component, the call sequence is as follows:

1. The atmospheric model (IFS) runs for one coupling time step and produces an updated wind field for the wave model (WAM) as well as updated radiation (solar and non-solar) and evaporation minus precipitation fields for the ocean model (NEMO).
2. WAM runs for the same period and produces updated sea surface roughness for atmosphere model and updated Stokes drift, and turbulent kinetic energy (Φ_{oc} in section 2.2) for the ocean model (NEMO).
3. NEMO runs for the same period and produces updates sea surface temperature and surface currents as input to the IFS model.

After the call to the NEMO model the cycle repeats itself. The flow chart of the coupled model is given in Fig. 9.

It is possible to have different periods for the different model components. For example, for the atmospheric model running at T255L91 with a 45 minutes timestep we can exchange data with the ocean model running at ORCA1L42 resolution with a 1 hour time step every 3 hours by running the atmosphere model for 4 time steps before we run the ocean model for 3 time steps. More details on the single executable coupled system can be found in Mogensen *et al.* (2012).

4.2 Results of the coupled simulations

To test the effects of including the wave coupling a series of three experiments was performed. One experiment was done with the reference settings of the NEMO v3.4.1 TKE scheme (CTRL hereafter), another experiment was done with a change to the e_{bb} parameter, reducing the magnitude of the surface value of TKE, from 67.83 to 20.0 (TKE-20), and finally an experiment was done where both the sea state dependent mixing and the Stokes-Coriolis effect were activated (TKE-WAM).

The reasons to perform the additional experiment TKE-20 are the following. In §3.4 we have noted that imposing a surface boundary condition on TKE gives rise to too much mixing if an ocean model with a thick uppermost layer is used. This is because TKE, as induced by wave breaking, varies quite rapidly with depth. Therefore we introduced a modification to NEMO where instead of the surface value we impose the average TKE over the uppermost layer. This average depends, however, on the sea state. As an alternative solution, we did forced mode experiments where we reduced the surface value to such an extent that biases in SST are minimal. It turned out that for 42 vertical levels $e_{bb} = 20$ gave a satisfactory solution (but note that the optimal value depends on the vertical resolution).

For all experiments CY39R1 of the coupled model was used with an atmospheric resolution of T255L91 and using the ORCA1 configuration with 42 vertical levels for the NEMO model. The runs were based on the seasonal forecasting setup with 3 ensemble members with a forecast length of 7 months starting from the 1st May and the 1st November from 1981 to 2010 equalling a total of 60 start dates. No stochastic physics was used in these runs so the difference between ensemble members was created by choosing different ocean ensemble members from the ORAS4 ocean reanalysis and from the application of SST perturbations at initial time.

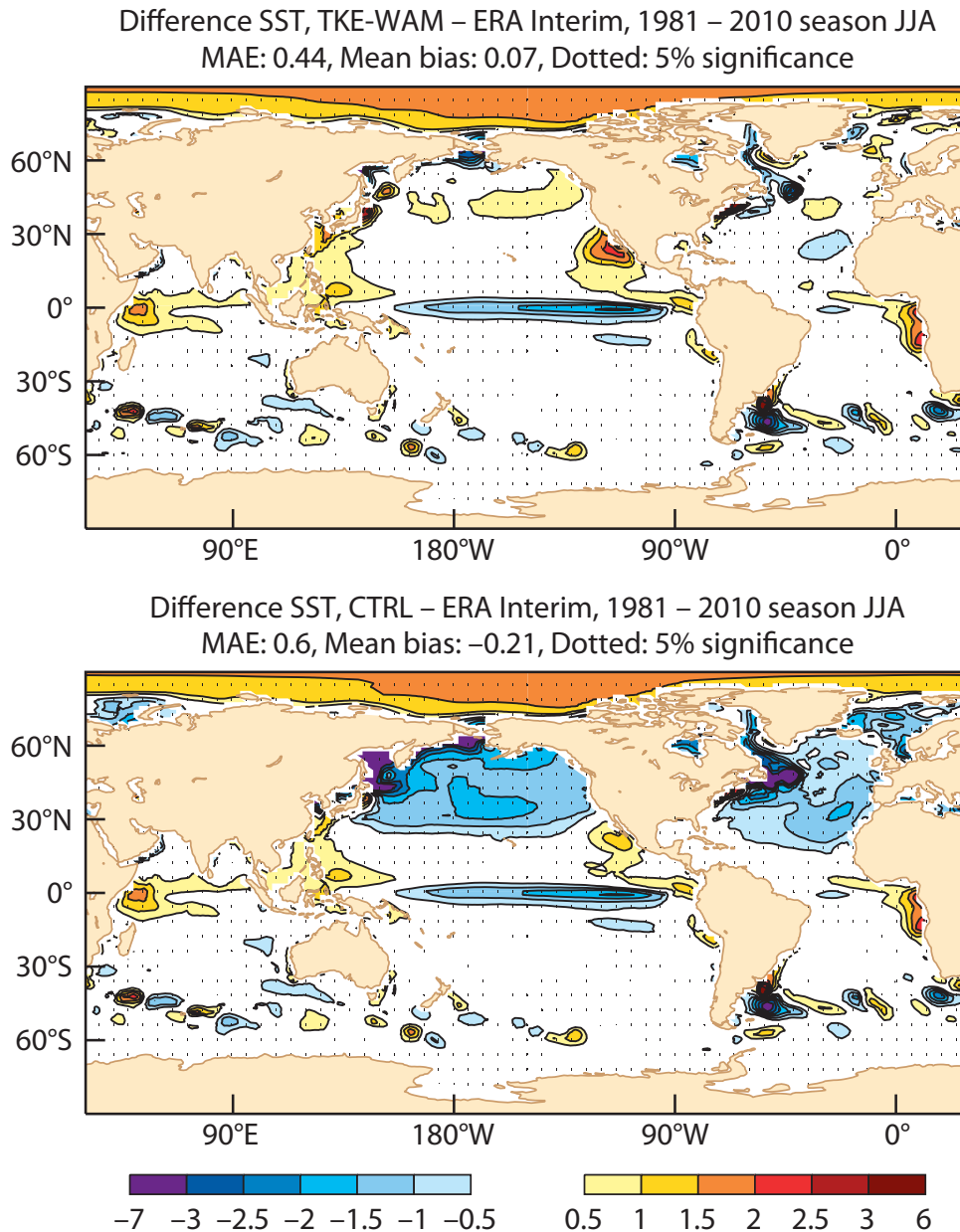


Figure 10: Systematic differences in SST with respect to the OIv2 analysis for JJA with start dates in May. Top panel the experiment TKE-WAM, bottom panel the CTRL experiment.

Impact on the mean state

Figure 10 shows the SST bias for the seasonal experiments initiated in May for JJA. The CTRL experiment shows a pronounced cold bias at high latitudes in the summer hemisphere, in both the Pacific and the Atlantic basins. For November starts, the cold bias appears in the Southern Hemisphere, not shown. In experiment TKE-WAM, where the TKE input is obtained directly from the wave model, the cold bias disappears, especially in the Atlantic basin, while in the Pacific a weak warm bias is now present. The

warm bias in the eastern part of the Pacific basin, associated with the weak coastal upwelling and poor representations of the stratocumulus, which was weak in CTRL, appears enhanced when the TKE input is from the waves, suggesting that in CTRL there might have been compensation of errors. Both experiments exhibit a pronounced cold tongue bias, slightly reduced in the TKE-WAM only for November starts (see later in Fig 11), and a warm bias in the Western tropical Pacific and Indian Ocean. There is little impact on SST in the winter hemisphere.

The different mean state in SST impacts the mean atmospheric circulation, with experiment TKE-WAM showing a reduced (improved) mid-latitude circulation in response to weaker meridional gradients in SST, with a weaker summer-time subtropical high (not shown).

The experiment TKE-20 shows very similar SST as experiment TKE-WAM and is therefore not shown.

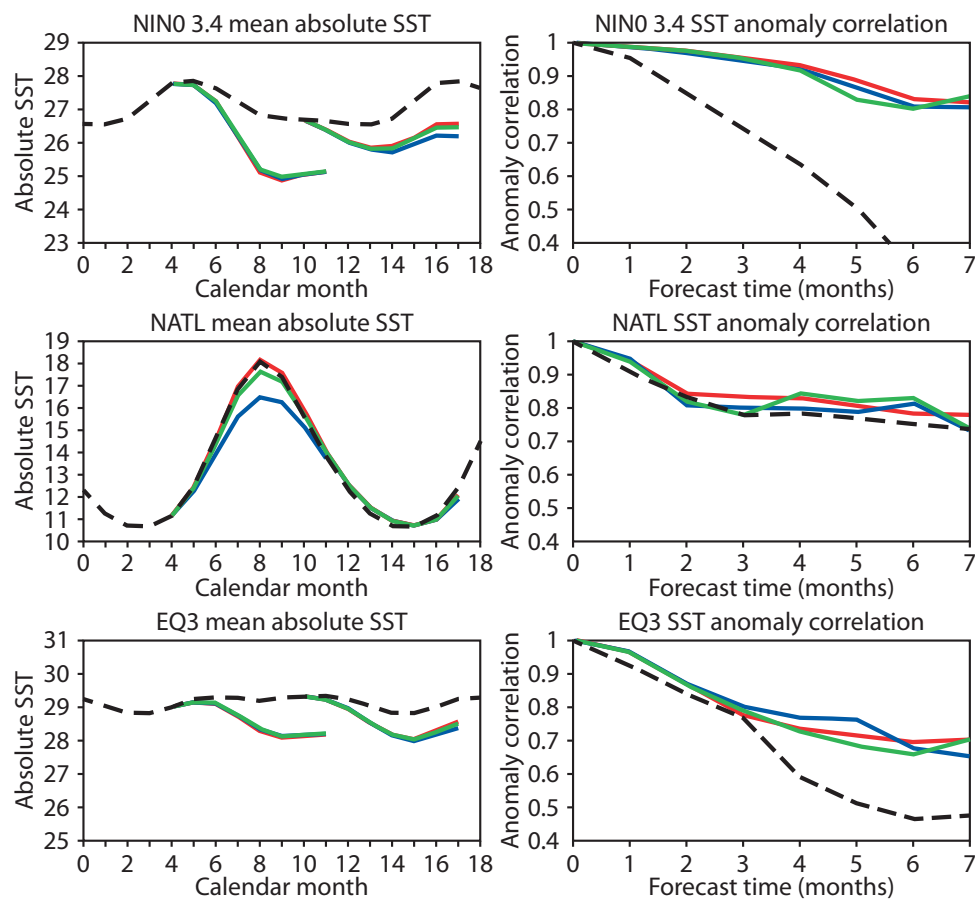


Figure 11: Absolute SST (left column) and correlation (right column) for the seasonal forecasts with CTRL (blue), TKE-WAM (red) and TKE-20 (green) in selected areas: NINO3.4 (170W-120W, 5N-5S), North Atlantic (30N-60N), Equatorial Western Pacific (region EQ3, 150E-170W, 5N-5S). In the left column results are compared with observations (dashed black), while the anomaly scores on the right are compared with persistence (dashed black).

Impact on seasonal forecasts

The skill of seasonal forecast of SST has been estimated for the different experiments above. Although the number of ensemble members is small (only 3) there are a substantial number of starting dates. Nevertheless the following results should be considered preliminary. Fig. 11 shows the absolute SST (left column) and correlation (right column) for the seasonal forecasts with CTRL, TKE-WAM and TKE-20 in different areas. Results show that TKE-WAM has some positive impact on the anomaly correlation skill over the Central Pacific (NINO3.4, 170W-120W, 5N-5S) and North Atlantic (30N-60N), and a slight degradation in the Equatorial Western Pacific (region EQ3, 150E-170W, 5N-5S). In other regions the impact of the TKE modifications on forecast skill is not so clear.

It is interesting to notice that the improvement in NINO3.4 is only apparent with TKE-WAM and not with TKE-20, in spite of the fact that both have a similar mean SST. In the North Atlantic, TKE-WAM is the best in reproducing the amplitude and phase of the seasonal cycle of the SST, followed by TKE-20, since the latter slightly underestimates the summer warming. The seasonality is substantially weaker in the CTRL experiment. The usual expectation is that the improved mean state is associated with improvements in skill, but this is not easy to demonstrate, and it is definitively not the case for the experiment TKE-20. However, it should be realized that the anomaly scores are obtained from SST's that have been corrected for the model drift shown in the left column of Fig. 11. This could therefore very well mask improvements in skill caused by improvements in the mean state.

Finally, the explanation of the fact that both TKE-WAM and TKE-20 appear to degrade the skill in the Equatorial Western Pacific remains unknown. It may be related to the slightly increased easterly bias in wind in TKE-WAM with respect to the CTRL (not shown). However, the level of wind and SST variability in all experiments is very similar. This result is surprising, since, compared to CTRL, both the TKE-WAM and the TKE-20 experiments do not seem to degrade the mean state in SST, but their skill scores are slightly worse compared to CTRL. This needs to be investigated further.

5 Coupling from Day 0

In the present operational medium-range/monthly ensemble forecasting system the forecast range is split in two parts, called leg A and leg B. In leg A, which consists of the first 10 Days of the forecast, the atmospheric model has high resolution while the ocean is passive. In Leg B the atmospheric model has half the resolution while the ocean becomes an active part of the coupled system. It is therefore of interest whether there are further benefits in forecasting by coupling the atmosphere with the ocean from initial time. In this section we list, based on numerical simulations, a number of advantages of coupling from Day 0. This two-way interaction turns out to be beneficial for forecasting slowly moving hurricanes, it improves the prediction of the MJO and some definite improvements in the statistical skill scores of ENS are found, in particular in the tropics.

The ocean model used in the ENS experiments is NEMO v3.4.1 with sea-state dependent TKE (Option 1) and Stokes-Coriolis forcing activated. In NEMO v3.4.1 the sea-state dependent stress τ_{oc} gave due to interpolation errors occasionally noisy results and therefore it was switched off for security reasons. This has since been corrected. The default light penetration scheme of v3.4.1 consists of three bands and includes the mean effects of chlorophyll. In upwelling areas this scheme resulted in a considerable overestimation of SST and therefore we reverted to a 2-band penetration scheme which is the scheme used in operations.

The ocean model used in the experiments testing the impact of coupling on hurricanes and on the forecast of the MJO was an earlier version of NEMO which did not include sea state effects on upper ocean mixing while for the atmosphere Cy38R1 was chosen. It is strongly emphasized that in this § the principal interest is in testing whether coupling from Day 0 is beneficial, we have not studied in detail whether sea state effects in upper ocean mixing and the introduction of the Stokes-Coriolis force have impact on the medium-range and monthly time scales.

5.1 Impact on hurricanes

Recent studies have shown that in certain circumstances, the ocean can have impact on hurricane intensification (Shay *et al.* 2000; Moon *et al.* 2007; Yablonski and Ginis 2008; Shay and Uhlhorn 2008). The wind circulation associated with a hurricane tends to reduce the sea surface temperature below the hurricane by several degrees. The cooling of sea surface is then likely to weaken the intensity of the hurricane, because the heat flux reduces. This feedback effect is expected to be stronger for slowly moving hurricanes.

In ENS the IFS is forced by persisted SST anomalies during the first 10 days of integrations. As a consequence, the air-sea interaction described above is not simulated by the model during the first 10 days of integrations, and this may result in an overestimation of the intensity of some hurricanes. This was indeed the case for hurricanes Nadine and Leslie during the 2012 Atlantic hurricane season. To evaluate the impact of coupling IFS to ORCA1L42 NEMO on the intensity of hurricanes, 15-day ENS forecasts of Leslie and Nadine have been reproduced with the same setup as in operations, but with IFS coupled to NEMO during the first 10 days of integrations. The forecast starting dates are 19 September 2012 for Nadine and 3 September 2012 at 12 UTC for Leslie. In both cases, the coupled integrations produce a significant cooling of SSTs below the hurricane. For instance Fig. 12 shows the difference of ensemble mean SSTs between day 5 and day 0 in the coupled integrations starting on 19 September 2012 (Nadine case). This Figure shows an extensive area over the North Atlantic with cooler SSTs at day 5. The amplitude of the cooling reaches 2.5°C over some areas near the centre of hurricane Nadine. As illustrated in the bottom part of Fig. 12, the intensity of Nadine is weaker in the coupled integrations than in the control integrations (ensemble mean maximum sustained wind of 26.5 m/s in the coupled integrations instead of 30.9 in the uncoupled integrations and a mean sea level pressure of 979 hPa in the coupled integrations instead of 971 hPa in the ensemble mean). The difference of hurricane intensity between the coupled and uncoupled integrations is statistically significant within the 1% level of confidence. The intensity of Nadine in the coupled integrations is closer to observations (observed mean sea level pressure of 978 hPa) than in the uncoupled integrations.

Leslie is another example of a slow moving hurricane during the 2012 Atlantic hurricane season. The operational EPS overestimated strongly its intensity. For instance, the ENS forecasts starting on 3 September 2012 predicted a mean sea level pressure of 957 hPa, which is 13 hPa lower than the observed mean sea level pressure (970 hPa). ENS integrations coupled from day 0 predict a mean sea level pressure of 968 hPa (ensemble mean), which is very close to the observed value. The difference of hurricane intensity between the coupled and uncoupled ENS integrations is statistically significant within the 1% level of confidence. As for Nadine, there is no significant difference in the tracks of the hurricane between both experiments.

Coupled experiments have also been performed for other tropical storms during the 2012 Atlantic season, showing in general little impact. Coupling from Day 0 had no significant impact on the intensity of Sandy, but the experiment with coupling from Day 0 displays higher hurricane strike probability over New York than the uncoupled experiment (not shown).

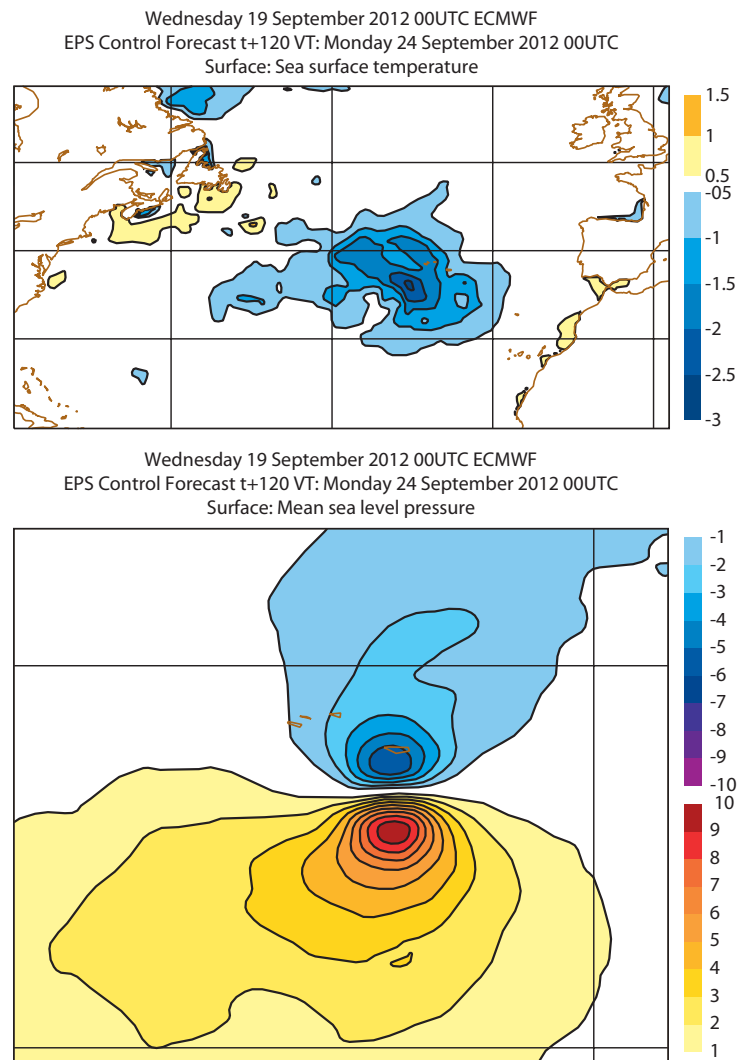


Figure 12: **Top:** Ensemble mean SST difference between day 5 and day 0 from the 51-ensemble integrations starting on 19 September 2012 with IFS coupled to NEMO with 1° resolution during the first 10 days of the integrations. **Bottom:** Difference in ensemble mean surface pressure between coupled and control for the 5 day forecast from 19 September 2012.

5.2 Impact on the MJO

Another justification for including an interactive ocean below the atmospheric model from Day 0 is the impact of the ocean-atmosphere interactions on the propagation of the Madden-Julian Oscillation (MJO) (see Woolnough et al 2007 for instance) which is a main source of predictability in the tropics on the sub-seasonal time scale. In order to assess the impact of ocean-atmosphere coupling in the current operational ENS configuration, a series of re-forecasts has been produced with and without coupling from Day 0. The re-forecasts consist of a fifteen-member ensemble of 45-day integrations starting on the 1st February, May, August and November 1989-2008 with IFS cycle 38R2. The MJO is diagnosed by projecting each ensemble member onto the two leading combined Empirical Orthogonal Functions (EOFs) of zonal winds at 850 hPa and 200 hPa and outgoing long-wave radiation (OLR) averaged between 15N and 15S (Wheeler and Hendon, 2003, Gottschalk et al, 2010). The skill of the monthly forecasting system is then estimated by computing the anomaly correlations of principal components 1 and 2 (PC1 and

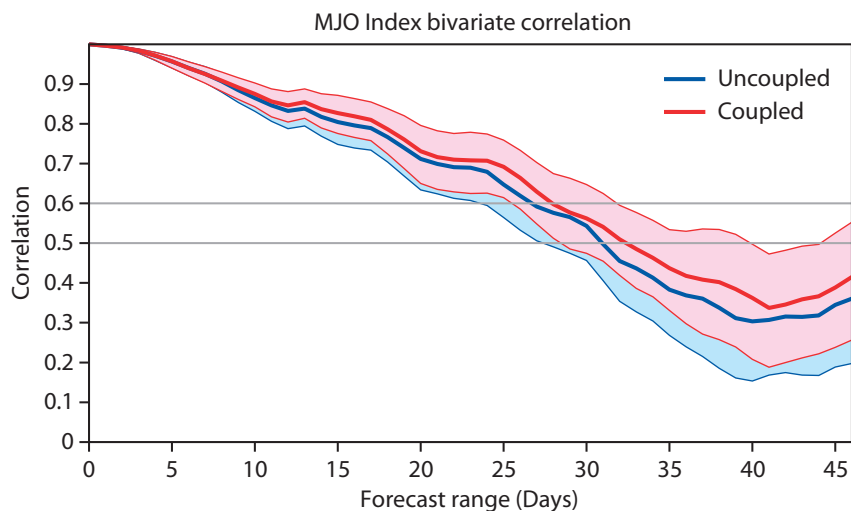


Figure 13: MJO Bivariate correlation for the control runs (leg A uncoupled, blue curve) and coupled from day 0 integrations (leg A coupled, red curve). The shaded areas represent the 5% level of confidence using a 10,000 re-sampling bootstrap procedure.

PC2) predicted by the model with the PC1 and PC2 computed from the analysis (in this case ECMWF reanalysis dataset, ERA-Interim). Fig. 13 suggests that model integrations with leg A coupled from Day 0 display higher skill in predicting the MJO than the control runs. The gain in skill is about 1 day of predictive skill.

5.3 Impact of coupling on ENS in the medium-range

An overview is given here of the impact of coupling from initial time using ENS with the configuration that is planned to be implemented. Two ENS experiments have been run using model cycle 39r1. Experiment \mathcal{C} is coupled from initial time, while experiment \mathcal{P} uses persisted SST anomalies in leg A, i.e. up to Day 10. In leg B of experiment \mathcal{P} , the IFS is coupled to NEMO. The initial conditions for leg B are obtained by forcing the ocean model with the wind stresses of the leg A integration. This corresponds to the coupling configuration of the operational ENS configuration in cycles prior to 39r1. Experiment \mathcal{C} uses tendency coupling during the first five days. Then, between Day 5 and Day 9, the observed SST anomalies are decreased leading to full coupling from Day 9.

Apart from the differences in the ocean-atmosphere coupling in leg A the two experiments are identical and the configuration corresponds to the one planned for operational implementation in cycle 40r1. This cycle includes a revision of the physics with a change to the representation of the vertical turbulent fluxes in the atmosphere. Furthermore, the vertical discretisation changes from 62 levels with a model top at 5 hPa to 91 levels with a top at 1 Pa. The horizontal resolution is as in the operational ENS with truncations T_L639 and T_L319 in leg A and leg B, respectively. The ENS consists of 50 perturbed forecasts and one unperturbed control member. The experimentation covers 33 cases in a boreal winter period (10 January to 14 March 2012) and 28 cases in boreal summer period (6 June to 13 August 2012).

First, noticeable changes to the SST errors are presented. Thereafter, the impact on upper air scores in the medium-range is summarized.

Sea surface temperature

Replacing the persisted SST anomalies in leg A by the coupled model may lead, because of model drift, to larger systematic errors. This is obvious as the persisted, observed SST anomalies are by definition unbiased for a large sample when compared to the observed data set. On the other hand, the random errors of the persistence forecast increase with lead time and there is the potential that the coupled model forecast is overall more accurate than the persistence forecast in regions that evolve significantly during the first ten days. Therefore the key question is whether the benefit of the latter outweighs the degradation due to the increased bias.

Fig. 14a and b show the mean SST error of the 10-day ensemble mean for experiment \mathcal{C} and \mathcal{P} , respectively. For experiment \mathcal{P} , the bias in the mean state is small and not statistically significant, as expected. For experiment \mathcal{C} , we see many different structures and many of them are small scale. The regions east of North America and Japan stand out because the positions of the boundary currents are not well reproduced by the model, leading to increased systematic errors. The eastern equatorial Pacific starts to develop a cold bias in the coupled model, which corresponds to the early phase of the “cold tongue problem”, which for the ECMWF coupled model is discussed in e.g. Magnusson et al. (2012). Finally, a warm bias starts to develop in Southern Ocean, south of 55S, in agreement with the systematic errors found in the standalone runs of §3.

Fig. 14c shows the day-10 difference between experiment \mathcal{C} and experiment \mathcal{P} of the ensemble mean absolute error which is a measure of RMS error. Negative values indicate improved forecast quality. In the extended tropical region (30N–30S), the SST forecasts are generally improved by introducing the coupling from Day 0. The largest improvement is found west of the Maritime continent, which could be related to the interaction between MJO and SSTs. Improvements are also found west of South America that can be related to better interaction between the atmospheric winds and/or cloud and upwelling of cold water in the ocean. For the northern extratropics, we see a degradation of the forecast quality along the boundary currents as expected from the increase in the systematic errors.

Tropospheric ensemble skill

The continuous ranked probability score (CRPS) has been computed for a set of tropospheric variables (500 hPa geopotential, temperature and wind at 850 hPa and 200 hPa) to quantify the impact on the ensemble skill. The verification is against the analysis produced by the 38r2 rd e-suite. As the results for the boreal summer and the boreal winter periods are similar, we focus on the combined sample of 61 cases.

Scores in the extratropics display a neutral to small positive impact of coupling from initial time. Fig. 15 shows the CRPS of 500 hPa geopotential in the northern extratropics (20N–90N). A more substantial impact is evident in the tropics (Fig. 16). At later lead times, there is a considerable positive impact on the ensemble skill which is generally statistically significant after about day 7. There is also a minor negative impact in the lower troposphere at early lead times. This may be caused by the increased systematic difference between the coupled model and the analysis that uses observed SSTs. The ensemble spread is not changed significantly due to the coupling from initial time (not shown).

Additional insight into the geographical distribution of the impact can be obtained by studying maps of the change of the ensemble mean rms error. The improvement in the SST is mirrored in the temperature at 1000 hPa. In the tropics, coupling leads to a reduced rms error in the late medium-range (day 6 to 10), which is most pronounced over the Maritime continent. The winds in the lower troposphere improve over

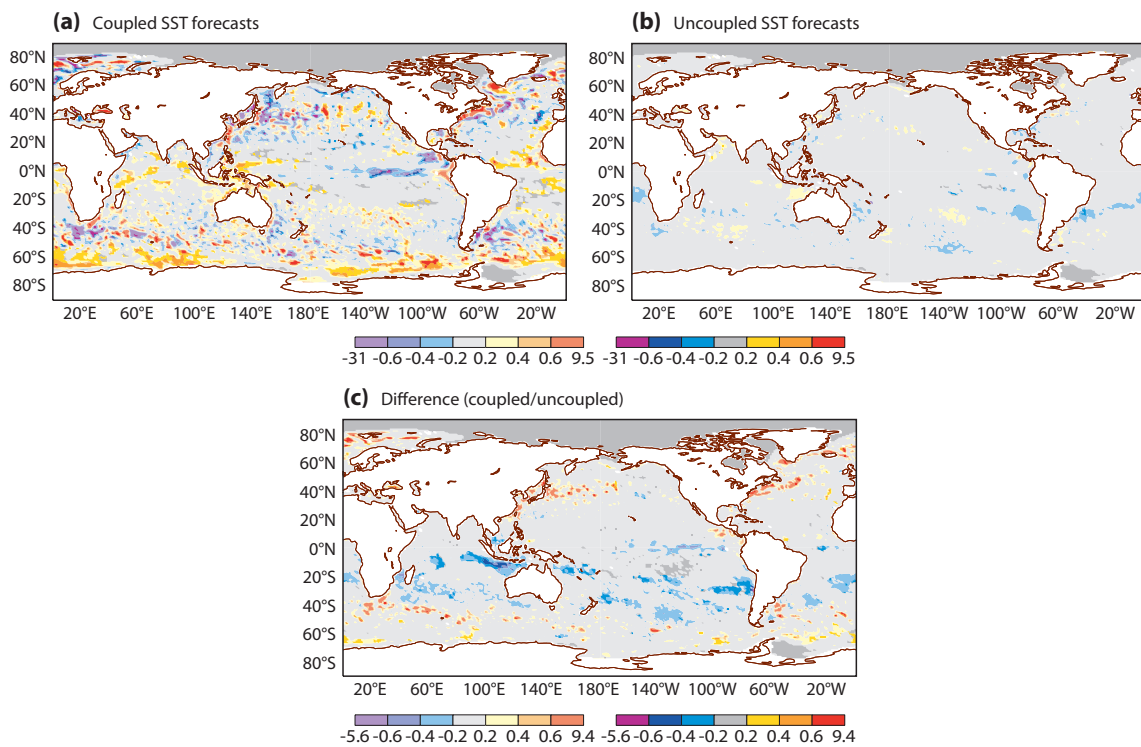


Figure 14: Mean error of 10-day ensemble mean forecast for (a) coupled and (b) uncoupled SST forecasts as well as (c) difference (coupled–uncoupled) in mean absolute error of day-10 ensemble mean forecasts. 33 cases in January–March 2012. Bold colours indicate statistical significance at the 95% level.

the Indian Ocean while the upper tropospheric winds improve more globally. Finally, there is a distinct reduction in error evident around 200 hPa east of the Himalayas for both temperature and zonal winds, but this change needs more diagnostics to understand the mechanisms behind and possible relations to the improvements over Indian Ocean and the Maritime continent.

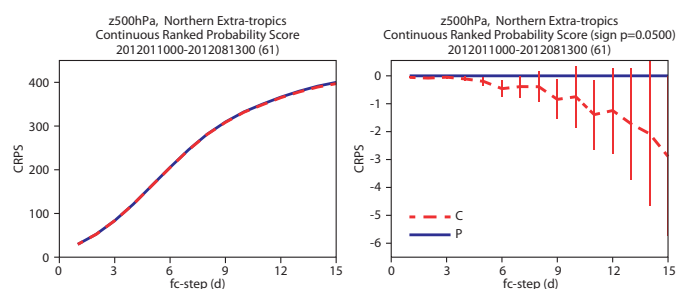


Figure 15: Impact of coupling with the ocean model from initial time on the continuous ranked probability score (CRPS) of 500 hPa geopotential in the northern extratropics (20N–90N). Panel (a) shows the CRPS of experiments \mathcal{C} and \mathcal{P} while (b) shows the CRPS difference between \mathcal{C} and \mathcal{P} with confidence intervals indicating the 95% probability level. Combined sample of 61 cases.

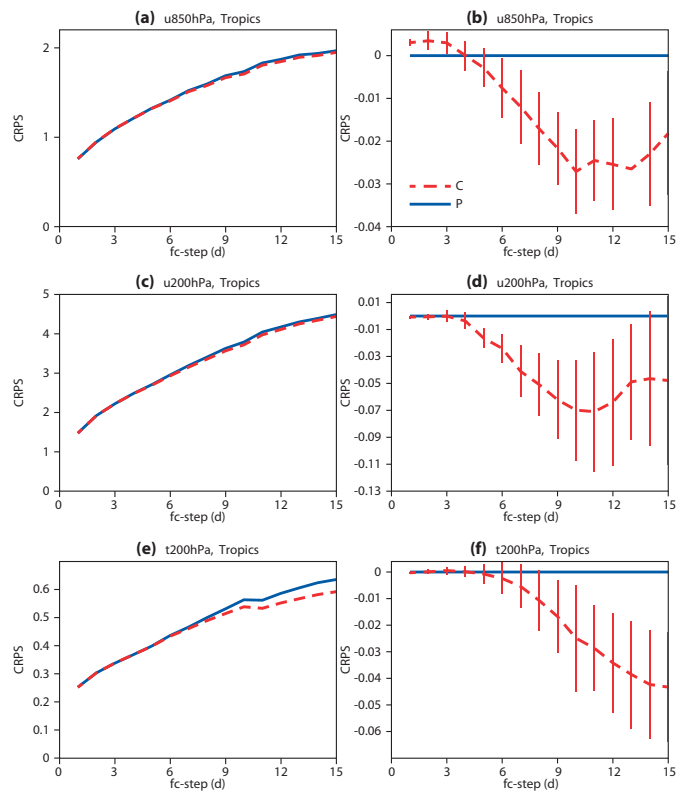


Figure 16: As previous figure but for the tropics and (a,b) zonal wind at 850 hPa, (c,d) zonal wind at 200 hPa and (e,f) temperature at 200 hPa.

6 Conclusions

In this paper an overview has been presented of the role ocean waves play in air-sea interaction, in particular for upper-ocean mixing and dynamics. We have studied the impact of sea-state dependent forcing, the Stokes-Coriolis force and the enhanced mixing by breaking ocean waves on the mean SST fields from NEMO in forced mode and in fully coupled integrations with the IFS-WAM-NEMO model. It is concluded that the sea-state dependent mixing is the main contributor to the impact on the ocean. Errors in SST obtained from standalone runs and from coupled simulations on the seasonal timescale show a certain degree of similarity. In the Summertime, in particular, the introduction of the sea-state dependent mixing gives a considerable improvement of the SST field and also of the seasonal cycle in, for example, the North Atlantic area. In addition, considerable improvements are found in the Kuro-Shio current and in the Gulfstream. Furthermore, impact on aspects of the ocean circulation such as the MOC were studied as well, but as far as we could see the sea-state dependent mixing did not influence the deep ocean.

It is, however, more difficult to assess whether sea state effects influence the skill of the seasonal forecasting system. At the moment there is weak evidence of improved skill in e.g. NINO3.4 and the North Atlantic area, but in other areas this is not so clear cut. However, as already pointed out in §4.2 the anomaly scores are obtained from SST's that have been corrected for the model drift, and therefore if the model drift is reduced this does not necessarily imply that there is improved skill. It is clear that more experimentation is required.

In the second part of this paper we have discussed possible benefits of coupling of the ocean and the

atmosphere from Day 0. Evidence has been presented that there are benefits for the prediction of hurricanes, for MJO prediction and there are also improvements in the skill of the ensemble prediction system, in particular in the tropics and to a lesser extent in the extra-tropics.

We conclude by pointing out that our work on the interaction of ocean waves and ocean circulation is still at its very beginning. Here, we have reported already some promising developments. Combined with the prospect of a sea-ice prediction capability and the prospect of a weakly coupled data assimilation system, very exciting times are indeed expected to lie ahead in the field of the interaction of ocean, atmosphere and ocean waves.

Acknowledgements. This work was partly supported by the European Union FP7 project MyWave (grant no 284455).

Appendix

A Supplementary Figures

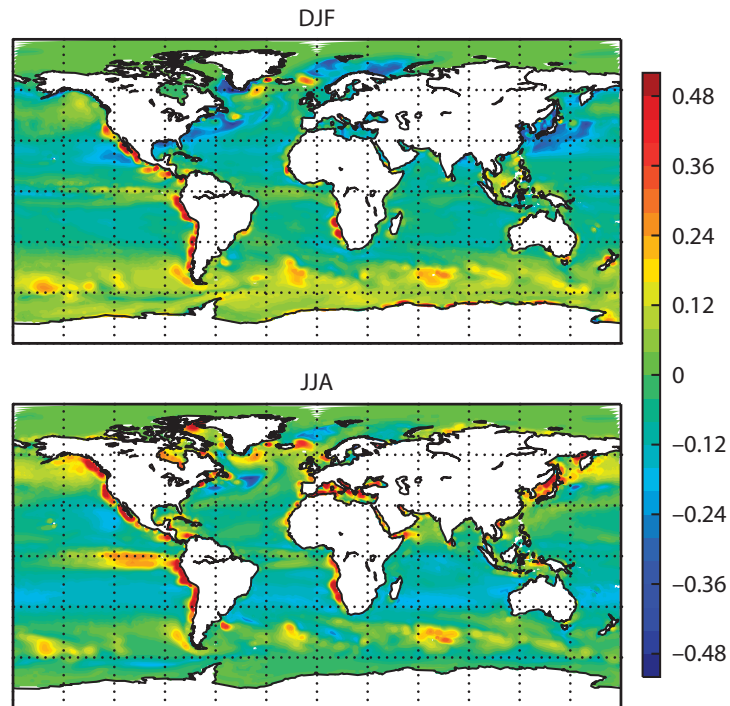


Figure A1: 20-yr average SST difference between CTRL (fsei) and a run with water-side stress from the ERA-Interim WAM model (TAUOC=fxdz).

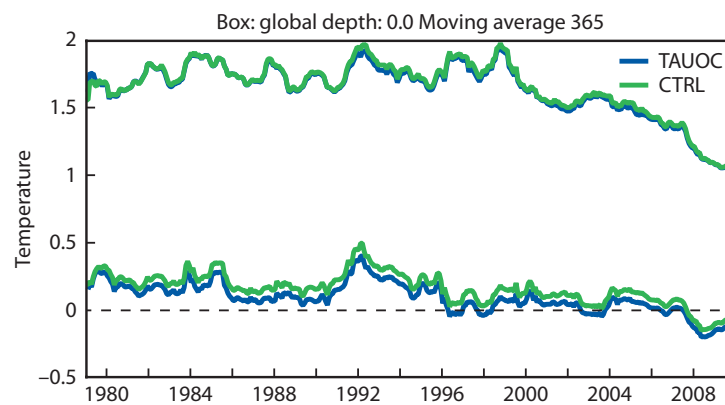


Figure A2: Time series of model bias (lower curves) and standard deviation (upper curves) for SST globally (CTRL=green, TAUOC=blue). A slight lowering of the bias is found. The trend is spurious and is the result of a substantial increase in observations over the model period.

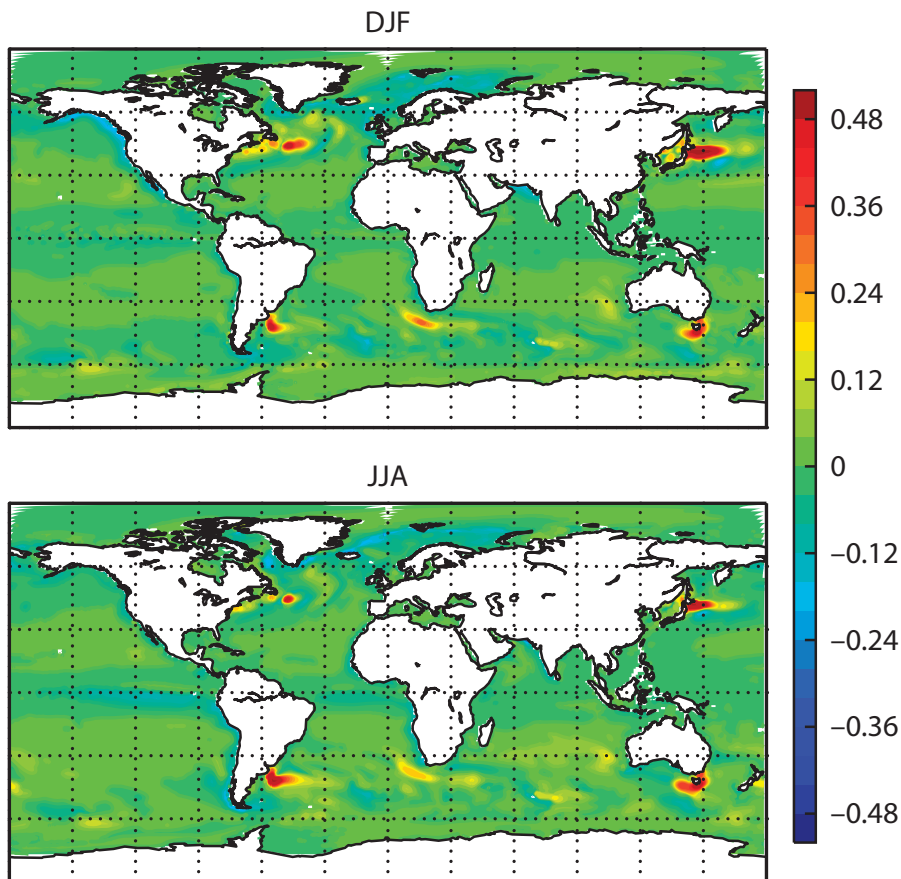


Figure A3: 20-yr average SST difference between CTRL (fsei) and a run with Stokes-Coriolis forcing as determined by the Stokes drift from the ERA-interim WAM model (STCOR=fsee). The differences are on the order of 0.5 K in the extratropics. The colour scale is ± 0.5 K.

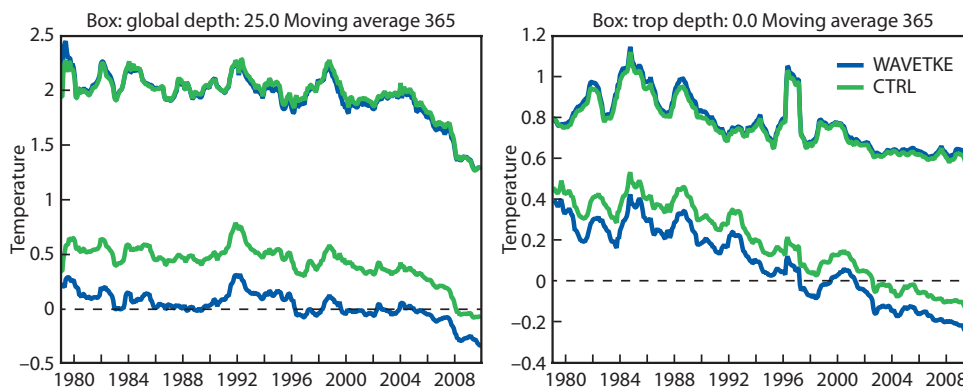


Figure A4: Panel a: Time series of model bias (lower curves) and standard deviation (upper curves) for observed temperature at 25 m depth globally (CTRL=green, TKEW=blue). Panel b: Same for surface temperature in the tropics. The trend is spurious and is the result of a substantial increase in observations over the model period. The bias at 25 m depth is greatly reduced most pronounced in the summer hemisphere, where the mixing is reduced, leading to higher SST.

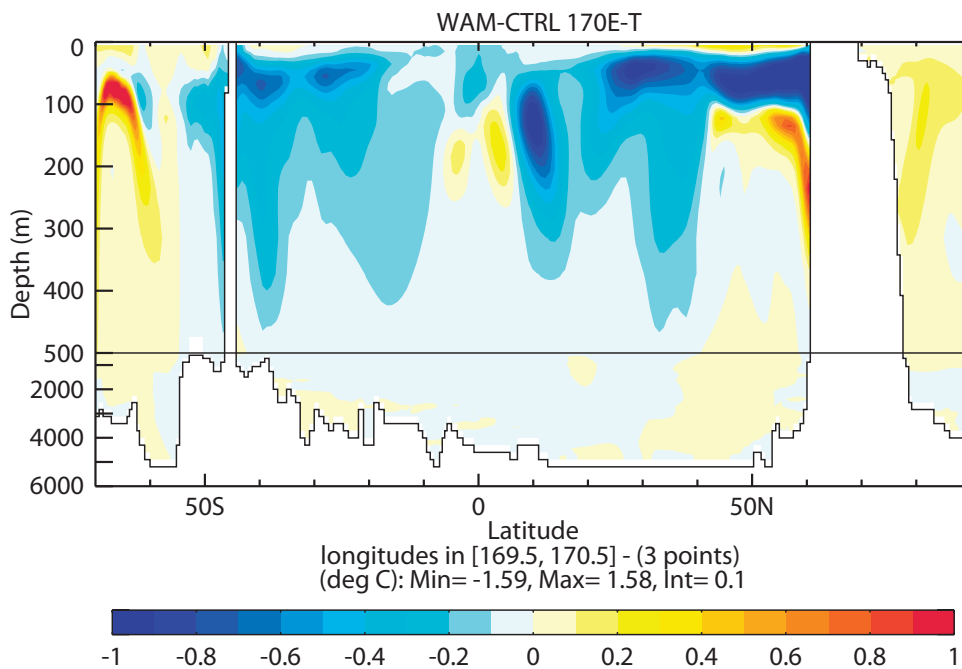


Figure A5: Panel a: Cross section at 170 E of the difference between temperature of WAM and CTRL. Impact of sea state dependent mixing is seen down to 400 m depth.

References

- Abramowitz, M., Stegun, I. A. (Eds.), 1972. Handbook of Mathematical Functions, with Formulas, Graphs, and Mathematical Tables. Dover, New York.
- Burchard, H., 2001. Simulating the Wave-Enhanced Layer under Breaking Surface Waves with Two-Equation Turbulence Models. *J. Phys. Oceanogr.* **31**, 3133-3145.
- Craig, P.D. and M.L. Banner, 1994. Modeling wave-enhanced turbulence in the ocean surface layer. *J. Phys. Oceanogr.* **24**, 2546-2559.
- Dee, D.P., S. M. Uppala, A. J. Simmons, P. Berrisford, P. Poli, S. Kobayashi, U. Andrae, M. A. Balmaseda, G. Balsamo, P. Bauer, P. Bechtold, A. C. M. Beljaars, L. van de Berg, J. Bidlot, N. Bormann, C. Delsol, R. Dragani, M. Fuentes, A. J. Geer, L. Haimberger, S. B. Healy, H. Hersbach, E. V. Hólm, L. Isaksen, P. Kållberg, M. Köhler, M. Matricardi, A. P. McNally, B. M. Monge-Sanz, J.-J. Morcrette, B.-K. Park, C. Peubey, P. de Rosnay, C. Tavalato, J.-N. Thépaut, F. Vitart, 2011. The ERA-Interim reanalysis: configuration and performance of the data assimilation system. *Quart. J. Roy. Meteor. Soc.*, **137**, 553-597.
- Edson, J., V. Jampana, R. Weller, S. Bigorre, A. Plueddemann, C. Fairall, S. Miller, L. Mahrt, D. Vickers, and H. Hersbach, 2013. On the exchange of Momentum over the open Ocean. *J. Phys. Oceanogr.*, doi:10.1175/JPO-D-12-0173.1, in press.
- Gemmrich, J., 2010. Strong turbulence in the Wave Crest Region, *J. Phys. Oceanogr.* **40**, 583-595.
- Gottschalk J., M. Wheeler, K. Weickmann, F. Vitart, N. Savage, H. Hendon, H. Lin, M. Flatau, D. Waliser, K. Sperber, W. Higgins and A. Vintzileos, 2009: Establishing and Assessing Operational Model

- MJO Forecasts: A Project of the CLIVAR Madden-Julian Oscillation Working Group. *Bull. Am. Meteor. Soc.*, **91**, 1247-1258.
- Grant A.L.M. and S.E. Belcher, 2009. Characteristics of Langmuir Turbulence in the Ocean Mixed layer, *J. Phys. Oceanogr.* **39**, 1871-1887.
- Hasselmann, K., 1970. Wave-driven inertial oscillations. *Geophys. Fluid Dyn.* **1**, 463-502.
- Hasselmann, K., 1971. On the mass and momentum transfer between short gravity waves and larger-scale motions. Part 1. *J. Fluid Mech.* **50**, 189-205.
- Janssen, Peter, 2004. *The interaction of Ocean Waves and Wind*. Cambridge University Press, 308+viii pp.
- Janssen, P., 2008. Air-sea interaction through waves. In: ECMWF Workshop on Ocean-Atmosphere Interactions, 10-12 November 2008. Available online at <http://www.ecmwf.int/publications/>. pp. 47-60.
- Janssen, P.A.E.M., 2012. Ocean wave effects on the daily cycle in SST. *J. Geophys. Res.*, **117**, C00J32, 24 pp., doi:10.1029/2012JC007943.
- Janssen, P.A.E.M. and P. Viterbo, 1996. Ocean Waves and the atmospheric Climate. *J. Climate* **9**, 1269-1287.
- Janssen, P.A.E.M., J.D. Doyle, J. Bidlot, B. Hansen, L. Isaksen and P. Viterbo, 2002: Impact and feedback of ocean waves on the atmosphere. in *Advances in Fluid Mechanics*, **33**, Atmosphere-Ocean Interactions, Vol. I, Ed. W.Petrie.
- Janssen, P.A.E.M., O. Sætra, C. Wettre, H. Hersbach and J. Bidlot, 2004. Impact of the sea state on the atmosphere and ocean. *Annales Hydrographiques 6e série*, **3** (772), 3,1,3,23.
- Jenkins, A.D., 1987a. A lagrangian model for wind- and wave-induced near-surface currents. *Coastal Engineering* **11**, 513-526.
- Komen, G.J., L. Cavaleri, M. Donelan, K. Hasselmann, S. Hasselmann, and P.A.E.M. Janssen, 1994: *Dynamics and Modelling of Ocean waves* (Cambridge University Press, Cambridge)
- Longuet-Higgins, M.S. and R.W. Stewart, 1961. The changes in amplitude of short gravity waves on steady non-uniform currents. *J. Fluid Mech.* **10**, 529-549.
- Magnusson, L., M. Alonso-Balmaseda, F. Molteni, 2012. On the dependence of ENSO simulation on the coupled model mean state. *Clim. Dyn.*, doi: 10.1007/s00382-012-1574-y
- Mastenbroek, C., G.J.H. Burgers and P.A.E.M. Janssen, 1993. The dynamical coupling of a wave model and a storm surge model through the atmospheric boundary layer. *J. Phys. Oceanogr.* **23**, 1856-1866.
- McWilliams, J.C., and J.M. Restrepo, 1999. The wave-driven ocean circulation. *J. Phys. Oceanogr.* **29**, 2523-2540.
- Mellor, G.L. and A. Blumberg, 2004. Wave breaking and Ocean Surface Layer Thermal Response. *J. Phys. Oceanogr.* **34**, 693-698.
- Mellor, G.L. and T. Yamada, 1982. Development of a turbulence closure model for geophysical fluid problems. *Rev. Geophys. Space Phys.* **20**, 851-875.
- Mogensen, K., S. Keeley and P. Towers, Coupling of the NEMO and IFS models in a single executable, ECMWF Technical Memorandum No 673, 2012.

- Moon, I., I. Ginis, T. Hara, and B. Thomas, 2007: Physics-based parameterization of air-sea momentum at high wind speeds and its impact on hurricane intensity predictions. *Mon. Wea. Rev.*, **135**, 2869-2878.
- Phillips, O.M., 1977. The dynamics of the upper ocean, Cambridge University Press, Cambridge, 336p.
- Rascle, N., Ardhuin, F. and E. Terray, 2006. Drift and mixing under the ocean surface: A coherent one-dimensional description with application to unstratified conditions. *J Geophys Res* 111 (C3), C03016, 16pp, doi:10.1029/2005JC003004.
- Reynolds RW, Rayner NA, Smith TM, C SD, Wang W. 2002. An improved in situ and satellite SST analysis for climate. *J. Climate*.**15**, 1609-1625.
- Saetra, Ø., Albrechtsen, J. and P. Janssen, 2007. Sea-State-Dependent Momentum Fluxes for Ocean Modeling. *J Phys Oceanogr* 37 (11), 2714-2725, doi:10.1175/2007JPO3582.1.
- Shay, L.K., G.J. Ginis and P.G. Black, 2000: Effects of a warm oceanic feature on hurricane Opal. *Mon. Wea. Rev.* **125(5)**, 1366-1383.
- Shay, L.K., and W. Uhlhorn, 2008: Loop Current response to hurricanes isodore and Lili. *Mon. Wea. Rev.*, **136**, 3248-3274.
- Terray, E.A., M.A. Donelan, Y.C. Agrawal, W.M. Drennan, K.K. Kahma, A.J. Williams, P.A. Hwang and S.A. Kitaigorodskii, 1996. Estimates of Kinetic Energy Dissipation under Breaking Waves. *J. Phys. Oceanogr.* **26**, 792-807.
- Wheeler, M.C. and H.H. Hendon, 2004: An all-season real-time multivariate MJO index: Development of an index for monitoring and prediction. *Mon. Wea. Rev.*, **132**, 1917-1932.
- Whitham, G.B. (1962). Mass, momentum and energy flux in water waves. *J. Fluid Mech.* **12**, 135-147.
- Whitham, G.B., 1974. *Linear and nonlinear waves*, Wiley, New York, 636p.
- Woolnough, S. J., F. Vitart and M. A. Balmaseda, 2007: The role of the ocean in the Madden-Julian Oscillation: Implications for MJO prediction. *Quart. J. Roy. Meteor. Soc.*, **133**, 117-128.
- Yablonski. R.M. and I. Ginis, 2008: Improving the initialization of coupled hurricane-ocean models by assimilating mesoscale oceanic features. *Mon. Wea. Rev.*, **136**, 2592-2607.

Heat-Budget Terms

Let's look at the factors influencing each term in the heat budget.

Factors Influencing Insolation Incoming solar radiation is primarily determined by latitude, season, time of day, and cloudiness. The polar regions are heated less than the tropics, areas in winter are heated less than the same area in summer, areas in early morning are heated less than the same area at noon, and cloudy days have less sun than sunny days.

The following factors are important:

1. The height of the sun above the horizon, which depends on latitude, season, and time of day. Don't forget, there is no insolation at night!
2. The length of day, which depends on latitude and season.
3. The cross-sectional area of the surface absorbing sunlight, which depends on height of the sun above the horizon.
4. Attenuation, which depends on: i) Clouds, which absorb and scatter radiation. ii) Path length through the atmosphere, which varies as $\csc \phi$, where ϕ is angle of the sun above the horizon. iii) Gas molecules which absorb radiation in some bands (figure 5.2). H_2O , O_3 , and CO_2 are all

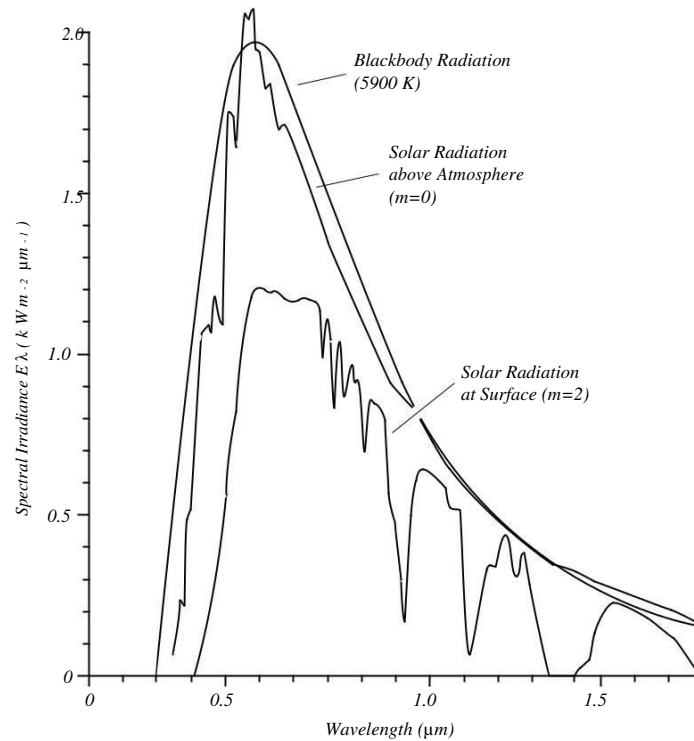


Figure 5.2 Insolation (spectral irradiance) of sunlight at top of the atmosphere and at the sea surface on a clear day. The dashed line is the best-fitting curve of blackbody radiation the size and distance of the sun. The number of standard atmospheric masses is designated by m . Thus $m = 2$ is applicable for sunlight when the sun is 30° above the horizon. After Stewart (1985: 43).

important. iv) Aerosols which scatter and absorb radiation. Both volcanic and marine aerosols are important. And v) dust, which scatters radiation, especially Saharan dust over the Atlantic.

5. Reflectivity of the surface, which depends on solar elevation angle and roughness of sea surface.

Solar inclination and cloudiness dominate. Absorption by ozone, water vapor, aerosols, and dust are much weaker.

The average annual value for insolation (figure 5.3) is in the range:

$$30 \text{ W/m}^2 < Q_{\text{SW}} < 260 \text{ W/m}^2 \quad (5.5)$$

Factors Influencing Infrared Flux The sea surface radiates as a blackbody having the same temperature as the water, which is roughly 290 K. The distribution of radiation as a function of wavelength is given by Planck's equation. Sea water at 290 K radiates most strongly at wavelengths near 10 μm . These wavelengths are strongly absorbed by clouds, and somewhat by water vapor. A plot of atmospheric transmittance as a function of wavelength for a clear

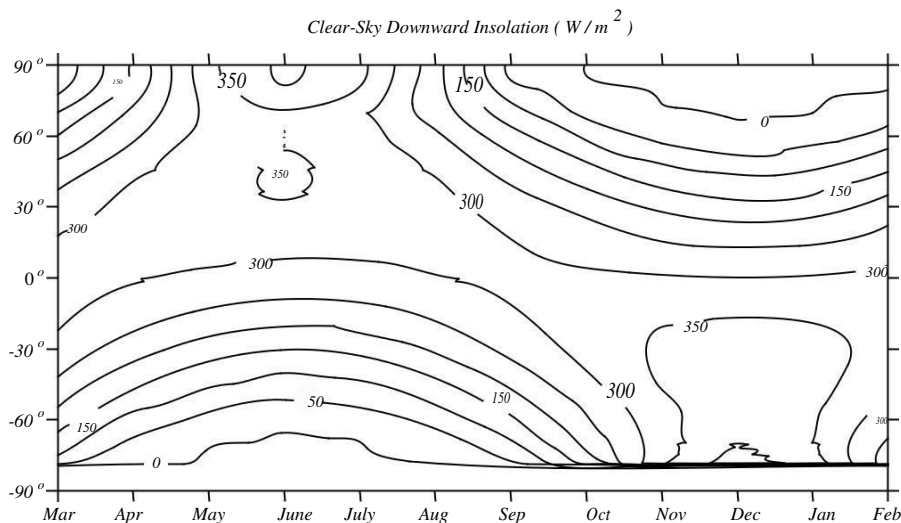


Figure 5.3 Monthly average of downward flux of sunlight through a cloud-free sky and into the ocean in W/m^2 during 1989 calculated by the Satellite Data Analysis Center at the nasa Langley Research Center (Darnell et al. 1992) using data from the International Satellite Cloud Climatology Project.

atmosphere but with varying amounts of water vapor (figure 5.4) shows the atmosphere is nearly transparent in some wavelength bands called windows.

The transmittance on a cloud-free day through the window from $8 \mu m$ to $13 \mu m$ is determined mostly by water vapor. Absorption in other bands, such as those at $3.5 \mu m$ to $4.0 \mu m$ depends on CO_2 concentration in the atmosphere. As the concentration of CO_2 increases, these windows close and more radiation is trapped by the atmosphere.

Because the atmosphere is mostly transparent to incoming sunlight, and somewhat opaque to outgoing infrared radiation, the atmosphere traps radiation. The trapped radiation, coupled with convection in the atmosphere, keeps earth's surface 33° warmer than it would be in the absence of a convecting, wet atmosphere but in thermal equilibrium with space. The atmosphere acts like the panes of glass on a greenhouse, and the effect is known as the **greenhouse effect**. See Hartmann (1994: 24–26) for a simple discussion of the radiative balance of a planet. CO_2 , water vapor, methane, and ozone are all important greenhouse gasses.

The net infrared flux depends on:

1. Clouds thickness. The thicker the cloud deck, the less heat escapes to space.
2. Cloud height, which determines the temperature at which the cloud radiates heat back to the ocean. The rate is proportional to t^4 , where t is the temperature of the radiating body in Kelvins. High clouds are colder than low clouds.
3. Atmospheric water-vapor content. The more humid the atmosphere the less heat escapes to space.

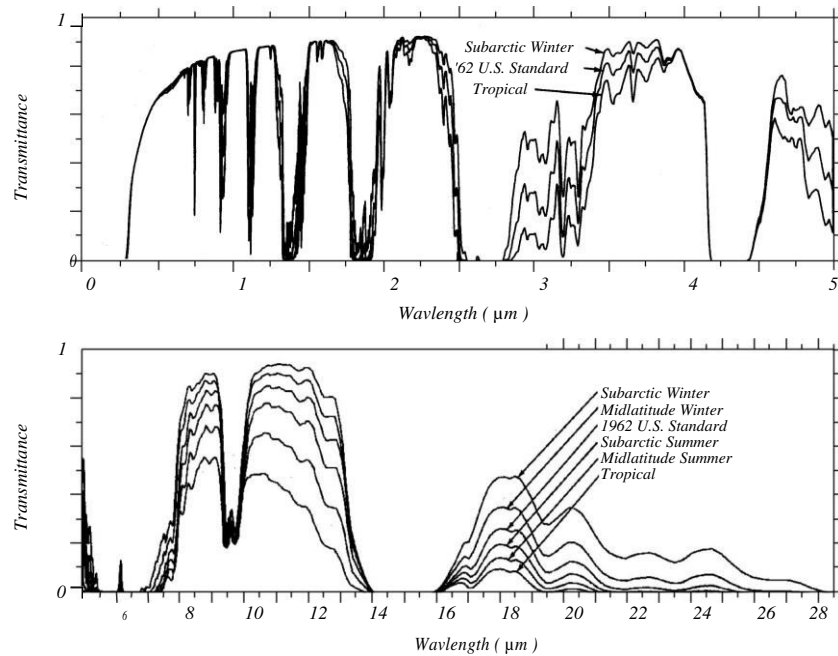


Figure 5.4 Atmospheric transmittance for a vertical path to space from sea level for six model atmospheres with very clear, 23 km, visibility, including the influence of molecular and aerosol scattering. Notice how water vapor modulates the transparency of the 10-14 μm atmospheric window, hence it modulates Q_{LW} , which is a maximum at these wavelengths. After Selby and McClatchey (1975).

4. Water Temperature. The hotter the water the more heat is radiated. Again, radiation depends of t^4 .
5. Ice and snow cover. Ice emits as a black body, but it cools much faster than open water. Ice-covered seas are insulated from the atmosphere.

Water vapor and clouds influence the net loss of infrared radiation more than surface temperature. Hot tropical regions lose less heat than cold polar regions. The temperature range from poles to equator is $0^\circ\text{C} < t < 25^\circ\text{C}$ or $273\text{K} < t < 298\text{K}$, and the ratio of maximum to minimum temperature in Kelvins is $298/273 = 1.092$. Raised to the fourth power this is 1.42. Thus there is a 42% increase in emitted radiation from pole to equator. Over the same distance water vapor can change the net emitted radiance by 200%.

The average annual value for net infrared flux is in the narrow range:

$$-60 \text{ W/m}^2 < Q_{LW} < -30 \text{ W/m}^2 \quad (5.6)$$

Factors Influencing Latent-Heat Flux Latent heat flux is influenced primarily by wind speed and relative humidity. High winds and dry air evaporate much more water than weak winds with relative humidity near 100%. In polar regions, evaporation from ice covered ocean is much less than from open water. In the arctic, most of the heat lost from the sea is through leads (ice-free areas). Hence the percent open water is very important for the arctic heat budget.

The average annual value for latent-heat flux is in the range:

$$-130 \text{ W/m}^2 < Q_L < -10 \text{ W/m}^2 \quad (5.7)$$

Factors Influencing Sensible-Heat Flux Sensible heat flux is influenced by wind speed and air-sea temperature difference. High winds and large temperature differences cause high fluxes. Think of this as a wind-chill factor for the ocean.

The average annual value for sensible-heat flux is in the range:

$$-42 \text{ W/m}^2 < Q_S < -2 \text{ W/m}^2 \quad (5.8)$$

Direct Calculation of Fluxes

Before we can describe the geographical distribution of fluxes into and out of the ocean, we need to know how they are measured or calculated.

Gust-Probe Measurements of Turbulent Fluxes There is only one accurate method for calculating fluxes of sensible and latent heat and momentum at the sea surface: from direct measurement of turbulent quantities in the atmospheric boundary layer made by gust probes on low-flying aircraft or offshore platforms. Very few such measurements have been made. They are expensive, and they cannot be used to calculate heat fluxes averaged over many days or large areas. The gust-probe measurements are used only to calibrate other methods of calculating fluxes.

1. Measurements must be made in the surface layer of the atmospheric boundary layer (See §4.3), usually within 30 m of the sea surface, because fluxes are independent of height in this layer.
2. Measurements must be made by fast-response instruments (gust probes) able to make several observations per second on a tower, or every meter from a plane.
3. Measurements include the horizontal and vertical components of the wind, the humidity, and the air temperature.

Fluxes are calculated from the correlation of vertical wind and horizontal wind, humidity, or temperature: Each type of flux is calculated from different measured variables, u , w , t , and q :

$$T = \overline{h \rho_a u' w' i} = \rho_a \overline{h u' w' i} \equiv \rho_a u'^2_* \quad (5.9a)$$

$$Q_S = C_p \overline{h \rho_a w' t' i} = \rho_a C_p \overline{h w' t' i} \quad (5.9b)$$

$$= L_E \overline{h w' q' i} \quad (5.9c)$$

where the brackets denotes time or space averages, and the notation is given in table 5.1. Note that **specific humidity** mentioned in the table is the mass of water vapor per unit mass of air.

Table 5.1 Notation Describing Fluxes

Symbol	Variable	Value and Units
C_p	Specific heat capacity of air	$1030 \text{ J} \cdot \text{kg}^{-1} \cdot \text{K}^{-1}$
C_D	Drag coefficient (see 4.3)	$(0.50 + 0.071 U_{10}) \times 10^{-3}$
C_L	Latent heat transfer coefficient	1.2×10^{-3}
C_S	Sensible heat transfer coefficient	1.0×10^{-3}
L_E	Latent heat of evaporation	$2.5 \times 10^6 \text{ J/kg}$
q	Specific humidity of air	$\text{kg (water vapor)/kg (air)}$
q_a	Specific humidity of air 10 m above the sea	$\text{kg (water vapor)/kg (air)}$
q_s	Specific humidity of air at the sea surface	$\text{kg (water vapor)/kg (air)}$
Q_S	Sensible heat flux	W/m^2
Q_L	Latent heat flux	W/m^2
T	Wind stress	Pascals
t_a	Temperature of the air 10 m above the sea	$\text{K or } ^\circ\text{C}$
t_s	Sea-surface temperature	$\text{K or } ^\circ\text{C}$
t'	Temperature fluctuation	$^\circ\text{C}$
u	Horizontal component of fluctuation of wind	m/s
u_*	Friction velocity	m/s
U_{10}	Wind speed at 10 m above the sea	m/s
w	Vertical component of wind fluctuation	m/s
ρ_a	Density of air	1.3 kg/m^3
\mathbf{T}	Vector wind stress	Pa

C_S and C_L from Smith (1988).

Radiometer Measurements of Radiative Fluxes Radiometers on ships, offshore platforms, and even small islands are used to make direct measurements of radiative fluxes. Wideband radiometers sensitive to radiation from $0.3 \mu\text{m}$ to $50 \mu\text{m}$ can measure incoming solar and infrared radiation with an accuracy of around 3% provided they are well calibrated and maintained. Other, specialized radiometers can measure the incoming solar radiation, the downward infrared radiation, and the upward infrared radiation.

Indirect Calculation of Fluxes: Bulk Formulas

The use of gust-probes is very expensive, and radiometers must be carefully maintained. Neither can be used to obtain long-term, global values of fluxes. To calculate these fluxes from practical measurements, we use observed correlations between fluxes and variables that can be measured globally.

For fluxes of sensible and latent heat and momentum, the correlations are called **bulk formulas**. They are:

$$T = \rho_a C_D U_{10}^2 \quad (5.10a)$$

$$Q_S = \rho_a C_p C_S U_{10} (t_s - t_a) \quad (5.10b)$$

$$Q_L = \rho_a L_E C_L U_{10} (q_s - q_a) \quad (5.10c)$$

Air temperature t_a is measured using thermometers on ships. It cannot be measured from space using satellite instruments. t_s is measured using thermometers on ships or from space using infrared radiometers such as the avhrr.

Table 5.2 Accuracy of Wind and Fluxes Observed Globally From Space

Variable	Accuracy	Comments
Wind Speed	± 1.5 m/s	Instrument Error
	± 1.5 m/s	Sampling Error (Monthly Average)
Wind Stress	± 10 %	Drag Coefficient Error
	± 14 Pa	Assuming 10 m/s Wind Speed
Insolation	± 5 %	Monthly Average
	± 15 W/m ²	Monthly Average
	± 10 %	Daily Average
Rain Rate	± 50 %	
Rainfall	± 10 %	5° × 5° area for trmm
Net Long Wave Radiation	$\pm 4-8$ %	Daily Average
	$\pm 15-27$ W/m ²	
Latent Heat Flux	± 35 W/m ²	Daily Average
	± 15 W/m ²	Monthly Average

The specific humidity of air at 10 m above the sea surface q_a is calculated from measurements of relative humidity made from ships. Gill (1982: pp: 39– 41, 43–44, & 605–607) describes equations relating water vapor pressure, vapor density, and specific heat capacity of wet air. The specific humidity at the sea surface q_s is calculated from t_s assuming the air at the surface is saturated with water vapor. U_{10} is measured or calculated using the instruments or techniques described in Chapter 4. Note that wind stress is a vector with magnitude and direction. It is parallel to the surface in the direction of the wind.

The problem now becomes: How to calculate the fluxes across the sea surface required for studies of ocean dynamics? The fluxes include: 1) stress; 2) solar heating; 3) evaporation; 4) net infrared radiation; 5) rain; 5) sensible heat; and 6) others such as CO₂ and particles (which produce marine aerosols). Furthermore, the fluxes must be accurate. We need an accuracy of approximately ± 15 W/m². This is equivalent to the flux of heat which would warm or cool a column of water 100 m deep by roughly 1 °C in one year. Table 5.2 lists typical accuracies of fluxes measured globally from space. Now, let's look at each variable.

The Equations of Motion

In this chapter I consider the response of a fluid to internal and external forces. This leads to a derivation of some of the basic equations describing ocean dynamics. In the next chapter, we will consider the influence of viscosity, and in chapter 12 we will consider the consequences of vorticity.

Fluid mechanics used in oceanography is based on Newtonian mechanics modified by our evolving understanding of turbulence. Conservation of mass, momentum, angular momentum, and energy lead to particular equations having names that hide their origins (table 7.1).

Table 7.1 Conservation Laws Leading to Basic Equations of Fluid Motion

Conservation of Mass:	Leads to Continuity Equation.
Conservation of Energy:	Conservation of heat leads to Heat Budgets.
	Conservation of mechanical energy leads to
	Wave Equation.
Conservation of Momentum:	Leads to Momentum (Navier-Stokes) Eq.
Conservation of Angular Momentum:	Leads to Conservation of Vorticity.

Dominant Forces for Ocean Dynamics

Only a few forces are important in physical oceanography: gravity, friction, and Coriolis (table 7.2). Remember that forces are vectors. They have magnitude and direction.

1. **Gravity** is the dominant force. The weight of the water in the ocean produces pressure. Changes in gravity, due to the motion of sun and moon relative to earth produces tides, tidal currents, and tidal mixing in the interior of the ocean.

Buoyancy is the upward or downward force due to gravity acting on a parcel of water that is more or less dense than other water at its level. For example, cold air blowing over the sea cools surface waters causing them

to be more dense than the water beneath. Gravity acting on the difference in density results in a force that causes the water to sink.

Horizontal pressure gradients are due to the varying weight of water in different regions of the ocean.

2. **Friction** is the force acting on a body as it moves past another body while in contact with that body. The bodies can be parcels of water or air.

Wind stress is the friction due to wind blowing across the sea surface. It transfers horizontal momentum to the sea, creating currents. Wind blowing over waves on the sea surface leads to an uneven distribution of pressure over the waves. The pressure distribution transfers energy to the waves, causing them to grow into bigger waves.

3. **Pseudo-forces** are apparent forces that arise from motion in curvilinear or rotating coordinate systems. For example, Newton’s first law states that there is no change in motion of a body unless a resultant force acts on it. Yet a body moving at constant velocity seems to change direction when viewed from a rotating coordinate system. The change in direction is due to a pseudo-force, the Coriolis force.

Coriolis Force is the dominant pseudo-force influencing motion in a coordinate system fixed to the earth.

Table 7.2 Forces in Geophysical Fluid Dynamics

Dominant Forces	
Gravity	Gives rise to pressure gradients, buoyancy, and tides.
Coriolis	Results from motion in a rotating coordinate system
Friction	Is due to relative motion between two fluid parcels. Wind stress is an important frictional force.
Other Forces	
Atmospheric Pressure	Results in inverted barometer effect.
Seismic	Results in tsunamis driven by earthquakes.

Note that the last two forces are much less important than the first three.

7.2 Coordinate System

Coordinate systems allow us to find locations in theory and practice. Various systems are used depending on the size of the features to be described or mapped. I will refer to the simplest systems; descriptions of other systems can be found in geography and geodesy books.

1. **Cartesian Coordinate System** is the one I will use most commonly in the following chapters to keep the discussion as simple as possible. We can describe most processes in Cartesian coordinates without the mathematical complexity of spherical coordinates. The standard convention in geophysical fluid mechanics is x is to the east, y is to the north, and z is up.

f-Plane is a Cartesian coordinate system in which the Coriolis force is assumed constant. It is useful for describing flow in regions small compared with the radius of the earth and larger than a few tens of kilometers.

β -plane is a Cartesian coordinate system in which the Coriolis force is assumed to vary linearly with latitude. It is useful for describing flow over areas as large as ocean basins.

2. **Spherical coordinates** are used to describe flows that extend over large distances and in numerical calculations of basin and global scale flows.

7.3 Types of Flow in the ocean

Many terms are used for describing the ocean circulation. Here are a few of the more commonly used terms for describing currents and waves.

1. **General Circulation** is the permanent, time-averaged circulation.
2. **Abysal** also called the **Deep Circulation** is the circulation of mass, in the meridional plane, in the deep ocean, driven by mixing.
3. **Wind-Driven Circulation** is the circulation in the upper kilometer of the ocean forced by the wind. The circulation can be caused by local winds or by winds in other regions.
4. **Gyres** are wind-driven cyclonic or anticyclonic currents with dimensions nearly that of ocean basins.

5. **Boundary Currents** are currents flowing parallel to coasts. Two types of boundary currents are important:

- Western boundary currents on the western edge of the ocean tend to be fast, narrow jets such as the Gulf Stream and Kuroshio.
- Eastern boundary currents are weak, e.g. the California Current.

6. **Squirts** or **Jets** are long narrow currents, with dimensions of a few hundred kilometers, that are nearly perpendicular to west coasts.

7. **Mesoscale Eddies** are turbulent or spinning flows on scales of a few hundred kilometers.

In addition to flow due to currents, there are many types of oscillatory flows due to waves. Normally, when we think of waves in the ocean, we visualize waves breaking on the beach or the surface waves influencing ships at sea. But many other types of waves occur in the ocean.

1. **Planetary Waves** depend on the rotation of the earth for a restoring force, and they including Rossby, Kelvin, Equatorial, and Yanai waves.
2. **Surface Waves** sometimes called gravity waves, are the waves that eventually break on the beach. The restoring force is due to the large density contrast between air and water at the sea surface.
3. **Internal Waves** are sub-sea wave similar in some respects to surface waves. The restoring force is due to change in density with depth.
4. **Tsunamis** are surface waves with periods near 15 minutes generated by earthquakes.
5. **Tidal Currents** are horizontal currents and currents associated with internal waves driven by the tidal potential.
6. **Edge Waves** are surface waves with periods of a few minutes confined to shallow regions near shore. The amplitude of the waves drops off exponentially with distance from shore.

7.4 Conservation of Mass and Salt

Conservation of mass and salt can be used to obtain very useful information about flows in the ocean. For example, suppose we wish to know the net loss of fresh water, evaporation minus precipitation, from the Mediterranean Sea. We could carefully calculate the latent heat flux over the surface, but there are probably too few ship reports for an accurate application of the bulk formula. Or we could carefully measure the mass of water flowing in and out of the sea through the Strait of Gibraltar, but the difference is small and perhaps impossible to measure accurately.

We can, however, calculate the net evaporation knowing the salinity of the flow in S_i and out S_o , together with a rough estimate of the volume of water V_o flowing out, where V_o is a volume flow in units of m^3/s (figure 7.1).

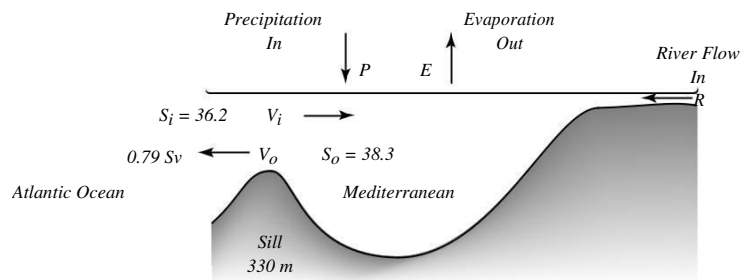


Figure 7.1 Schematic diagram of flow into and out of a basin.
Values from Bryden and Kinder (1991).

The mass flowing out is, by definition, $\rho_o V_o$. If the volume of the sea does not change, conservation of mass requires:

$$\rho_i V_i = \rho_o V_o \quad (7.1)$$

where, ρ_i , ρ_o are the densities of the water flowing in and out. We can usually assume, with little error, that $\rho_i = \rho_o$.

If there is precipitation P and evaporation E at the surface of the basin and conservation of mass becomes:

$$V_i + R + P = V_o + E \quad (7.2)$$

Solving for $(V_o - V_i)$:

$$V_o - V_i = (R + P) - E \quad (7.3)$$

which states that the net flow of water into the basin must balance precipitation plus river inflow minus evaporation when averaged over a sufficiently long time.

Because salt is not deposited or removed from the sea, conservation of salt requires :

$$\rho_i V_i S_i = \rho_o V_o S_o \quad (7.4)$$

Where ρ_i , S_i are the density and salinity of the incoming water, and ρ_o , S_o are density and salinity of the outflow. With little error, we can again assume that $\rho_i = \rho_o$.

An Example of Conservation of Mass and Salt Using the values for the flow at the Strait of Gibraltar measured by Bryden and Kinder (1991) and shown in figure 7.1, solving (7.4) for V_i assuming that $\rho_i = \rho_o$, and using the estimated value of V_o , gives $V_i = 0.836 Sv = 0.836 \times 10^6 \text{ m}^3/\text{s}$, where $Sv = \text{Sverdrup} = 10^6 \text{ m}^3/\text{s}$ is the unit of volume transport used in oceanography. Using V_i and V_o in (7.3) gives $(R + P - E) = -4.6 \times 10^4 \text{ m}^3/\text{s}$.

Knowing V_i we can also calculate a minimum flushing time for replacing water in the sea by incoming water. The minimum flushing time T_m is the volume of the sea divided by the volume of incoming water. The Mediterranean has a volume of around $4 \times 10^6 \text{ km}^3$. Converting $0.836 \times 10^6 \text{ m}^3/\text{s}$ to km^3/yr we obtain $2.64 \times 10^4 \text{ km}^3/\text{yr}$. Then, $T_m = 4 \times 10^6 \text{ km}^3 / 2.64 \times 10^4 \text{ km}^3/\text{yr}$

= 151 yr. The actual time depends on mixing within the sea. If the waters are well mixed, the flushing time is close to the minimum time, if they are not well mixed, the flushing time is longer.

Our example of flow into and out of the Mediterranean Sea is an example of a **box model**. A box model replaces large systems, such as the Mediterranean Sea, with boxes. Fluids or chemicals or organisms can move between boxes, and conservation equations are used to constrain the interactions within systems.

7.5 The Total Derivative (D/Dt)

If the number of boxes in a system increases to a very large number as the size of each box shrinks, we eventually approach limits used in differential calculus. For example, if we subdivide the flow of water into boxes a few meters on a side, and if we use conservation of mass, momentum, or other properties within each box, we can derive the differential equations governing fluid flow.

Consider the example of acceleration of flow in a small box of fluid. The resulting equation is called the **total derivative**. It relates the acceleration of a particle Du/Dt to derivatives of the velocity field at a fixed point in the fluid. We will use the equation to derive the equations for fluid motion from Newton's Second Law which requires calculating the acceleration of a particles passing a fixed point in the fluid.

We begin by considering the flow of a quantity q_{in} into and q_{out} out of the small box sketched in figure 7.2. If q can change continuously in time and space, the relationship between q_{in} and q_{out} is:

$$q_{out} = q_{in} + \frac{\partial q}{\partial t} \delta t + \frac{\partial q}{\partial x} \delta x \quad (7.5)$$

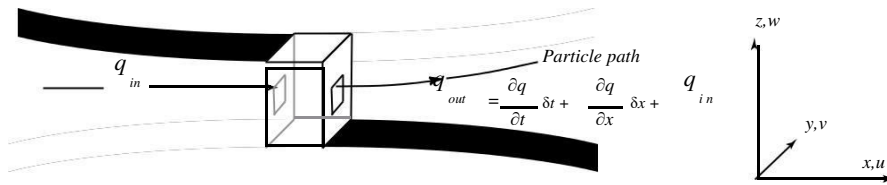


Figure 7.2 Sketch of flow used for deriving the total derivative.

The rate of change of the quantity q within the volume is:

$$\frac{Dq}{Dt} = \frac{q_{\text{out}} - q_{\text{in}}}{\delta t} = \frac{\partial q}{\partial t} + \frac{\partial q}{\partial x} \frac{\delta x}{\delta t} \quad (7.6)$$

But $\delta x/\delta t$ is the velocity u , and therefore:

$$\frac{Dq}{Dt} = \frac{\partial q}{\partial t} + u \frac{\partial q}{\partial x}$$

In three dimensions, the total derivative becomes:

$$\frac{D}{Dt} = \frac{\partial}{\partial t} + u \frac{\partial}{\partial x} + v \frac{\partial}{\partial y} + w \frac{\partial}{\partial z} \quad (7.7a)$$

$$\frac{D}{Dt} = \frac{\partial}{\partial t} + \mathbf{u} \cdot \nabla() \quad (7.7b)$$

where \mathbf{u} is the vector velocity and ∇ is the operator **del** of vector field theory (See Feynman, Leighton, and Sands 1964: 2–6).

This is an amazing result. Transforming coordinates from one following a particle to one fixed in space converts a simple linear derivative into a non-linear partial derivative. Now let's use the equation to calculate the change of momentum of a parcel of fluid.

7.6 Momentum Equation

Newton's Second Law relates the change of the momentum of a fluid mass due to an applied force. The change is:

$$\frac{D(m\mathbf{v})}{Dt} = \mathbf{F} \quad (7.8)$$

where \mathbf{F} is force, m is mass, and \mathbf{v} is velocity. I have emphasized the need to use the total derivative because we are calculating the force on a particle. We can assume that the mass is constant, and (7.8) can be written:

$$\frac{D\mathbf{v}}{Dt} = \frac{\mathbf{F}}{m} = \mathbf{f}_m \quad (7.9)$$

where \mathbf{f}_m is force per unit mass.

Four forces are important: pressure gradients, Coriolis force, gravity, and friction. Without deriving the form of these forces (the derivations are given in the next section), we can write (7.9) in the following form.

$$\frac{D\mathbf{v}}{Dt} = -\frac{1}{\rho} \nabla p - 2\boldsymbol{\Omega} \times \mathbf{v} + \mathbf{g} + \mathbf{F}_f \quad (7.10)$$

Acceleration equals the negative pressure gradient minus the Coriolis force plus gravity plus other forces. Here \mathbf{g} is acceleration of gravity, \mathbf{F}_f is friction, and the magnitude Ω of $\boldsymbol{\Omega}$ is the **Rotation Rate of earth**, 2π radians per sidereal day or

$$\Omega = 7.292 \times 10^{-5} \text{ radians/s} \quad (7.11)$$

Momentum Equation in Cartesian coordinates: Expanding the derivative in (7.10) and writing the components in a Cartesian coordinate system gives the **Momentum Equation**:

$$\frac{\partial u}{\partial t} + u \frac{\partial u}{\partial x} + v \frac{\partial u}{\partial y} + w \frac{\partial u}{\partial z} = -\frac{1}{\rho} \frac{\partial p}{\partial x} + 2 \Omega v \sin \phi + F_x \quad (7.12a)$$

$$\frac{\partial v}{\partial t} + u \frac{\partial v}{\partial x} + v \frac{\partial v}{\partial y} + w \frac{\partial v}{\partial z} = -\frac{1}{\rho} \frac{\partial p}{\partial y} - 2 \Omega u \sin \phi + F_y \quad (7.12b)$$

$$\frac{\partial w}{\partial t} + u \frac{\partial w}{\partial x} + v \frac{\partial w}{\partial y} + w \frac{\partial w}{\partial z} = -\frac{1}{\rho} \frac{\partial p}{\partial z} + 2 \Omega u \cos \phi - g + F_z \quad (7.12c)$$

where F_i are the components of any frictional force per unit mass, and ϕ is latitude. In addition, we have assumed that $w \ll v$, so the $2 \Omega w \cos \phi$ has been dropped from equation in (7.12a).

Equation (7.12) appears under various names. Leonhard Euler (1707–1783) first wrote out the general form for fluid flow with external forces, and the equation is sometimes called the **Euler equation** or the **acceleration equation**. Louis Marie Henri Navier (1785–1836) added the frictional terms, and so the equation is sometimes called the **Navier-Stokes equation**.

The term $2 \Omega u \cos \phi$ in (7.12c) is small compared with g , and it can be ignored in ocean dynamics. It cannot be ignored, however, for gravity surveys made with gravimeters on moving ships.

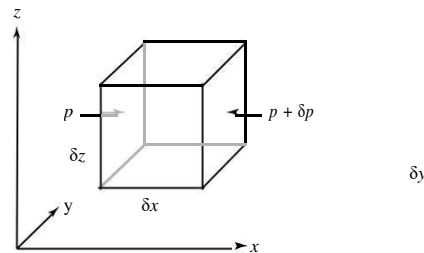


Figure 7.3 Sketch of flow used for deriving the pressure term in the momentum equation.

Derivation of Pressure Term Consider the forces acting on the sides of a small cube of fluid (figure 7.3). The net force δF_x in the x direction is

$$\delta F_x = p \delta y \delta z - (p + \delta p) \delta y \delta z$$

$$\delta F_x = -\delta p \delta y \delta z$$

But

$$\delta p = \frac{\partial p}{\partial x} \delta x$$

and therefore

$$\delta F_x = -\frac{\partial p}{\partial x} \delta x \delta y \delta z$$

$$\delta F_x = -\frac{\partial p}{\partial x} \delta V$$

Dividing by the mass of the fluid δm in the box, the acceleration of the fluid in the x direction is:

$$a_x = \frac{\delta F_x}{\delta m} = - \frac{\partial p}{\partial x} \frac{\delta V}{\delta m}$$

$$\boxed{a_x = - \frac{1}{\rho} \frac{\partial p}{\partial x}} \quad (7.13)$$

The pressure forces and the acceleration due to the pressure forces in the y and z directions are derived in the same way.

The Coriolis Term in the Momentum Equation The Coriolis term exists because we describe currents in a reference frame fixed on earth. The derivation of the Coriolis terms is not easy. Henry Stommel, the noted oceanographer at the Woods Hole Oceanographic Institution even wrote a book on the subject with Dennis Moore (Stommel & Moore, 1989).

Usually, we just state that the force per unit mass, the acceleration of a parcel of fluid in a rotating system, can be written:

$$\frac{D\mathbf{v}}{Dt}_{\text{fixed}} = \frac{D\mathbf{v}}{Dt}_{\text{rotating}} + (2\boldsymbol{\Omega} \times \mathbf{v}) + \boldsymbol{\Omega} \times (\boldsymbol{\Omega} \times \mathbf{R}) \quad (7.14)$$

where \mathbf{R} is the vector distance from the center of earth, $\boldsymbol{\Omega}$ is the angular velocity vector of earth, and \mathbf{v} is the velocity of the fluid parcel in coordinates fixed to earth. The term $2\boldsymbol{\Omega} \times \mathbf{v}$ is the Coriolis force, and the term $\boldsymbol{\Omega} \times (\boldsymbol{\Omega} \times \mathbf{R})$ is the centrifugal acceleration. The latter term is included in gravity (figure 7.4).

The Gravity Term in the Momentum Equation The gravitational attraction of two masses M_1 and m is:

$$\mathbf{F}_g = \frac{G M_1 m}{R^2}$$

where R is the distance between the masses, and G is the gravitational constant.

The vector force \mathbf{F}_g is along the line connecting the two masses.

The force per unit mass due to gravity is:

$$\frac{\mathbf{F}_g}{m} = \mathbf{g}_f = \frac{G M_E}{R^2} \quad (7.15)$$

where M_E is the mass of earth. Adding the centrifugal acceleration to (7.15) gives gravity \mathbf{g} (figure 7.4):

$$\mathbf{g} = \mathbf{g}_f - \boldsymbol{\Omega} \times (\boldsymbol{\Omega} \times \mathbf{R}) \quad (7.16)$$

Note that gravity does not point toward earth's center of mass. The centrifugal acceleration causes a plumb bob to point at a small angle to the line directed to earth's center of mass. As a result, earth's surface including the ocean's surface is not spherical but it is an oblate ellipsoid. A rotating fluid planet has an equatorial bulge.

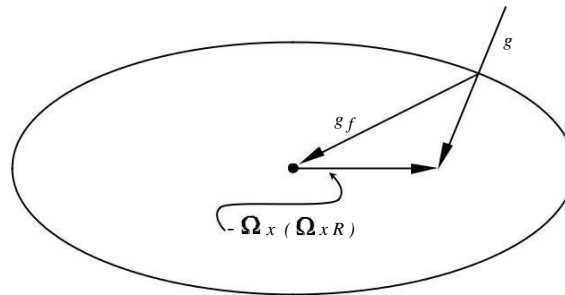


Figure 7.4 Downward acceleration g of a body at rest on earth's surface is the sum of gravitational acceleration between the body and earth's mass gf and the centrifugal acceleration due to earth's rotation $\Omega \times (\Omega \times R)$. The surface of an ocean at rest must be perpendicular to g , and such a surface is close to an ellipsoid of rotation. earth's ellipticity is greatly exaggerated here.

7.7 Conservation of Mass: The Continuity Equation

Now let's derive the equation for the conservation of mass in a fluid. We begin by writing down the flow of mass into and out of a small box (figure 7.5).

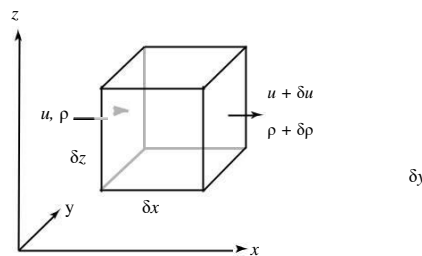


Figure 7.5 Sketch of flow used for deriving the continuity equation.

$$\begin{aligned} \text{Mass flow in} &= \rho u \delta z \delta y \\ \text{Mass flow out} &= (\rho + \delta\rho)(u + \delta u)\delta z \delta y \end{aligned}$$

The mass flux into the volume must be (mass flow out) - (mass flow in). There-fore,
 Mass flux = $(\rho \delta u + u \delta\rho + \delta\rho \delta u)\delta z \delta y$

But

$$\delta u = \frac{\partial u}{\partial x} \delta x; \quad \delta\rho = \frac{\partial \rho}{\partial x} \delta x$$

Therefore

$$\underline{\frac{\partial u}{\partial x}} \quad \underline{\frac{\partial \rho}{\partial x}} \quad \underline{\frac{\partial \rho}{\partial x} \frac{\partial u}{\partial x}}$$

$$\text{Mass flux} = \rho \frac{\partial u}{\partial x} + u \frac{\partial \rho}{\partial x} + \frac{\partial \rho}{\partial x} \frac{\partial u}{\partial x} \delta x \delta x \delta y \delta z$$

The third term inside the parentheses becomes much smaller than the first two terms as $\delta x \rightarrow 0$, and

$$\text{Mass flux} = \frac{\partial(\rho u)}{\partial x} \delta x \delta y \delta z$$

In three dimensions:

$$\text{Mass flux} = \frac{\partial(\rho u)}{\partial x} + \frac{\partial(\rho v)}{\partial y} + \frac{\partial(\rho w)}{\partial z} \delta x \delta y \delta z$$

The mass flux must be balanced by a change of mass inside the volume, which is:

$$\frac{\partial \rho}{\partial t} \delta x \delta y \delta z$$

and conservation of mass requires:

$$\frac{\partial \rho}{\partial t} + \frac{\partial(\rho u)}{\partial x} + \frac{\partial(\rho v)}{\partial y} + \frac{\partial(\rho w)}{\partial z} = 0 \quad (7.17)$$

This is the **continuity equation** for compressible flow, first derived by Leonhard Euler (1707–1783).

The equation can be put in an alternate form by expanding the derivatives of products and rearranging terms to obtain:

$$\frac{\partial \rho}{\partial t} + u \frac{\partial \rho}{\partial x} + v \frac{\partial \rho}{\partial y} + w \frac{\partial \rho}{\partial z} + \rho \frac{\partial u}{\partial x} + \rho \frac{\partial v}{\partial y} + \rho \frac{\partial w}{\partial z} = 0$$

The first four terms constitute the total derivative of density $D\rho/Dt$ from (7.7), and we can write (7.17) as:

$$\boxed{\frac{1}{\rho} \frac{D\rho}{Dt} + \frac{\partial u}{\partial x} + \frac{\partial v}{\partial y} + \frac{\partial w}{\partial z} = 0} \quad (7.18)$$

This is the alternate form for the continuity equation for a compressible fluid.

The Boussinesq Approximation Density is nearly constant in the ocean, and Joseph Boussinesq (1842–1929) noted that we can safely assume density is constant except when it is multiplied by g in calculations of pressure in the ocean. The assumption greatly simplifies the equations of motion.

Boussinesq's assumption requires that:

1. Velocities in the ocean must be small compared to the speed of sound c . This ensures that velocity does not change the density. As velocity approaches the speed of sound, the velocity field can produce large changes of density such as shock waves.
2. The phase speed of waves or disturbances must be small compared with c . Sound speed in incompressible flows is infinite, and we must assume the fluid is compressible when discussing sound in the ocean. Thus the approximation is not true for sound. All other waves in the ocean have speeds small compared to sound.
3. The vertical scale of the motion must be small compared with c^2/g , where g is gravity. This ensures that as pressure increases with depth in the ocean, the increase in pressure produces only small changes in density.

The approximations are true for oceanic flows, and they ensure that oceanic flows are incompressible. See Kundu (1990: 79 and 112), Gill (1982: 85), Batchelor (1967: 167), or other texts on fluid dynamics for a more complete description of the approximation.

Compressibility The Boussinesq approximation is equivalent to assuming sea water is incompressible. Now let's see how the assumption simplifies the continuity equation. We define the **coefficient of compressibility**

$$\beta = -\frac{1}{V} \frac{dV}{dp} = -\frac{1}{V} \frac{dV}{dt} \cdot \frac{dt}{dp}$$

where V is volume, and p is pressure. For incompressible flows, $\beta = 0$, and:

$$\frac{1}{V} \frac{dV}{dt} = 0$$

because $dp/dt \neq 0$. Remembering that density is mass m per unit volume V , and that mass is constant:

$$\frac{d}{dt} \left(\frac{m}{V} \right) = \frac{1}{V} \frac{dm}{dt} - \frac{m}{V^2} \frac{dV}{dt} = -\frac{1}{\rho} \frac{D\rho}{Dt} = 0$$

If the flow is incompressible, (7.18) becomes:

$$\frac{\partial u}{\partial x} + \frac{\partial v}{\partial y} + \frac{\partial w}{\partial z} = 0 \tag{7.19}$$

This is the **Continuity Equation for Incompressible Flows**.

7.8 Solutions to the Equations of Motion

Equations (7.12) and (7.19) are four equations, the three components of the momentum equation plus the continuity equation, with four unknowns: u, v, w, p . Note, however, that these are non-linear partial differential equations. Conservation of momentum, when applied to a fluid, converted a simple, first-order, ordinary, differential equation for velocity (Newton's Second Law), which is usually easy to solve, into a non-linear partial differential equation, which is almost impossible to solve.

Boundary Conditions: In fluid mechanics, we generally assume:

1. No velocity normal to a boundary, which means there is no flow through the boundary; and
2. No flow parallel to a solid boundary, which means no slip at the solid boundary.

Solutions We expect that four equations in four unknowns plus boundary conditions give a system of equations that can be solved in principle. In practice, solutions are difficult to find even for the simplest flows. First, as far as I know, there are no exact solutions for the equations with friction. There are very few exact solutions for the equations without friction. Those who are interested in ocean waves might note that one such exact solution is Gerstner's solution for water waves (Lamb, 1945: 251). Because the equations are almost impossible to solve, we will look for ways to greatly simplify the equations. Later, we will find that even numerical calculations are difficult.

Analytical solutions can be obtained for much simplified forms of the equations of motion. Such solutions are used to study processes in the ocean, including waves. Solutions for oceanic flows with realistic coasts and bathymetric features must be obtained from numerical solutions. In the next few chapters we seek solutions to simplified forms of the equations. In Chapter 15 we will consider numerical solutions.

7.9 Important Concepts

1. Gravity, buoyancy, and wind are the dominant forces acting on the ocean.
2. Earth's rotation produces a pseudo force, the Coriolis force.
3. Conservation laws applied to flow in the ocean lead to equations of motion. Conservation of salt, volume and other quantities can lead to deep insights into oceanic flow.
4. The transformation from equations of motion applied to fluid parcels to equations applied at a fixed point in space greatly complicates the equations of motion. The linear, first-order, ordinary differential equations describing Newtonian dynamics of a mass accelerated by a force become nonlinear, partial differential equations of fluid mechanics.
5. Flow in the ocean can be assumed to be incompressible except when describing sound. Density can be assumed to be constant except when density is multiplied by gravity g . The assumption is called the Boussinesq approximation.
6. Conservation of mass leads to the continuity equation, which has an especially simple form for an incompressible fluid.

UNIT – 5

Intertropical Convergence Zone

The ITCZ (Intertropical Convergence Zone) play important role in the global circulation system and also known as the Equatorial Convergence Zone or Intertropical Front. It is a basically low pressure belt encircling Earth near the Equator. It is a zone of convergence where the trade winds meet. Here, we are giving the concept, causes and impact of ITCZ (Intertropical Convergence Zone) for general awareness.

It is a zone between the northern and southern hemisphere where winds blowing equator-ward from the mid-latitudes and winds flowing pole ward from the tropics meet. It shifts from north and south seasonally according to the movement of the Sun. For Example- when the ITCZ is shifted to north of the Equator, the southeast trade wind changes to a southwest wind as it crosses the Equator. The ITCZ shifts only between 40° to 45° of latitude north or south of the equator based on the pattern of land and ocean

ITCZ (Intertropical Convergence Zone) is caused by the convergence of northeast and southeast trade winds in the area encircling Earth near the Equator. For better understanding, we must know about the trade winds and air masses.

It affects rainfall in equatorial region due to the variation of location resulting in the wet and dry seasons of the tropics rather than the cold and warm seasons of higher latitudes.

Tropical cyclones

Tropical cyclone, also called **typhoon** or **hurricane**, an intense circular storm that originates over warm tropical oceans and is characterized by low atmospheric pressure, high winds, and heavy rain. Drawing energy from the sea surface and maintaining its strength as long as it remains over warm water, a tropical cyclone generates winds that exceed 119 km (74 miles) per hour. In extreme cases winds may exceed 240 km (150 miles) per hour, and gusts may surpass 320 km (200 miles) per hour. Accompanying these strong winds are torrential rains and a

devastating phenomenon known as the storm surge, an elevation of the sea surface that can reach 6 metres (20 feet) above normal levels. Such a combination of high winds and water makes cyclones a serious hazard for coastal areas in tropical and subtropical areas of the world. Every year during the late summer months (July–September in the Northern Hemisphere and January–March in the Southern Hemisphere), cyclones strike regions as far apart as the Gulf Coast of North America, northwestern Australia, and eastern India and Bangladesh. Tropical cyclones are known by various names in different parts of the world. In the North Atlantic Ocean and the eastern North Pacific they are called hurricanes, and in the western North Pacific around the Philippines, Japan, and China the storms are referred to as typhoons. In the western South Pacific and Indian Ocean they are variously referred to as severe tropical cyclones, tropical cyclones, or simply cyclones. All these different names refer to the same type of storm.

Formation

The fuel for a tropical cyclone is provided by a transfer of water vapor and heat from the warm ocean to the overlying air, primarily by evaporation from the sea surface. As the warm, moist air rises, it expands and cools, quickly becoming saturated and releasing latent heat through the condensation of water vapor. The column of air in the core of the developing disturbance is warmed and moistened by this process. The temperature difference between the warm, rising air and the cooler environment causes the rising air to become buoyant, further enhancing its upward movement.

If the sea surface is too cool, there will not be enough heat available, and the evaporation rates will be too low to provide the tropical cyclone enough fuel. Energy supplies will also be cut off if the warm surface water layer is not deep enough, because the developing tropical system will modify the underlying ocean. Rain falling from the deep convective clouds will cool the sea surface, and the strong winds in the Centre of the storm will create turbulence. If the resulting mixing brings cool water from below the surface layer to the surface, the fuel supply for the tropical system will be removed.

The vertical motion of warm air is by itself inadequate to initiate the formation of a tropical system. However, if the warm, moist air flows into a preexisting atmospheric disturbance, further development will occur. As the rising air warms the core of the disturbance by both release of

latent heat and direct heat transfer from the sea surface, the atmospheric pressure in the centre of the disturbance becomes lower. The decreasing pressure causes the surface winds to increase, which in turn increases the vapor and heat transfer and contributes to further rising of air. The warming of the core and the increased surface winds thus reinforce each other in a positive feedback mechanism.

Anatomy of A Cyclone

The eye

A characteristic feature of tropical cyclones is the eye, a central region of clear skies, warm temperatures, and low atmospheric pressure. Typically, atmospheric pressure at the surface of Earth is about 1,000 millibars. At the centre of a tropical cyclone, however, it is typically around 960 millibars, and in a very intense “super typhoon” of the western Pacific it may be as low as 880 millibars. In addition to low pressure at the centre, there is also a rapid variation of pressure across the storm, with most of the variation occurring near the centre. This rapid variation results in a large pressure gradient force, which is responsible for the strong winds present in the eye wall

Horizontal winds within the eye, on the other hand, are light. In addition, there is a weak sinking motion, or subsidence, as air is pulled into the eye wall at the surface. As the air subsides, it compresses slightly and warms, so that temperatures at the centre of a tropical cyclone are some 5.5 °C (10 °F) higher than in other regions of the storm. Because warmer air can hold more moisture before condensation occurs, the eye of the cyclone is generally free of clouds. Reports of the air inside the eye being “oppressive” or “sultry” are most likely a psychological response to the rapid change from high winds and rain in the eyewall to calm conditions in the eye.

The eyewall

The most dangerous and destructive part of a tropical cyclone is the eye wall. Here winds are strongest, rainfall is heaviest, and deep convective clouds rise from close to Earth’s surface to a height of 15,000 metres (49,000 feet). As noted above, the high winds are driven by rapid changes in atmospheric pressure near the eye, which creates a large pressure gradient force.

Winds actually reach their greatest speed at an altitude of about 300 meters (1,000 feet) above the surface. Closer to the surface they are slowed by friction, and higher than 300 meters they are weakened by a slackening of the horizontal pressure gradient force. This slackening is related to the temperature structure of the storm. Air is warmer in the core of a tropical cyclone, and this higher temperature causes atmospheric pressure in the centre to decrease at a slower rate with height than occurs in the surrounding atmosphere. The lessened contrast in atmospheric pressure with altitude causes the horizontal pressure gradient to weaken with height, which in turn results in a decrease in wind speed.

Rainbands

In addition to deep convective cells (compact regions of vertical air movement) surrounding the eye, there are often secondary cells arranged in bands around the centre. These bands, commonly called rainbands, spiral into the centre of the storm. In some cases the rainbands are stationary relative to the centre of the moving storm, and in other cases they seem to rotate around the centre. The rotating cloudbands often are associated with an apparent wobbling of the storm track. If this happens as the tropical cyclone approaches a coastline, there may be large differences between the forecast landfall positions and actual landfall.

As a tropical cyclone makes landfall, surface friction increases, which in turn increases the convergence of airflow into the eyewall and the vertical motion of air occurring there. The increased convergence and rising of moisture-laden air is responsible for the torrential rains associated with tropical cyclones, which may be in excess of 250 mm (10 inches) in a 24-hour period. At times a storm may stall, allowing heavy rains to persist over an area for several days. In extreme cases, rainfall totals of 760 mm (30 inches) in a five-day period have been reported.

Classification

cyclones are classified on the basis of the wind speed.

Deep Depression: If the depression intensifies further then it will become a Deep Depression, which has speeds of between 32–38 mph (50–61 km/h).

Cyclonic storm: If the Deep Depression develops gale force wind speeds of between 39–54 mph (62–88 km/h), it is called a Cyclonic storm and the IMD assigns a name to it.

Severe Cyclonic Storm: Severe Cyclonic Storms have storm force wind speeds of between 55–72 mph (89–117 km/h)

Very Severe Cyclonic Storm: Very Severe Cyclonic Storms have hurricane-force winds of 73–102 mph (118–166 km/h).

Extremely Severe Cyclonic Storm: Extremely Severe Cyclonic Storms have hurricane-force winds of 166–221 km/h (104–137 mph).

Super Cyclonic Storm: The highest classification used in the North Indian Ocean is a Super Cyclonic Storm, which have hurricane-force winds of above 138 mph (222 km/h).

Storm surge

A **storm surge**, **storm flood** or **storm tide** is a coastal flood or tsunami-like phenomenon of rising water commonly associated with low pressure weather systems (such as tropical cyclones and strong extratropical cyclones), the severity of which is affected by the shallowness and orientation of the water body relative to storm path, as well as the timing of tides. Most casualties during tropical cyclones occur as the result of storm surges. It is a measure of the rise of water beyond what would be expected by the normal movement related to tides. Storm surge is caused primarily by the strong winds in a hurricane or tropical storm. The low pressure of the storm has minimal contribution!

Factors affecting

Central Pressure: Lower pressure will produce a higher surge. However, as was shown on page 2, the central pressure is a minimal contributor compared to the other factors.

Storm Intensity : Stronger winds will produce a higher surge. The two images below show how much storm surge is produced by two different storms, the second one having maximum winds that are 15 mph stronger than the first. All other variable are equal.

Storm Forward Speed : On the open coast, a faster storm will produce a higher surge. However, a higher surge is produced in bays, sounds, and other enclosed bodies of water with a slower

storm. The two images below show the surge generated by two hypothetical hurricanes hitting the Florida Panhandle— one moving 5 mph and the other 25 mph.

Angle of Approach: to Coast The angle at which a storm approaches a coastline can affect how much surge is generated. A storm that moves onshore perpendicular to the coast is more likely to produce a higher storm surge than a storm that moves parallel to the coast or moves inland at an oblique angle.

Size: A larger storm will produce higher surge. There are two reasons for this. First, the winds in a larger storm are pushing on a larger area of the ocean. Second, the strong winds in a larger storm will tend to affect an area longer than a smaller storm. Size is a key difference between the surge generated by storms like Katrina and Charley.

El Niño/Southern Oscillation (ENSO)

El Niño and the Southern Oscillation, also known as ENSO is a periodic fluctuation in sea surface temperature (El Niño) and the air pressure of the overlying atmosphere (Southern Oscillation) across the equatorial Pacific Ocean. This phenomenon has a major influence on climate patterns in various parts of the world. Scientific progress on the understanding and modelling of ENSO has improved prediction skills within a range of one to nine months in advance, helping society to prepare for the associated hazards such as heavy rains, floods and drought. El Niño and La Niña are the oceanic components while the Southern Oscillation is the atmospheric counterpart, thus giving rise to the term El Niño/Southern Oscillation.

Though ENSO is a single climate phenomenon, it has three states, or phases, it can be in. The two opposite phases, “El Niño” and “La Niña,” require certain changes in both the ocean **and** the atmosphere because ENSO is a *coupled* climate phenomenon. “Neutral” is in the middle of the continuum.

1. El Niño: A warming of the ocean surface, or above-average sea surface temperatures (SST), in the central and eastern tropical Pacific Ocean. Over Indonesia, rainfall tends to become reduced while rainfall increases over the tropical Pacific Ocean. The low-level surface winds, which normally blow from east to west along the equator (“easterly winds”), instead weaken or, in some cases, start blowing the other direction (from west to east or “westerly winds”).

2. La Niña: A cooling of the ocean surface, or below-average sea surface temperatures (SST), in the central and eastern tropical Pacific Ocean. Over Indonesia, rainfall tends to increase while rainfall decreases over the central tropical Pacific Ocean. The normal easterly winds along the equator become even stronger.
3. Neutral: Neither El Niño or La Niña. Often tropical Pacific SSTs are generally close to average. However, there are some instances when the ocean can look like it is in an El Niño or La Niña state, but the atmosphere is not playing along (or vice versa).

Weather forecasting techniques

Persistence

The simplest method of forecasting the weather, persistence, relies upon today's conditions to forecast the conditions tomorrow. This can be a valid way of forecasting the weather when it is in a steady state, such as during the summer season in the tropics. This method of forecasting strongly depends upon the presence of a stagnant weather pattern. Therefore, when in a fluctuating weather pattern, this method of forecasting becomes inaccurate. It can be useful in both short range forecasts and long range forecasts.

Use of a barometer

Measurements of barometric pressure and the pressure tendency (the change of pressure over time) have been used in forecasting since the late 19th century. The larger the change in pressure, especially if more than 3.5 hPa (2.6 mmHg), the larger the change in weather can be expected. If the pressure drop is rapid, a low pressure system is approaching, and there is a greater chance of rain. Rapid pressure rises are associated with improving weather conditions, such as clearing skies.

Looking at the sky

Along with pressure tendency, the condition of the sky is one of the more important parameters used to forecast weather in mountainous areas. Thickening of cloud cover or the invasion of a higher cloud deck is indicative of rain in the near future. High thin cirrostratus clouds can create halos around the sun or moon, which indicates an approach of a warm front and its associated rain. Morning fog portends fair conditions, as rainy conditions are preceded by wind or clouds that prevent fog formation. The approach of a line of thunderstorms could indicate the approach of a cold front. Cloud-free skies are indicative of fair weather for the near future. A bar can indicate a coming tropical cyclone. The use of sky cover in weather prediction has led to various weather lore over the centuries.

Nowcasting

The forecasting of the weather within the next six hours is often referred to as **nowcasting**. In this time range it is possible to forecast smaller features such as individual showers and thunderstorms with reasonable accuracy, as well as other features too small to be resolved by a

computer model. A human given the latest radar, satellite and observational data will be able to make a better analysis of the small scale features present and so will be able to make a more accurate forecast for the following few hours. However, there are now expert systems using those data and mesoscale numerical model to make better extrapolation, including evolution of those features in time.

Use of forecast models

In the past, the human forecaster was responsible for generating the entire weather forecast based upon available observations. Today, human input is generally confined to choosing a model based on various parameters, such as model biases and performance. Using a consensus of forecast. However, regardless how small the average error becomes with any individual system, large errors within any particular piece of guidance are still possible on any given model run. Humans are required to interpret the model data into weather forecasts that are understandable to the end user. Humans can use knowledge of local effects that may be too small in size to be resolved by the model to add information to the forecast. While increasing accuracy of forecast models implies that humans may no longer be needed in the forecast process at some point in the future, there is currently still a need for human intervention.

Analog technique

The analog technique is a complex way of making a forecast, requiring the forecaster to remember a previous weather event that is expected to be mimicked by an upcoming event. What makes it a difficult technique to use is that there is rarely a perfect analog for an event in the future. Some call this type of forecasting pattern recognition. It remains a useful method of observing rainfall over data voids such as oceans as well as the forecasting of precipitation amounts and distribution in the future. A similar technique is used in medium range forecasting, which is known as teleconnections, when systems in other locations are used to help pin down the location of another system within the surrounding regime. An example of teleconnections are by using El Niño-Southern Oscillation (ENSO) related phenomena.

Standard tool in weather forecasting

A **THERMOMETER** measures the air temperature. Most thermometers are closed glass tubes containing liquids such as alcohol or mercury. When air around the tube heats the liquid, the liquid expands and moves up the tube. A scale then shows what the actual temperature is.

A **BAROMETER** measures air pressure. It tells you whether or not the pressure is rising or falling. A rising barometer means sunny and dry conditions, while a falling barometer means stormy and wet conditions. An Italian scientist named Torricelli built the first barometer in 1643.

A **SLING PSYCHROMETER** measures relative humidity, using the cooling effect of evaporation. Two thermometers are used in a sling psychrometer. Wet the cloth of one of the thermometers and swing the psychrometer around a few times. Water evaporates from the cloth, causing the temperatures on that thermometer to be lower than the other.

A **RAIN GAUGE** measures the amount of rain that has fallen over a specific time period.

A **WIND VANE** is an instrument that determines the direction from which the wind is blowing.

An **ANEMOMETER** measures wind speed. The cups catch the wind, turning a dial attached to the instrument. The dial shows the wind speed.

A **WIND SOCK** is a conical textile tube, which resembles a giant sock, designed to indicate wind direction and relative wind speed.

WEATHER MAPS indicate atmospheric conditions above a large portion of the Earth's surface. Meteorologists use weather maps to forecast the weather.

A **HYGROMETER** measures the water vapor content of air or the humidity.

A **WEATHER BALLOON** measures weather conditions higher up in the atmosphere.

A **COMPASS** is a navigational instrument for finding directions.

WEATHER SATELLITES are used to photograph and track large-scale air movements. Then meteorologists compile and analyze the data with the help of computers.

Satellite in Weather Forecasting

The **weather satellite** is a type of satellite that is primarily used to monitor the weather and climate of the Earth. Satellites can be polar orbiting, covering the entire Earth asynchronously, or geostationary, hovering over the same spot on the equator.

Meteorological satellites see more than clouds and cloud systems: city lights, fires, effects of pollution, auroras, sand and dust storms, snow cover, ice mapping, boundaries of ocean currents, energy flows, etc. Other types of environmental information are collected using weather satellites. Weather satellite images helped in monitoring the volcanic ash cloud from Mount St. Helens and activity from other volcanoes such as Mount Etna.^[2] Smoke from fires in the western United States such as Colorado and Utah have also been monitored.

Types

Geostationary

Geostationary weather satellites orbit the Earth above the equator at altitudes of 35,880 km (22,300 miles). Because of this orbit, they remain stationary with respect to the rotating Earth and thus can record or transmit images of the entire hemisphere below continuously with their

visible-light and infrared sensors. The news media use the geostationary photos in their daily weather presentation as single images or made into movie loops. These are also available on the city forecast pages of www.noaa.gov (example Dallas, TX).

Polar orbiting

Polar orbiting weather satellites circle the Earth at a typical altitude of 850 km (530 miles) in a north to south (or vice versa) path, passing over the poles in their continuous flight. Polar orbiting weather satellites are in sun-synchronous orbits, which means they are able to observe any place on Earth and will view every location twice each day with the same general lighting conditions due to the near-constant local solar time. Polar orbiting weather satellites offer a much better resolution than their geostationary counterparts due their closeness to the Earth.

Uses

Snowfield monitoring, especially in the Sierra Nevada, can be helpful to the hydrologist keeping track of available snowpack for runoff vital to the watersheds of the western United States. This information is gleaned from existing satellites of all agencies of the U.S. government (in addition to local, on-the-ground measurements). Ice floes, packs and bergs can also be located and tracked from weather space craft.

Even pollution whether it is nature-made or man-made can be pinpointed. The visual and infrared photos show effects of pollution from their respective areas over the entire earth. Aircraft and rocket pollution, as well as condensation trails, can also be spotted. The ocean current and low level wind information gleaned from the space photos can help predict oceanic oil spill coverage and movement. Almost every summer, sand and dust from the Sahara Desert in Africa drifts across the equatorial regions of the Atlantic Ocean. GOES-EAST photos enable meteorologists to observe, track and forecast this sand cloud. In addition to reducing visibilities and causing respiratory problems, sand clouds suppress hurricane formation by modifying the solar radiation balance of the tropics. Other dust storms in Asia and mainland China are common and easy to spot and monitor, with recent examples of dust moving across the Pacific Ocean and reaching North America.

In remote areas of the world with few local observers, fires could rage out of control for days or even weeks and consume millions of acres before authorities are alerted. Weather satellites can

be a tremendous asset in such situations. Nighttime photos also show the burn-off in gas and oil fields. Atmospheric temperature and moisture profiles have been taken by weather satellites since 1969

Inter Tropical Convergence Zone (ITCZ),

The Intertropical Convergence Zone (ITCZ) is a zone of low-pressure near the equator where two easterly trade winds originating from the Northern and Southern hemispheres converge. This zone of enhanced convection, cloudiness, and rainfall constitutes the rising branch of the meridional Hadley circulation (Fig. 1.1). The non-uniform distribution of land and sea introduces zonal asymmetries in heating, which drive an eastwest overturning, known as the Walker circulation, wherein air rises at longitudes of the heating and sinks at the other longitudes. The three-quasi permanent centers of the rising branch of the Walker circulation are located over Indonesia, central Africa, and the Amazon basin (Fig. 1.2). From satellite data, the ITCZ can be identified as a meandering band of cold infrared effective temperature and high albedo located over the warmest equatorial region. The ITCZ plays an important role on the atmospheric energy balance (Waliser and Gautier 1993) and the earth's climate (Zhang 1993). The excessive heat absorbed at the surface over the tropical oceans is transferred to the lower troposphere through evaporation then transported to higher altitudes through convection and latent heat release and to higher latitudes through the Hadley circulation. The convective latent heat release plays a vital role in driving low-latitude circulations and in supplying energy to balance the radiative heat losses and 'fuel' the wind systems of middle and high latitudes. Furthermore, the enhanced cloudiness associated with convective cloud systems contributes significantly to the planetary albedo, absorptivity, and transmissivity of the incident solar radiation. Inside and outside the ITCZ, the fluxes of heat, moisture, and momentum and radiation through the ocean surface and in the atmosphere differ dramatically. Therefore, the structure, position, and migration of the ITCZ are important in defining and analyzing the earth's climate on a global scale. Accordingly, the strength and character of the air-sea coupling are important in determining the earth's climate on a local scale.

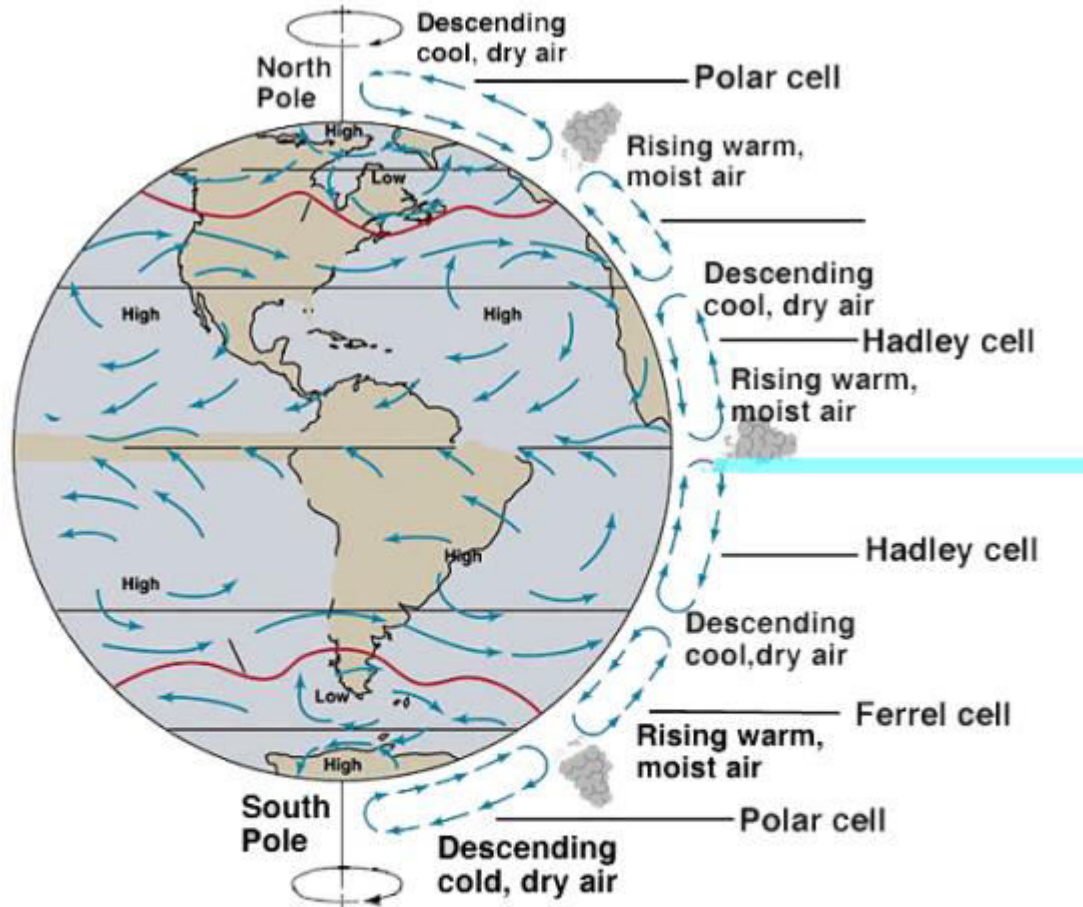


Figure 1.1. Schematic diagram of the Hadley circulation over the tropics which consists of rising air near the equator and sinking air at subtropical latitudes.

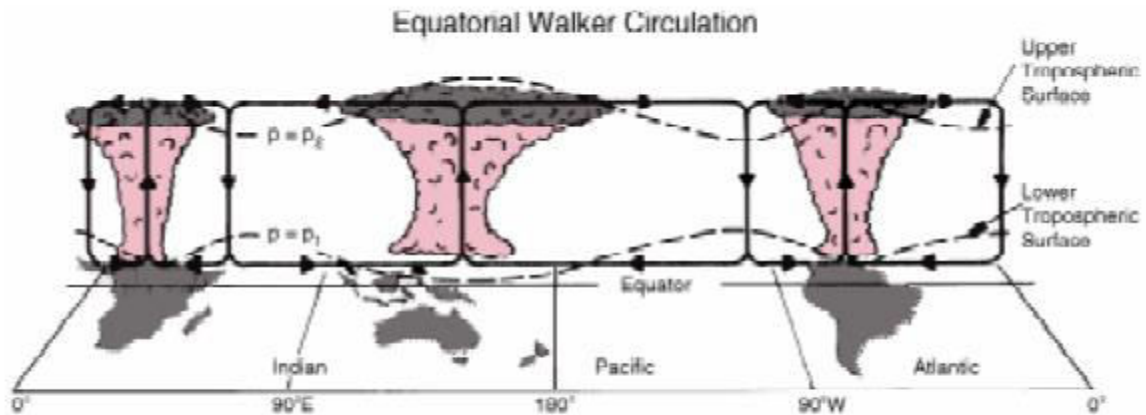


Figure 1.2. Schematic diagram of the Walker circulation along the equatorial region. Adapted from Salby (1992).

Nearly 45% of the world's population live in the tropics (World Bank Atlas, 1992). Almost all facets of societal and economic activities in the tropical countries are critically dependent on the climate variations in the regions. For example, the major agriculture productions in Asian countries can be accounted for by the fluctuation of the monsoon rainfall (World Market Atlas, 1992). Because of the strong linkage of the tropical climate to the rest of the world through coupling with the global climate and economic systems, variability in tropical climate affecting economic productivity will have major global impacts. Through the implications mentioned above, it is obvious that advanced understanding and better predictions of the tropical climate will greatly benefit the social and economic aspects not only for the population in the tropical region, but also for the whole world.

A considerable number of observational and theoretical studies on many aspects concerning the ITCZ have been undertaken over the last few decades. The emergence of satellite era with its broad spatial coverage and long period of records has produced the capability to estimate tropical convection with a variety of spatial and temporal scales (Winston and Krueger 1977; Heddinghaus and Krueger 1981; Waliser and Gautier 1993; Waliser et al. 1993). Therefore, rain estimation based on satellite-derived infra red and visible data appears to be the only way to obtain for a long continuous period over tropical oceans and inaccessible parts of land masses, though it is recognized that additional information derived from passive and active microwave sensors must be added to improve quantitative measurement of tropical rainfall (Simpson et al. 1988). On the theoretical side, the understanding gained from analytical and numerical modeling approaches have considerably advanced the knowledge of the physical processes of the tropical convection (Pike 1972; Ramage 1974; Helfand 1979; Rind and Rossow 1984; Lipps and Hemler 1986; Xie and Philander 1994; Xie 1996; Oort and Yienger 1996; Liu 1997). However, the complex interactions between the atmosphere, oceans, and land masses remain an outstanding

challenging problem for the understanding of the tropical climate. Observations readily verify this complexity. It appears that there is a distinct mode preference in response to the large-scale structure of the tropical atmosphere. Such preference scale would be described by the simple and linear dynamic methods. But, the tropical convection composes a wide spectrum of phenomenon that spans spatial scales ranging from planetary to mesoscale and time scales ranging from interannual to diurnal. The most dramatic, most energetic, and best-defined pattern of interannual variability in the tropics is the global set of climate anomalies referred to as El Niño/Southern Oscillation (ENSO). The ENSO-related changes in precipitation, temperature, and other environmental variables have both direct effects (through drought, flood, and extreme weather events) and indirect effects (through changes in transmission and outbreaks of infectious diseases) on human life as well as economic activities. Based on research achievements over the past fifteen years, scientist can now offer skillful experimental forecast of ENSO. Improved climate predictions related with ENSO, furthermore, will provide early warning of extreme climate events, and, thereby, reduce both societal and economic vulnerability. In view of the above considerations, the results of this study may have some practical implications. Based on improved analyses and modeling methods, the climate variations associated with the ITCZ in the tropics could be predicted, tested, and adjusted. The results could be made available as input information for the government, private organizations, and the public at large so as to adapt their plans and activities accordingly and to the best interest of the people. More specifically, this research aims to address six different tasks:

1. fundamental characteristics of the global ITCZ, such as the climatology, the standard deviation, the coefficient of variation, the meridional profiles, and the spatial and temporal variability.
 2. the role of large-scale atmospheric circulation and sea surface temperature on tropical convection over the tropical Indian, western Pacific, central Pacific, eastern Pacific, and Atlantic oceans.
 3. the relationships between sea surface temperature anomalies over the Pacific Ocean and convective anomalies over Indonesia during ENSO events and their longterm prediction.
 4. the physical processes and dynamical interpretations of the ITCZ over the Indian Ocean and Indonesia during a normal and during an ENSO event.
 5. the importance of meteorological processes associated with transport of air masses during forest fires in Indonesia.
 6. the planetary boundary structure over the Indian Ocean and its role on the connection between continental emissions and impacts over the ITCZ.
- To achieve these objectives, a hierarchy of methodologies from simple statistical analysis to intermediate numerical simulation is utilized. The statistical analysis including its key objectives - data reduction, inference, and the identification of relationships - is performed to provide a basic representation of observations. Meanwhile, the numerical simulation is used when the complexity and non-linearity of the air-sea-land interactions pose great difficulties if simple models are used.

Tropical cyclones- formation, classification and structure

- Tropical cyclones are violent storms that originate over oceans in **tropical areas** and move over to the coastal areas bringing about large scale destruction due to violent winds (squalls), very heavy rainfall (torrential rainfall) and **storm surge**.
- They are irregular wind movements involving **closed circulation** of air around a low pressure center. This closed air circulation (whirling motion) is a result of **rapid upward movement of hot air** which is subjected to Coriolis force. The low pressure at the center is responsible for the wind speeds.

Squall == a sudden violent gust of wind or localized storm, especially one bringing rain, snow, or sleet.

Torrent == a strong and fast-moving stream of water or other liquid.

- The cyclonic wind movements are **anti-clockwise in the northern hemisphere** and **clockwise in the southern hemisphere** (This is due to Coriolis force).
- The cyclones are often characterized by existence of an anticyclone between two cyclones.

Conditions Favourable for Tropical Cyclone Formation

1. Large sea surface with temperature higher than **27° C**,
2. Presence of the Coriolis force enough to create a cyclonic vortex,
3. Small variations in the vertical wind speed,
4. A pre-existing weak low-pressure area or low-level-cyclonic circulation,
5. Upper divergence above the sea level system,

Good Source of Latent Heat

- Ocean waters having temperatures of 27° C or more is the source of moisture which feeds the storm. The condensation of moisture releases enough latent heat of condensation to drive the storm.

Why tropical cyclones form mostly on the western margins of the oceans? OR

Why tropical cyclones don't form in the eastern tropical oceans?

- The depth of warm water (**26-27°C**) should extend for **60-70 m** from surface of the ocean/sea, so that deep convection currents within the water do not churn and mix the cooler water below with the warmer water near the surface.
- The above condition occurs only in western tropical oceans because of warm ocean currents (easterly trade winds pushes ocean waters towards west) that flow from east towards west forming a thick layer of water with temperatures greater than 27°C. This supplies enough moisture to the storm.
- The **cold currents** lower the surface temperatures of the eastern parts of the tropical oceans making them unfit for the breeding of cyclonic storms.

[One Exception: During strong El Niño years, strong hurricanes occur in the eastern Pacific. This is due to the accumulation of warm waters in the eastern Pacific due to **weak Walker Cell**]

Why cyclones occur mostly in late summers?

- Whirling motion is enhanced when the **doldrums** (region within ITCZ) over oceans are farthest from the equator. This happens during the autumnal equinox (August-September). At this time, there are two advantages—the air is overheated and the sun is exactly over the equator.

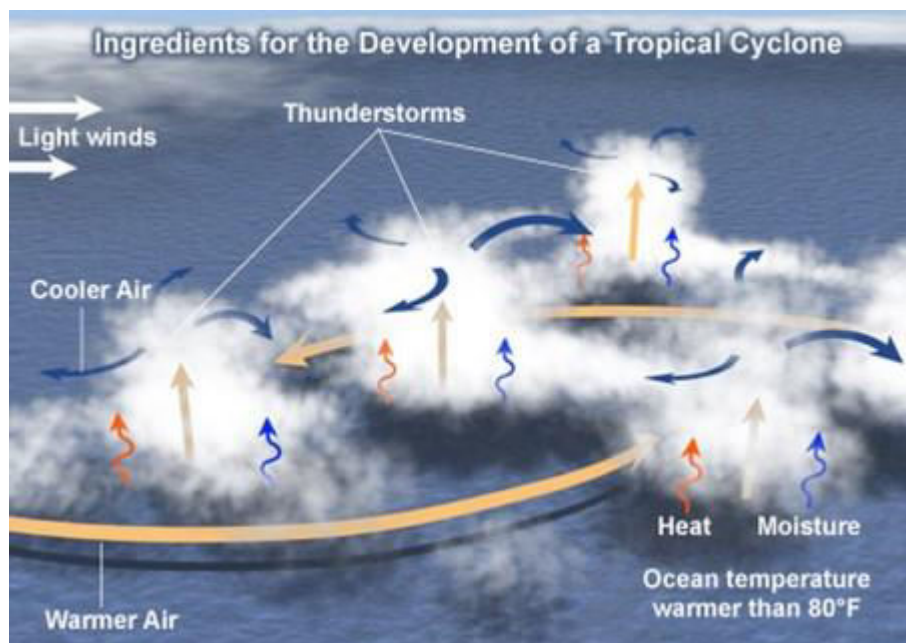
[Due to high specific heat of water, and mixing, the ocean waters in northern hemisphere attain maximum temperatures in August. (Continents attain maximum temperatures in June-July)]

Coriolis Force (f)

- The **Coriolis force is zero at the equator (no cyclones at equator because of zero Coriolis Force)** but it increases with latitude. Coriolis force at 5° latitude is significant enough to create a storm [cyclonic vortex].
- **About 65 per cent of cyclonic activity occurs between 10° and 20° latitude.**

Low-level Disturbances

- Low-level disturbance (thunderstorms – they are the seeds of cyclones) in the form of easterly wave disturbances in the Inter-Tropical Convergence Zone (ITCZ) should pre-exist.



- **Small local differences** in the temperature of water and of air produce various **low pressure centers** of small size. A weak cyclonic circulation develops around these areas.
- Then, because of the rising warm humid air, a true cyclonic vortex may develop very rapidly. However, only a few of these disturbances develop into cyclones.

[rising of humid air => adiabatic lapse rate => fall in temperature of air => condensation of moisture in air => latent heat of condensation released => air gets more hot and lighter => air is further uplifted => more air comes in to fill the gap => new moisture available for condensation => latent heat of condensation and the cycle repeats]

Temperature contrast between air masses

- Trade winds from both the hemispheres meet along inter-tropical front. Temperature contrasts between these air masses must exist when the ITCZ is farthest, from the equator.
- Thus, the convergence of these air masses of different temperatures and the resulting instability are the prerequisites for the origin and growth of violent tropical storms.

Upper Air Disturbance

- The remains of an upper tropospheric cyclone from the Westerlies move deep into the tropical latitude regions. As divergence prevails on the eastern side of the troughs, a rising motion occurs; this leads to the development of thunderstorms.
- Further, these old abandoned troughs (remnants of temperate cyclones) usually have cold cores, suggesting that the environmental lapse rate is steeper and unstable below these troughs. Such instability encourages thunderstorms (child cyclones).



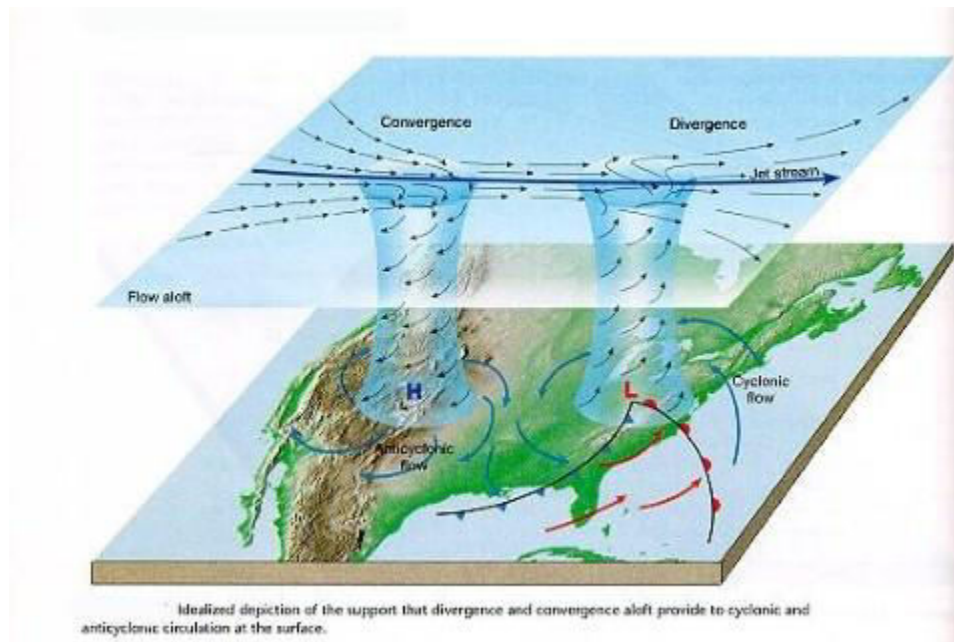
Vorticity provided by flow in the jet stream generates cyclonic flow near a trough and anticyclonic flow adjacent to a ridge.

Wind Shear

- Wind Shear == differences between wind speeds at different heights.
- Tropical cyclones develop when the wind is uniform.
- **Because of weak vertical wind shear, cyclone formation processes are limited to latitude equator ward of the [subtropical jet stream](#). [Jet streams]**
- In the temperate regions, wind shear is high due to westerlies and this inhibits convective cyclone formation.

Upper Tropospheric Divergence

- A well – developed divergence in the upper layers of the atmosphere is necessary so that the rising air currents within the cyclone continue to be pumped out and a low pressure maintained at the center.



Humidity Factor

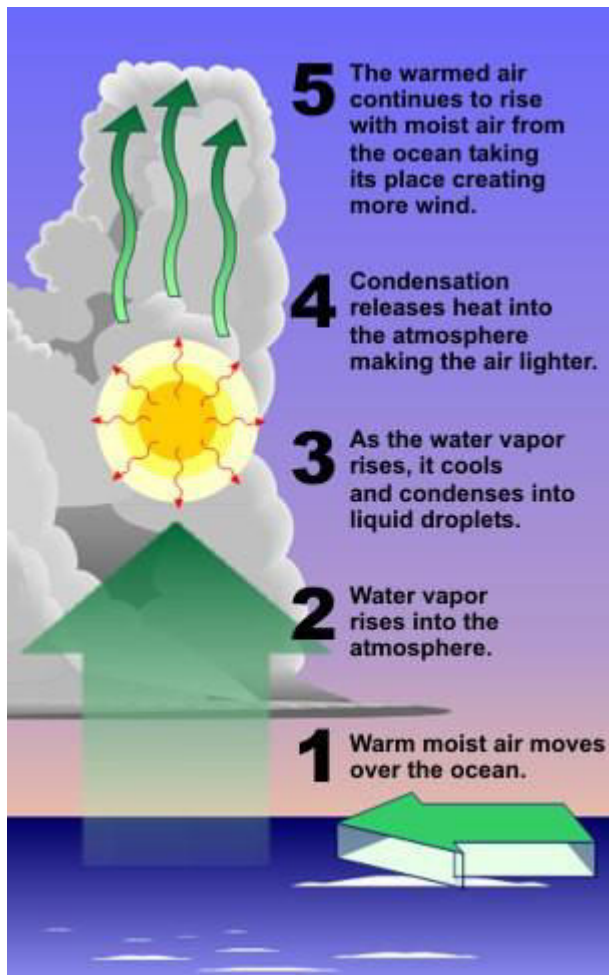
- High humidity (around 50 to 60 per cent) is required in the mid-troposphere, since the presence of moist air leads to the formation of [cumulonimbus cloud](#).
- Such conditions exist over the equatorial **doldrums**, especially in western margins of oceans (this is because of east to west movement of ocean currents), which have great moisture, carrying capacity because the **trade winds** continuously replace the saturated air.

Origin and Development of Tropical Cyclones

- The tropical cyclones have a **thermal origin**, and they develop over tropical seas during late summers (August to mid-November).
- At these locations, the strong local convective currents acquire a whirling motion because of the Coriolis force.
- After developing, these cyclones advance till they find a weak spot in the trade wind belt.

Origin

- Under favorable conditions, multiple thunderstorms originate over the oceans. These thunderstorms merge and create an intense low pressure system (wind is warm and lighter).



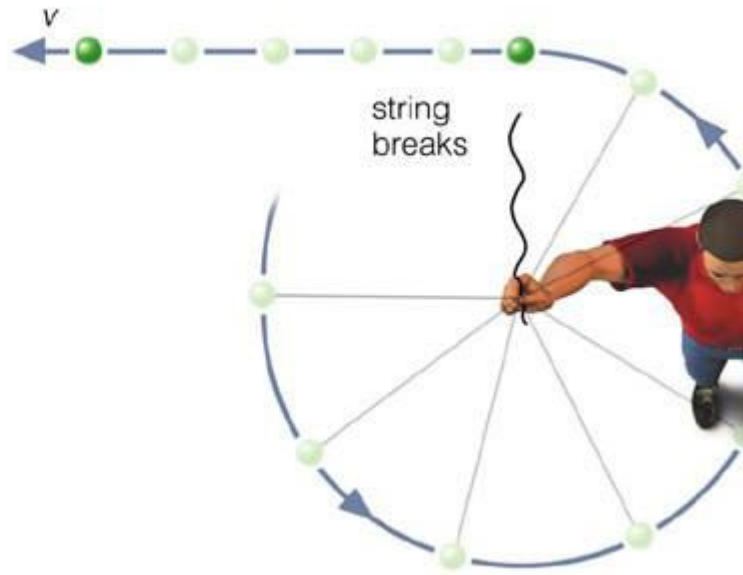
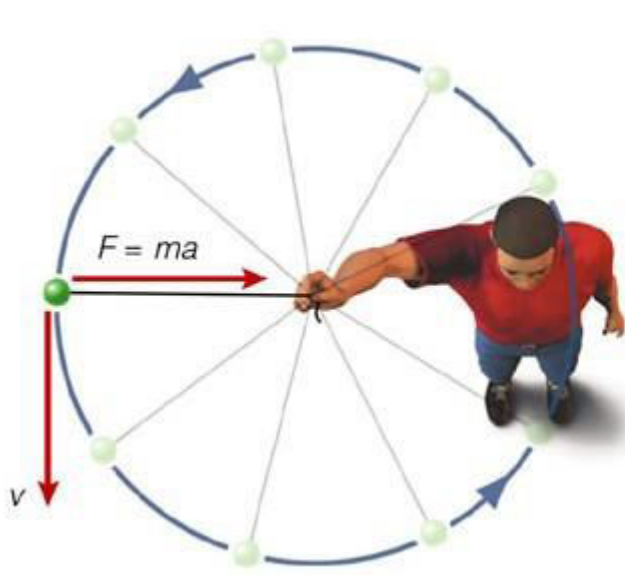
Early stage

- In the thunderstorm, air is uplifted as it is **warm and light**. At certain height, due to [lapse rate and adiabatic lapse rate](#), the temperature of air falls and moisture in the air undergoes **condensation**.
- Condensation releases [latent heat of condensation](#) making the air more warmer. It becomes much lighter and is further uplifted.

- The space is filled by fresh moisture laden air. Condensation occurs in this air and the cycle is repeated as long as the moisture is supplied.
- Due to excess moisture over oceans, the thunderstorm intensifies and sucks in air at much faster rate. The air from surroundings rushes in and undergoes deflection due to **Coriolis force** creating a **cyclonic vortex (spiraling air column. Similar to [tornado](#))**.



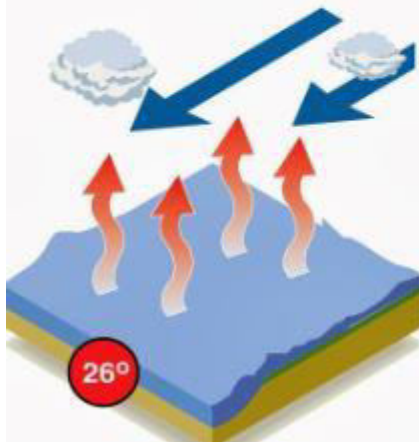
- Due to centripetal acceleration (centripetal force pulling towards the center is countered by an opposing force called centrifugal force), the air in the vortex is forced to form a region of calmness called an **eye** at the center of the cyclone. The inner surface of the vortex forms the **eye wall**, the **most violent region** of the cyclone.



How tropical storms are formed

High humidity and ocean temperatures of over 26°C are major contributing factors

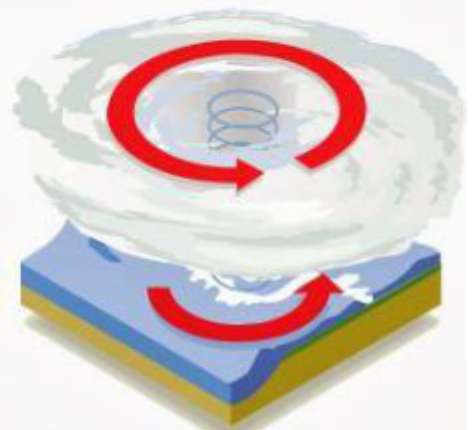
Water evaporates from the ocean surface and comes into contact with a **mass of cold air**, forming **clouds**



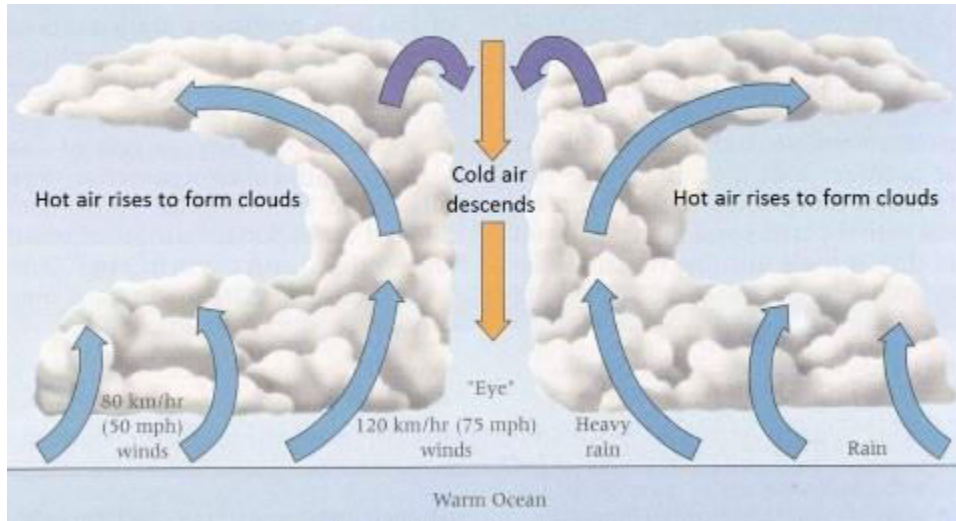
A **column of low pressure** develops at the centre. **Winds form** around the column



As pressure in the central column (the eye) weakens, the **speed of the wind around it increases**



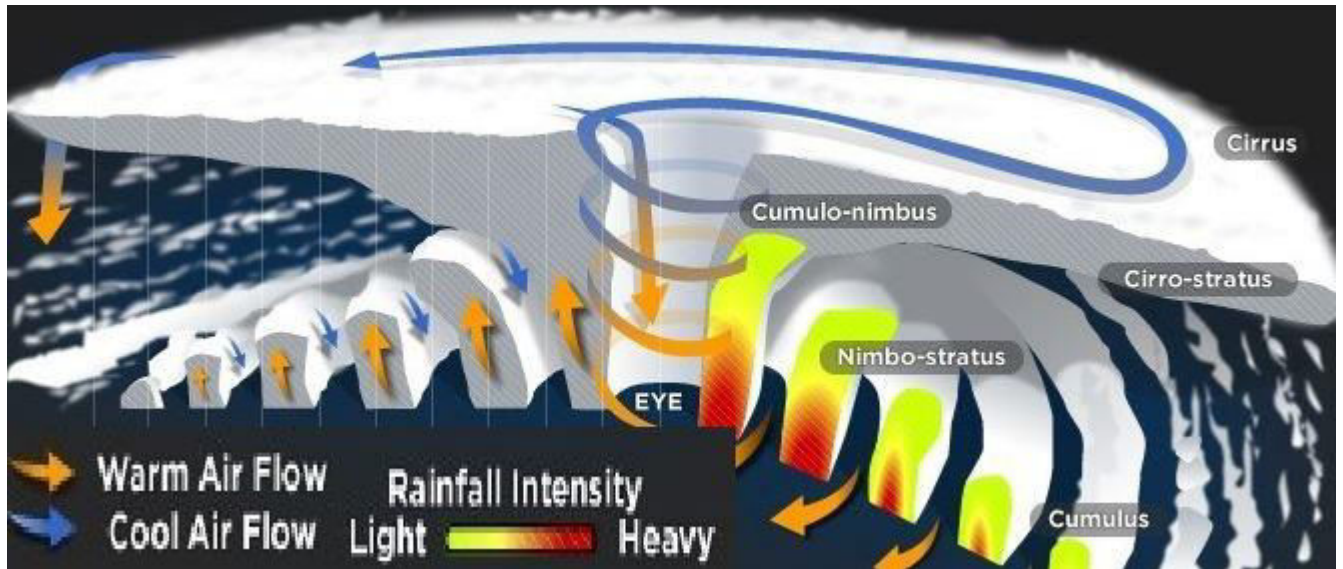
[Eye is created due to tangential force acting on wind that is following a curvy path]



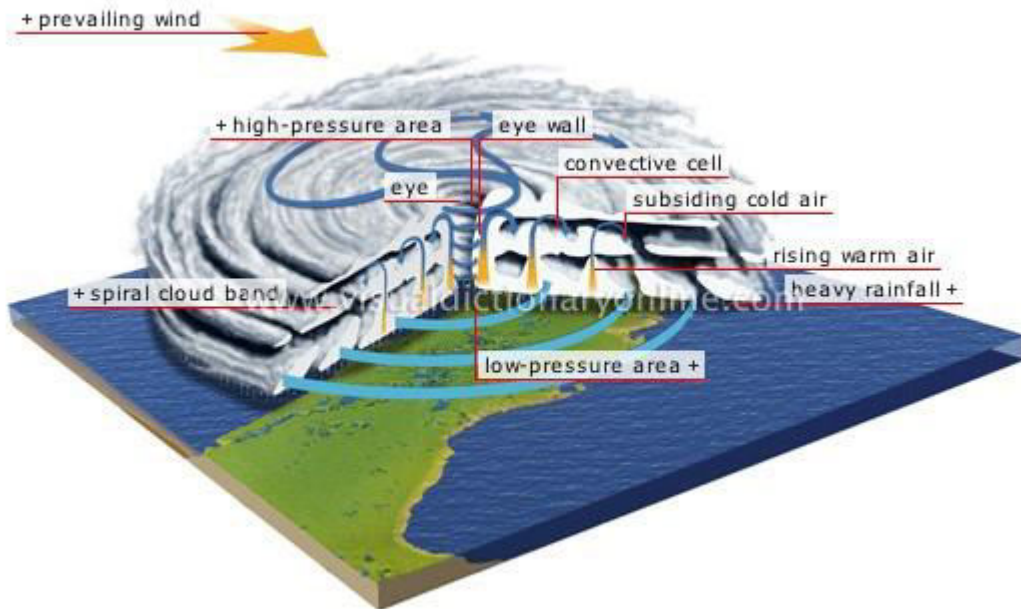
- All the wind that is carried upwards loses its moisture and becomes cold and dense. It descends to the surface through the cylindrical eye region and at the edges of the cyclone.
- Continuous supply of **moisture** from the sea is the major driving force behind every cyclone. On reaching the land the **moisture supply is cut off** and the storm dissipates.
- If ocean can supply more moisture, the storm will reach a mature stage.

Mature stage

- At this stage, the spiraling winds create multiple convective cells with successive calm and violent regions.
- The regions with cumulonimbus cloud (rising limbs of convective cell) formation are called **rain bands** below which intense rainfall occurs.
- The ascending air will lose moisture at some point and descends (subsides) back to surface through the calm regions (descending limbs of convection cell – subsiding air) that exist between two rain bands.
- Cloud formation is dense at the center. The cloud size decreases from center to periphery.
- Rain bands are mostly made up of cumulonimbus clouds. The ones at the periphery are made up of nimbostratus and cumulus clouds.
- The dense overcast at the upper levels of troposphere is due to cirrus clouds which are mostly made up of hexagonal ice crystals.
- The dry air flowing along the central dense overcast descends at the periphery and the eye region.



Structure of a tropical cyclone



Eye

- The “eye” is a roughly circular area of comparatively **light winds and fair weather** found at the center of a severe tropical cyclone.
- There is little or **no precipitation** and sometimes blue sky or stars can be seen.

- The eye is the region of **lowest surface pressure** and warmest temperatures aloft (in the upper levels) – the eye temperature may be 10°C warmer or more at an altitude of 12 km than the surrounding environment, but only 0-2°C warmer at the surface in the tropical cyclone.
- Eyes range in size from 8 km to over 200 km across, but most are approximately 30-60 km in diameter.

Eye wall

- The eye is surrounded by the “eye wall”, the roughly circular ring of **deep convection**, which is the area of **highest surface winds** in the tropical cyclone. Eye Wall region also sees the maximum sustained winds i.e. **fastest winds in a cyclone occur along the eye wall region**.
- The eye is composed of air that is slowly sinking and the eye wall has a net upward flow as a result of many moderate – occasionally strong – **updrafts and downdrafts [Explained in ‘Thunderstorms’]**.
- The eye’s warm temperatures are due to compressional warming (adiabatic) of the subsiding air.
- Most soundings taken within the eye show a low-level layer, which is relatively moist, with an inversion above – suggesting that the sinking in the eye **typically does not reach the ocean surface**, but instead only gets to around 1-3 km of the surface.

Spiral bands

- Another feature of tropical cyclones that probably plays a role in **forming and maintaining the eye** is the eye wall convection.
- Convection in tropical cyclones is organized into long, narrow rain bands which are oriented in the same direction as the horizontal wind.
- Because these bands **seem to spiral into the center** of a tropical cyclone, they are called “spiral bands”.
- Along these bands, low-level convergence is a maximum, and therefore, upper-level divergence is most pronounced above.
- A direct circulation develops in which warm, moist air converges at the surface, ascends through these bands, **diverges aloft**, and **descends on both sides of the bands**.
- Subsidence is distributed over a wide area on the outside of the rain band but is concentrated in the small inside area.
- As the air subsides, adiabatic warming takes place, and the air dries.
- Because subsidence is concentrated on the inside of the band, the adiabatic warming is stronger inward from the band causing a sharp contrast in pressure falls across the band since warm air is lighter than cold air.
- Because of the pressure falls on the inside, the tangential winds around the tropical cyclone increase due to increased pressure gradient. Eventually, the band moves toward the center and encircles it and the **eye and eye wall form**.

- Thus, the cloud-free eye may be due to a **combination of dynamically forced centrifuging of mass out of the eye into the eye wall and to a forced descent caused by the moist convection of the eye wall.**

Vertical Structure of a Tropical Cyclone

There are three divisions in the vertical structure of tropical cyclones.

- The lowest layer, extending up to 3 km and known as the inflow layer, is responsible for **driving the storm.**
- The middle layer, extending from 3 km to 7 km, is where the **main cyclonic storm** takes place.
- The outflow layer lies above 7 km. The maximum outflow is found at 12 km and above. The movement of air is **anticyclonic** in nature.

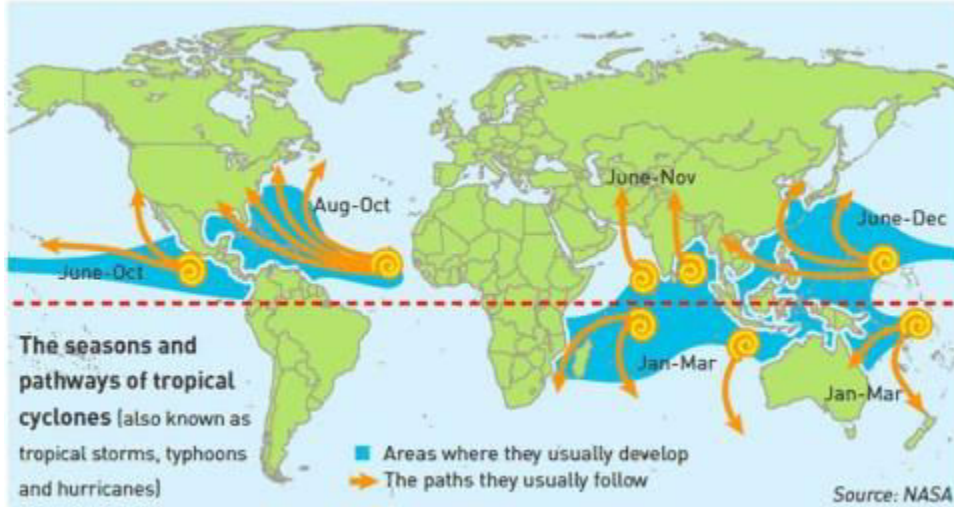
Categories of Tropical Cyclones



Cyclone Category	Wind Speed in Km/h	Damage Capacity	Type of Disturbances	Wind Speed in Km/h
			01	120-150
02	150-180	Moderate	Depression	31-49
03	180-210	Extensive	Deep Depression	49-61
04	210-250	Extreme	Cyclonic Storm	61-88
05	250 +	Catastrophic	Severe Cyclonic Storm	88-117
			Very Severe Cyclone	118-221
			Super Cyclone	More than 221

Category	Australian name	US*	NW Pacific	Arabian Sea / Bay of Bengal
-	Tropical low	Tropical depression	Tropical depression	Depression or severe depression
1	Tropical cyclone	Tropical storm	Tropical storm	Cyclonic storm
2	Tropical cyclone	Tropical storm	Severe tropical storm	Severe cyclonic storm
3	Severe tropical Cyclone	Hurricane	Typhoon	Very severe cyclonic storm
4	Severe tropical cyclone	Hurricane	Typhoon	Very severe cyclonic storm
5	Severe tropical cyclone	Hurricane	Typhoon	Super cyclonic storm

Favorite Breeding Grounds for Tropical Cyclones



- South-east Caribbean region where they are called hurricanes.
- Philippines islands, eastern China and Japan where they are called typhoons.
- Bay of Bengal and Arabian Sea where they are called cyclones.
- Around south-east African coast and Madagascar-Mauritius islands.
- North-west Australia.

Regional names for Tropical Cyclones

Regions	What they are called
Indian Ocean	Cyclones
Atlantic	Hurricanes
Western Pacific and South China Sea	Typhoons
Western Australia	Willy-willies

Characteristics of Tropical Cyclones

- The main features of tropical cyclones are as follows.

Size and Shape

- Tropical cyclones have symmetrical **elliptical shapes** (2:3 ratio of length and breadth) with steep pressure gradients. They have a compact size—80 km near center, which may develop up to 300 km to 1500 km.

Wind Velocity and Strength

- Wind velocity, in a tropical cyclone, is more in poleward margins than at center and is more over oceans than over landmasses, which are scattered with physical barriers. The wind velocity may range from nil to 1200 km per hour.

Path of Tropical Cyclones

- These cyclones start with a westward movement, but turn northwards around 20° latitude. They turn further north-eastwards around 25° latitude, and then eastwards around 30° latitude. They then lose energy and subside.
- Tropical cyclones follow a **parabolic path**, their axis being parallel to the isobars.
- Coriolis force or earth's rotation, easterly and westerly winds influence the path of a tropical cyclone.
- Tropical cyclones die at 30° latitude because of cool ocean waters and increasing wind shear due to westerlies.

Path of Tropical Cyclones

- a) These cyclones start with a westward movement — This is because the earth is rotating from west to east and the formation is under the influence of easterlies.
- b) but turn northwards around 20° latitude — Coriolis force deflects the path towards right.
- c) They turn further north-eastwards around 25° latitude — Coriolis force deflects it further towards the right.
- d) and then eastwards around 30° latitude — Because of westerly winds.
- e) They then lose energy and subside — Ocean water at 30° latitude is not warm enough to sustain a cyclone. Also in due to westerlies doesn't facilitate the formation of cyclonic vortex.

Warning of Tropical Cyclones

- Detection of any unusual phenomena in the weather leading to cyclones has three main parameters: **fall in pressure, increase in wind velocity, and the direction and movement (track) of storm.**
- There are a network of weather stations monitoring pressure fall and wind velocities in all countries of the world, including the Arctic and Antarctic regions.
- The islands attain special significance in this as they facilitate monitoring of these developments.
- In India, there are detection radars along both the coasts.
- Monitoring is also done by aircraft which carry a number of instruments including a weather radar.
- Cyclone monitoring by satellites is done through very high resolution radiometers, working in the visual and infra-red regions (for night view) of the spectrum to obtain an image of the cloud cover and its structure.
- Remote sensing by radars, aircraft and satellites helps predict where exactly the cyclone is going to strike. It helps in taking advance steps in the following areas:
 1. closing of ports and harbours,
 2. suspension of fishing activities,
 3. evacuation of population,
 4. stocking of food and drinking water, and
 5. provision of shelter with sanitation facilities (safety homes).
- Today, it is possible to detect a cyclone right from its genesis in the high seas and follow its course, giving a warning at least 48 hours prior to a cyclone strike.
- However, the predictions of a storm course made only 12 hours in advance do not have a very high rate of precision.

Strom surges

Storm surge is an abnormal rise of water generated by a storm, over and above the predicted astronomical tide.

- It's the change in the water level that is due to the presence of the storm • Since storm surge is a difference between water levels, it does not have a reference level

Storm tide is the water level rise during a storm due to the combination of storm surge and the astronomical tide.

- Since storm tide is the combination of surge and tide, it does require a reference level • A 15 ft. storm surge on top of a high tide that is 2 ft. above mean sea level produces a 17 ft. storm tide.

Storm surge is caused primarily by the strong winds in a hurricane or tropical storm. The low pressure of the storm has minimal contribution!

The wind circulation around the eye of a hurricane (blows on the ocean surface and produces a vertical circulation in the ocean). In deep water, there is nothing to disturb this circulation and there is very little indication of storm surge. Once the hurricane reaches shallower waters near the coast, the vertical circulation in the ocean becomes disrupted by the ocean bottom. The water can no longer go down, so it has nowhere else to go but up and inland.

Central Pressure: Lower pressure will produce a higher surge.

Storm Intensity: Stronger winds will produce a higher surge.

Storm Forward Speed: On the open coast, a faster storm will produce a higher surge. However, a higher surge is produced in bays, sounds, and other enclosed bodies of water with a slower storm.

Width and Slope of the Ocean Bottom: Higher storm surge occurs with wide, gently sloping continental shelves, while lower storm surge occurs with narrow, steeply sloping shelves

Size: A larger storm will produce higher surge.

Angle of Approach to Coast: The angle at which a storm approaches a coastline can affect how much surge is generated. A storm that moves onshore perpendicular to the coast is more likely to produce a higher storm surge than a storm that moves parallel to the coast or moves inland at an oblique angle.

Local Features Storm surge is highly dependent on local features and barriers that will affect the flow of water. A good example is the coast of North Carolina, which has the complexities of such features as barrier islands, inlets, sounds, bays, and rivers.

EL-Nino Southern Oscillation (ENSO)

The El Niño/Southern Oscillation (ENSO) is a naturally occurring phenomenon involving fluctuating ocean temperatures in the central and eastern equatorial Pacific, coupled with changes in the atmosphere. This phenomenon has a major influence on climate patterns in various parts of the world. Scientific progress on the understanding and modelling of ENSO has improved prediction skills within a range of one to nine months in advance, helping society to prepare for the associated hazards such as heavy rains, floods and drought. The value of these predictions can translate into hundreds of millions, if not billions, of dollars in potential savings.

El Niño and La Niña are the oceanic components while the Southern Oscillation is the atmospheric counterpart, thus giving rise to the term El Niño/Southern Oscillation.

The El Niño/Southern Oscillation comprises three phases: El Niño, La Niña and neutral. El Niño, meaning “boy child” in Spanish, was first used in the nineteenth century by fishermen in Peru and Ecuador to refer to the unusually warm waters that reduced their catch just before Christmas. El Niño events often

begin in the middle of the year with large-scale warming of surface water in the central and eastern equatorial Pacific Ocean and changes in the tropical atmospheric circulation (i.e. winds, pressure and rainfall). In general, El Niño reaches a peak during November–January and then decays over the first half of the following year. It occurs every two to seven years and can last up to 18 months. Strong and moderate El Niño events have a warming effect on average global surface temperatures.

The opposite of El Niño within the ENSO cycle is known as La Niña, which means “little girl” and refers to the large-scale cooling of the ocean surface temperatures in the same region in the equatorial Pacific, coupled with a reversal of the overlying atmospheric conditions. In many locations, especially in the tropics, La Niña (or cold episodes) produces the opposite climate variations to El Niño. During ENSO-neutral phases, atmospheric patterns are controlled more by other climate drivers.

The World Meteorological Organization (WMO) issues regular El Niño/La Niña Updates based on observational monitoring of the current situation, seasonal predictions through climate model simulations performed by advanced centres around the world, and input from top international experts. The last El Niño episode was in 2009/2010. The outcomes of each El Niño event are never exactly the same: they depend on the intensity of the event, the time of year when it develops and the interaction with other climate patterns. El Niño does not affect all regions, and even in a given region, the impacts are not the same. For the most accurate information at national or local level, it is important to consult National Meteorological and Hydrological Services.

REGIONAL CLIMATE EFFECTS OF EL NIÑO

During El Niño events, the pool of warm water in the central or eastern tropical Pacific heats the overlying atmosphere, causing the air to rise. As it rises, the air cools and produces rain. In contrast, on the western side of the Pacific, the ocean surface tends to cool and there is less rising motion. These changing patterns of ascending and descending air are part of the Southern Oscillation component of ENSO as explained above. This means that El Niño is often associated with warm and dry conditions in southern and eastern inland areas of Australia, as well as Indonesia, the Philippines, Malaysia and central Pacific islands such as Fiji, Tonga and Papua New Guinea. During the northern hemisphere summer season, the Indian monsoon rainfall generally tends to be less than normal, especially in the north-west of India. The magnitude and scale of the changes in atmospheric circulation associated with El Niño are such that the effects on regional climate extend beyond the tropical Pacific basin. In northern hemisphere winter, drier than normal conditions are typically observed over south-eastern Africa and northern Brazil. Wetter than normal conditions are typically observed along the Gulf Coast of the United States, the west coast of tropical South America (Colombia, Ecuador and Peru) and from southern Brazil to central Argentina. Parts of eastern Africa also usually receive above-normal rainfall. El Niño is associated with milder winters in north-western Canada and Alaska due to fewer cold air surges from the Arctic – a result of a large-scale region of lower pressure centred on the Gulf of Alaska/ North Pacific Ocean. It is important to stress that these are typical effects – not specific forecasts – and that actual conditions vary according to the strength and timing of the El Niño event. Other factors (such as the Indian Ocean Dipole or the North Atlantic Oscillation/Arctic Oscillation) can also have an important influence on seasonal climate. Regional Climate Outlook Forums in different parts of the world factor

the likely development of El Niño or La Niña events into their seasonal predictions for users in the sectors of agriculture and food security, water management, health, disaster risk reduction and energy.

EL NIÑO AND TROPICAL CYCLONE ACTIVITY

El Niño tends to lead to more tropical cyclone activity in the central and eastern Pacific basins and less in the Atlantic basin. Over the central and eastern Pacific, increased sea-level atmospheric pressure in the subtropical areas adjacent to the area of ocean warming is associated with weaker upper-level winds and reduced vertical wind shear, which favours more tropical cyclone activity. In the eastern Pacific, El Niño typically causes the track of tropical cyclones to shift northwards and tends to increase the intensity of associated rainfall. Over the Atlantic basin, the reduced sea-level atmospheric pressure is associated with stronger upper-level westerly winds and stronger lower-level easterly trade winds, both of which increase the vertical wind shear and hinder hurricane formation. El Niño also suppresses Atlantic hurricane activity by increasing atmospheric stability.

satellite in weather forecasting.

Reliable weather prediction holds the key for socio economic development and is essential for food security of the human society. Since time immemorial, human race has been fascinated by the ever changing and highly dynamic atmosphere around him and has made concerted efforts to understand the controlling processes and achieve better capabilities of weather forecasting. The recent attempts for satellite based observations, made over the past two decades, have provided new insights in these processes. Synoptic coverage provided by satellites is ideally suited to study weather related atmospheric processes on different scales. The recent advances in satellite technology in terms of high resolution, multi-spectral bands covering visible, infrared and microwave regions have made space data an inevitable component in weather monitoring and dynamic modeling. The impact of satellite data is phenomenal in certain areas of meteorological applications such as short-range forecasts, Tropical Cyclone (TC) monitoring, aviation forecasts etc. With improving trend in accuracy of satellite retrievals, improvements could be carried out in models leading to improved forecasts, especially in the tropics.

CONTRIBUTIONS OF SPACE OBSERVATIONS

z Synoptic view of large areas, bringing out the inter-relations of processes of different spatial scales. z Frequent observations from geostationary satellites provide continuous monitoring while polar orbiting satellites give typical twice daily coverage; such data is relevant for study of weather system dynamics. z The inherent spatial averaging is more representative than the point insitu observations and readily usable for weather prediction models. z High level of uniformity of space observations overcomes the problem of inter-calibration needed for ground based instruments. z Filling of gaps in observations;

Space data covers large oceanic areas and inaccessible and remote land areas, thus giving global coverage. z New types of data and observations; parameters such as sea surface (skin) temperature, sea surface wind stress, sea level, cloud liquid water content, radiation balance, aerosol are some of the unique parameters provided only by satellites. z Simultaneous observation of several dynamic parameters provided by different sensors in same platform facilitates study of inter-relationships and knowledge of processes (e.g. Sea Surface temperature and deep convection, cloud development and radiative forcing).

METEOROLOGICAL SATELLITES / PAYLOADS

Currently several operational meteorological satellites are providing global and regional observations. Six different types of satellite systems currently in use are : 1) Visible/ Infrared/Water Vapour Imagers, 2) Infrared Sounders, 3) Microwave Imagers, 4) Microwave Sounders, 5) Scatterometers and 6) Radar Altimeters. Though the water vapour imaging capability is available only on the geostationary satellite, the visible and infrared imagers are available on geostationary as well as polar orbiting satellites. The last four are currently available only on polar orbiting systems. We first describe in detail below the INSAT system which is the primary satellite for weather surveillance in this part of the globe. It is a multipurpose geostationary satellite that caters to the requirements of Meteorology and Communication. It carries a met payload called Very High Resolution Radiometer (VHRR) that enables us to have visible, infrared and now even water vapour images. It is designed to provide the following services:

Round the clock surveillance of weather systems including severe weather events around the Indian region. z Operational parameters for weather forecasting – cloud cover, cloud top temperature, sea surface temperature, snow cover, cloud motion vector, outgoing long wave radiation etc. z Collection and transmission of meteorological, hydrological and oceanographic data from remote/inaccessible areas through Data Collection Platforms. z Timely dissemination of warning of impending disasters such as cyclones through Cyclone Warning Dissemination Systems. z Dissemination of Meteorological information including processed images of weather systems through Meteorological Data dissemination system.

INSAT applications programme started with the launch of INSAT-1 series of satellites in early 1980s. INSAT-2 series that followed was designed based on user feedback. INSAT-2A and 2B launched in 1992 and 1993 carried VHRR payload with improved resolution of 2 km in visible and 8 km in thermal band.

The imaging capability included three modes, viz. full frame, normal mode and sector mode of 5 minutes for rapid coverage of severe weather systems. INSAT-2E launched in 1999 carried an advanced VHRR payload operating in three channels – visible (2 km), thermal and water vapour (8 km). The water vapour channel is capable of giving water vapour distribution and flow patterns in the middle troposphere. Besides this, INSAT-2E also carried a CCD camera with 3 channels – visible, near infrared and short wave infrared with 1 km resolution to map the vegetation cover. A geostationary meteorological satellite (METSAT) system devoted totally to meteorology was launched in 2002. It has been renamed as Kalpana-1 and is currently the operational satellite system being used by IMD. INSAT-3A has been launched in April 2003 and carries identical payloads as in INSAT-2E. INSAT-3D planned for future will also carry atmospheric sounder for temperature and water vapour profiles and split thermal channels for accurate sea surface temperature retrieval. Data from INSAT satellites are being used to retrieve a number of quantitative products. INSAT imagery is being used very exhaustively to provide support for synoptic analysis and weather forecasting. The quantitative products available from INSAT and its applications are described in subsequent sections.

FUTURE MISSIONS Several satellite missions have been planned to support the operational data needs and ongoing research efforts. The future Metsat missions will carry improved VHRR and vertical sounders for temperature/humidity profiles. The Megha -Tropiques Mission scheduled for 2004 launch will be a joint project by ISRO and CNES, France with the objective of studying the water cycle and energy exchanges in the tropics. With an equatorial inclined orbit, the satellite will have high repetitively over tropical regions. The future appears bright for our space-based observing system. Advanced, multispectral (visible, IR, and passive microwave) imagers, sounders (infrared and microwave) and scatterometers are planned for launch in the near future. Hyperspectral measurements from newly developed interferometers are expected to be flown experimentally by 2006. The information content will vastly exceed that of the current measuring devices. Instead of a few dozen viewing channels, these instruments will have more than a thousand channels over a wide spectral range. The satellite data downloads are expected to exceed several terabytes per day. Fortunately, communications and computing capacity are increasing at a rate that hopefully can accommodate this data explosion. Emerging new technologies (including the use of rapidly developing visualization tools) will be employed. It is important that the evolving spacebased observational system keeps one step ahead of the demands being placed by the user community and advances in numerical weather prediction. While it will become an enormous task and challenge to assimilate this wealth of data into meaningful

parameters, the outlook is bright for unlocking the stillunresolved mysteries towards improving our understanding and prediction of atmospheric circulation systems such as tropical cyclone.

standard tool in weather forecasting

Before the 1600s, knowledge of the Earth's atmosphere and weather was not exact. People mostly relied on experience with local weather events for forecasts. Aunt Sally could smell a snowstorm coming, and Uncle Jim's knee told of impending rain. Then simple devices, such as thermometers, barometers and weather vanes, were invented that gave recordable data. As technology advanced from the 1800s onward, more sophisticated equipment allowed detection of regional and global weather patterns, and modern radar, satellites and computer modeling programs allow long-term weather predictions.

Temperature Equipment

Glass thermometers filled with either alcohol or mercury are standard equipment for measuring air, soil and water temperatures. Maximum and minimum temperature thermometers register the lowest and highest temperatures during a specific time period. The resistance temperature detector determines air temperatures based on changes in electrical resistance of specific metals due to temperature and gives a digital readout. Preferred for automatic weather stations, RTDs can supply a temperature reading every second.

Atmospheric Pressure and Wind

Barometers measure atmospheric pressure. Liquid barometers usually measure mercury contained within an evacuated tube, and the mercury level changes as atmospheric pressure increases or decreases. Aneroid barometers contain a fixed volume of air sealed within a unit equipped with a flexible membrane. As the membrane expands and contracts with changes caused by atmospheric pressure conditions, an attached needle points to the correct reading. Wind anemometers measure the direction and speed of wind. They usually incorporate a weather vane tail and a fan to measure speed.

Moisture Indicators

There are several tools that measure humidity, or the percentage of water in air. The earliest was the hygrometer, which depends on a human hair expanding and contracting in response to humidity changes. The psychrometer detects the difference in temperature between a dry and a wet thermometer bulb to measure humidity. Other instruments include the electrical hygrometer, the dew-point hygrometer, the infrared hygrometer and the dew cell. Rain gauges measure rainfall, and snow gauges measure snowfall.

Weather Balloons

Weather balloons measure humidity, air pressure, temperature, wind speed and direction with units called radiosondes. Launched from 1,100 sites around the world twice a day, they rise to over 20 miles above the Earth, recording as they travel and transmitting the information back to meteorologists by radio waves. When the balloon bursts, the radiosonde parachutes back to Earth for recycling. Weather balloons give a vertical snapshot of atmospheric conditions in a given area.

High-Tech Tools

With the invention of radar in World War II, meteorological studies vastly improved. Conventional radar, Doppler radar and dual-polarization radar detect storm systems, their direction, speed, intensity and type of precipitation. Meteorological satellites orbiting the Earth began transmitting in 1962 and led to more complicated satellites. Geostationary Operational Environmental Satellites transmit photographic images of the Western Hemisphere every 15 minutes. Polar Operational Environmental Satellites take about 1.5 hours to orbit the Earth, providing information about weather, oceans and volcanic eruptions. Computer analysis of weather data and computer modeling of weather systems make long-term weather prediction on a global scale increasingly more accurate.

cyclone tracking thunderstorms-forecasting

In the first half of the 20th century the identification of tropical cyclones was based on changes in weather conditions, the state of the sea surface, and reports from areas that had already been affected by the [storm](#). This method left little time for advance warning and contributed to [high](#) death tolls.

Observation networks and techniques improved with time; with the advent

of [weather satellites](#) in the 1960s, the early detection and tracking of tropical cyclones was greatly improved.

Use of satellites and aircraft

An array of geostationary [satellites](#) (those that remain over a fixed position on Earth) is operated by a number of countries. Each of these satellites provides continuous displays of [Earth's](#) surface in visible light and in infrared wavelengths. It is the latter that are most important in tracking the stages of tropical [cyclone development](#). Infrared images show the temperatures of [cloud](#) tops, thus allowing the loosely organized convection associated with easterly waves to be detected by the presence of cold, high clouds. They also show the deep, organized convection characteristic of a tropical [cyclone](#). Satellite images not only show a storm's location but also can be used to estimate its intensity because certain cloud patterns are characteristic of particular [wind](#) speeds.

Although satellite images provide general information on the location and intensity of tropical cyclones, detailed information on a storm's strength and structure must be obtained directly, using [aircraft](#). This information is essential in providing the most accurate warnings possible. Operational reconnaissance is done only by the United States for storms that may affect its continental landmass. No other country does this type of reconnaissance. Tropical cyclones in other [ocean](#) basins occur over a larger region, and most countries do not have the financial resources to maintain research aircraft. When evidence of a developing circulation is detected in the Atlantic or Caribbean, a U.S. Air Force C-130 aircraft is dispatched to determine if a closed circulation is present. The centre of circulation is noted, and an instrument called a dropsonde is released through the bottom of the aircraft to measure the temperature, humidity, [atmospheric pressure](#), and wind speed. In many cases, the naming of a [tropical storm](#), or its upgrade from tropical storm to tropical cyclone, is based on aircraft observations.

Long-term forecasts

Forecasts of expected numbers of Atlantic tropical cyclones are now being made well in advance of the start of each year's tropical cyclone [season](#). The forecast model takes into account seasonal trends in factors related to tropical cyclone formation such as the presence of El Niño or La Niña oceanic conditions (see the section below), amount of rainfall over Africa, winds in the lower stratosphere, and atmospheric pressure and wind tendencies over the Caribbean. Based on these factors, forecasts are issued concerning the expected numbers of tropical storms, tropical cyclones, and intense tropical cyclones for the Atlantic. These forecasts are issued in December, and they are revised in June and again in [August](#) of each year for the current Atlantic tropical cyclone season. The forecast model has displayed reasonable skill in predicting the total number of storms each season.

Climatic variations and tropical cyclone frequency

The number of tropical cyclones generated during a given a year has been observed to vary with certain climatic conditions that modify the general circulation of the [atmosphere](#). One of these conditions is the [intermittent](#) occurrence of [El Niño](#), an oceanic phenomenon characterized by the presence every few years of unusually warm water over the equatorial eastern Pacific. The presence of unusually cool surface waters in the region is known as [La Niña](#). While the factors connecting El Niño and La Niña to tropical cyclones are complicated, there are a few general relationships. During years when El Niño conditions are present, upper-level winds over the Atlantic tend to be stronger than normal, which increases the vertical shear and decreases tropical cyclone activity. La Niña conditions result in weaker shear and [enhanced](#) tropical cyclone activity. The variation of sea surface temperature associated with El Niño and La Niña also changes the strength and location of the [jet stream](#), which in turn alters the tracks of tropical cyclones. There are indications that El Niño and La Niña modulate tropical cyclone activity in other parts of the world as well. More tropical cyclones seem to occur in the eastern portion of the South Pacific during El Niño years, and fewer occur during La Niña years.

The possibility is being examined that changes in Earth's [climate](#) might alter the numbers, intensity, or paths of tropical cyclones worldwide. Increasing the amount of [carbon dioxide](#) and other greenhouse gases in the atmosphere

through the burning of fossil fuels and other human activities may increase the global average temperature and the temperature of the sea surface. These potential changes would influence the maximum intensity reached by a tropical cyclone, which depends on both the sea surface temperature and the temperature of the upper [troposphere](#). An increase in global temperature, however, could actually decrease the number of tropical cyclones, because any change in temperature would be accompanied by changes in Earth's general circulation. If tropical [atmospheric circulation](#) were to change in such a way as to increase the winds at upper levels, then there could be a decrease in tropical cyclone activity. An [assessment](#) by the World Meteorological Organization of the effect of [climate change](#) on tropical cyclones concluded that there is no evidence to suggest that an enhanced [greenhouse effect](#) will cause any major changes in the global location of tropical cyclone genesis or the total area of Earth's surface over which tropical cyclones form. Furthermore, while the maximum potential intensity of tropical cyclones may increase by 10 to 20 percent with a doubling of the concentration of carbon dioxide in the atmosphere, factors such as increased cooling due to ocean spray and changes in the vertical temperature variation may offset these effects.